AL-Farahidi University / College of Technical Eng.Aircraft Structure/ 4th Year

Training Package

In

Aircraft Structures

For

Students of four class

Aeronautical Engineer Department/ Production

By

Muhsin J. Jweeg

Emad Q. Hussein

2021 -2022

AL-Farahidi University / College of Technical Eng.
Aircraft Structure/ 4th Year
General Viewing

Introduction

Aircraft design is driven by the goal to transport cargo and passengers quickly from point to point. Since aircraft are highly integrated systems, developments in propulsion, aerodynamics and structures feed on each other to produce aircraft that operate from relatively low speeds to hypersonic speeds.

It is important that all the different types of loads that aircraft will bear be well estimated and then the structure response to these loads be carefully calculated. Those forces produce results such as deformations in other words; the forces are an input the structure and the effect of the forces acting on the structure (deformation, cracking, etc.) are the output.

The various types of structural component found in aircraft construction and the various loads they support. We saw that an aircraft is basically an assembly of **stiffened shell structures** ranging from the single cell closed section fuselage to multicellular wings and tail surfaces each subjected to bending, shear, torsional and axial loads. Structural members such as these are known as *open section* **beams**, while the cellular components are termed *closed section* **beam**s; clearly, both types of beam are subjected to **axial, bending, shear and torsional loads.**

General type of Load Applied on Structure and Stresses

Airframes must be strong and light in weight. Many forces and structural stresses act on an aircraft when it is **flying and when it is static**. The stresses acting on an aircraft are shown in Figure 1.
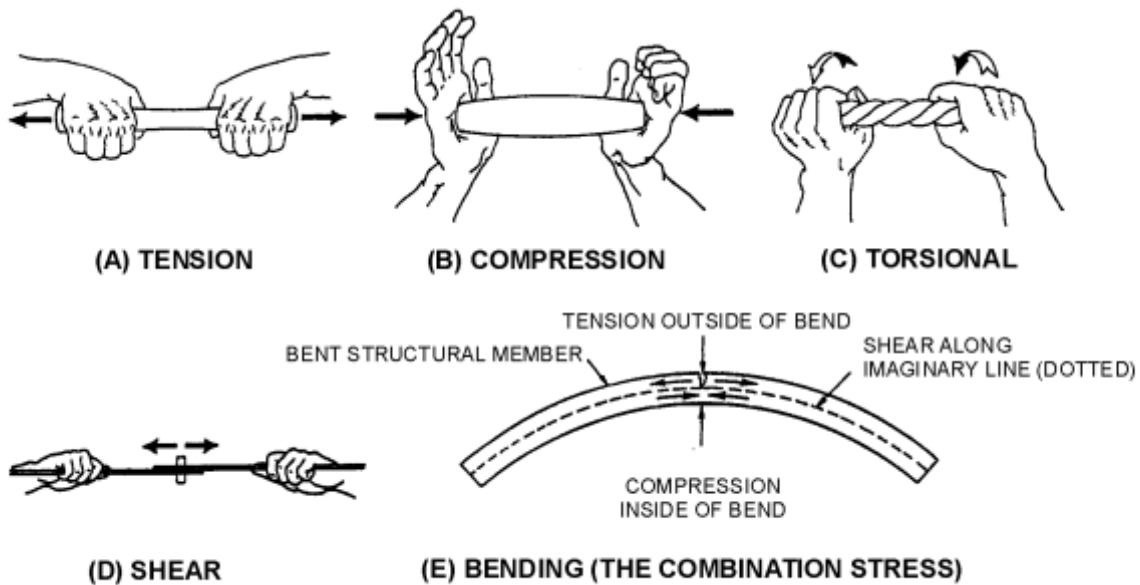
(A) TENSION   (B) COMPRESSION   (C) TORSIONAL

(D) SHEAR   (E) BENDING (THE COMBINATION STRESS)

Figure -1.—Five stresses acting on an aircraft.

<mark>Tension</mark>

The simplest type of loading on a member is tension (Fig. 1, view A). A tensile load applied (axially) in line with the center of gravity of the section will result in tensile stress distributed uniformly across the plane of the cross section lying at right angles to the line of loading.
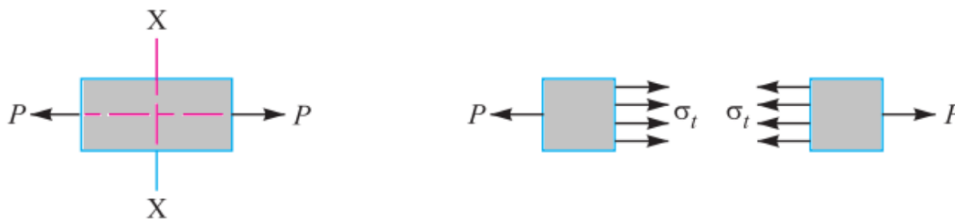
This internal force per unit area at any section of the body is known as **unit stress** or simply a **stress.** It is denoted by a Greek letter sigma (σ). Mathematically,

$$\textbf{Stress, } \sigma = \frac{P}{A}$$

Where;

        P - Force or load acting on a body, and
        A - Cross-sectional area of the body.

When a system of forces or loads acts on a body, it undergoes some deformation. This deformation per unit length is known as **unit strain** or simply a **strain.** It is denoted by a Greek letter epsilon (ε).Mathematically,

$$\text{Strain, } \varepsilon = \frac{\delta l}{l}$$

Where;

δl - Change in length of the body
l - Original length of the body.

For example, an **elevator control** cable is in additional tension when the pilot moves the control column.

Compression

If forces acting on an aircraft move toward each other to **squeeze** the material, the stress is called *compression*. Compression (Fig.1, view B) is the opposite of tension. Compression is the resistance to crushing produced by two forces pushing toward each other in the same straight line. Then the stress induced at any section of the body is known as *compressive stress* A little consideration will show that due to the compressive load, there will be an increase in cross-sectional area and a decrease in length of the body. The ratio of the decrease in length to the original length is known as *compressive strain.*
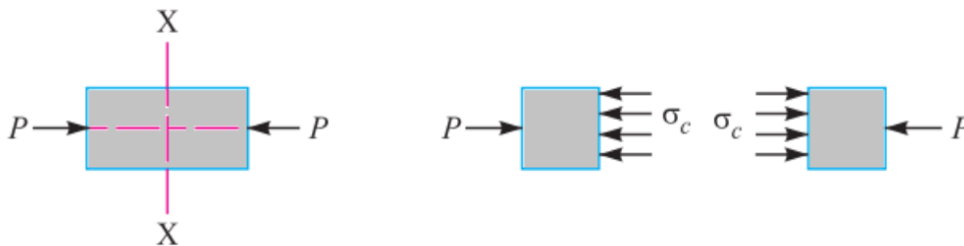
For example, when an airplane is on the ground, the **landing gear** struts are under a constant compression stress.

Torsion

Torsional (Fig.1, view C) stresses result from a **twisting force.** Torsional loading is the application of a force that tends to cause the member to twist about its structural axis. The principal deflection caused by torsion is measured by the angle of twist. The stress set up by torsion is known as *torsional shear stress*. It is zero at the centroid axis and maximum at the outer surface. The maximum torsional shear stress at the outer surface of the shaft may be obtained from the following equation;

3
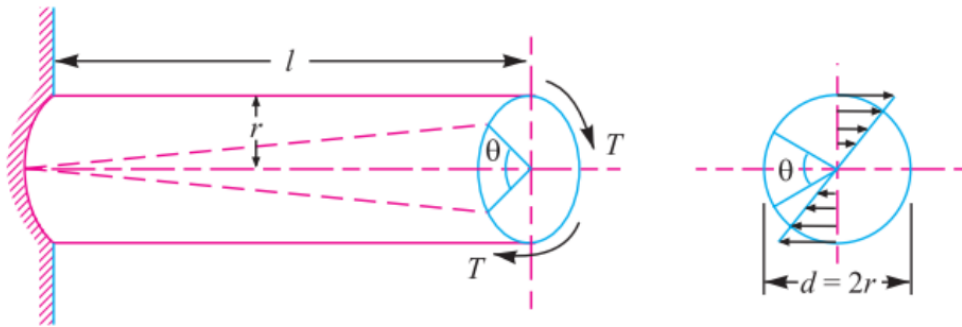
$$\frac{\tau}{r} = \frac{T}{J} = \frac{c\theta}{l}$$

where τ - Torsional shear stress induced at the outer surface of the shaft or maximum shear stress,

r - Radius of the shaft,

T - Torque or twisting moment,

J - Second moment of area of the section about its polar axis or polar moment of inertia,

C - Modulus of rigidity for the shaft material,

l -Length of the shaft, and

θ - Angle of twist in radians on a length l.

Torsional stress in a fuselage is created in several ways. For example, torsional stress is encountered in **engine torque** on turboprop aircraft. Engine torque tends to rotate the aircraft in the direction opposite to the direction the propeller is turning. This force creates a torsional stress in the fuselage as shown in Fig. 2. Also, torsional stress on the fuselage is created by the action of the **ailerons when the aircraft** is maneuvered.

Figure -2.—Engine torque creates torsion stress in aircraft fuselages.

Shear

Shear stress is presented when the load applied parallel to the area (Fig. 1, view D) , or due to bending, (A shear load is a force that tends to produce a sliding failure on a material along a plane that is parallel to the direction of the force).
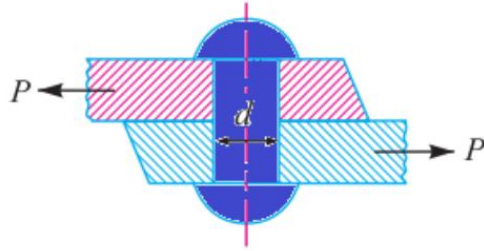
The corresponding strain is known as *shear strain* and it is measured by the angular deformation accompanying the shear stress, The shear stress and shear strain are denoted by the Greek letters tau(τ) and phi (ϕ) respectively. Mathematically,

Shear stress, τ = Tangential force / Resisting area

Bending

Bending is a combination of tension and compression. For example, when bending a piece of tubing, the upper portion compression and the lower portion tension together.
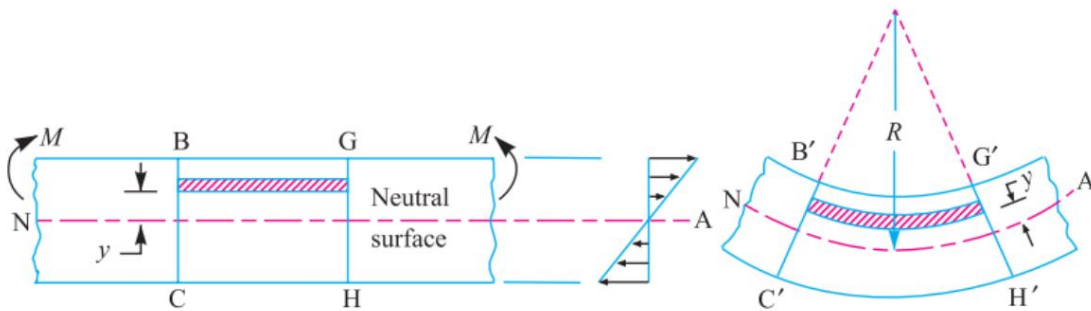
The bending equation is given by;

$$\frac{M}{I} = \frac{\sigma}{y} = \frac{E}{R}$$

Where; M - Bending moment acting at the given section,
  σ - Bending stress

  I - Moment of inertia of the cross-section about the neutral axis,
  y - Distance from the neutral axis to the extreme fiber,
  E - Young's modulus of the material of the beam, and
  R - Radius of curvature of the beam

For example, the **wing spars** of an aircraft in flight are subject to bending stresses.

Varying Stress

All structural members of an aircraft are subject to one or more stresses. Sometimes a structural member has **alternate stresses**; for example, it is under compression one instant and under tension the next. The strength of aircraft materials must be great enough to withstand maximum force of varying stresses.

When an aircraft is on the ground, there is a bending force on the fuselage. This force occurs because of the weight of the aircraft. **Bending increases** when the aircraft makes a carrier landing. This bending action creates a tension stress on the lower skin of the fuselage and a compression stress on the top skin as shown in Fig.(3)
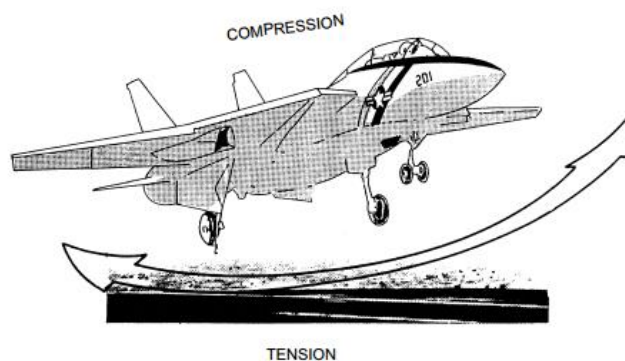

Figure -3.—Bending action occurring during carrier landing.

When the aircraft is in flight, lift forces act upward against the wings, tending to bend them upward. The wings are prevented from folding over the fuselage by the resisting strength of the wing structure. The bending action creates a tension stress on the bottom of the wings and a compression stress on the top of the wings.

Note that; during flight, any maneuver that causes acceleration or deceleration increases the forces and Stresses on the **wings, fuselage, and landing gear** of aircraft are **tension, compression, shear, bending, and torsion**. These stresses are absorbed by each component of the wing structure and transmitted to the **fuselage structure**. The empennage (**tail section**) absorbs the same stresses and transmits them to the fuselage.

Chapter One

Structural Components of

Aircraft

The aircraft is a complex engineering structure comprises the following units (Fig. 1.1):

- Airframe group including wing, fuselage and tail units.
- Airframe mechanisms, mechanism power actuators, hydraulic and pneumatic systems, and power plant,
- Aircraft equipment group(electronic and electric equipment, instrument and oxygen equipment, high altitude, etc..
- Radar equipment group (communication, navigation).

The aircraft construction can be sub-divided into many sub-assemblies. These are built in specially, in different parts of the factory or even in different factories before forward to the final assembly shop.
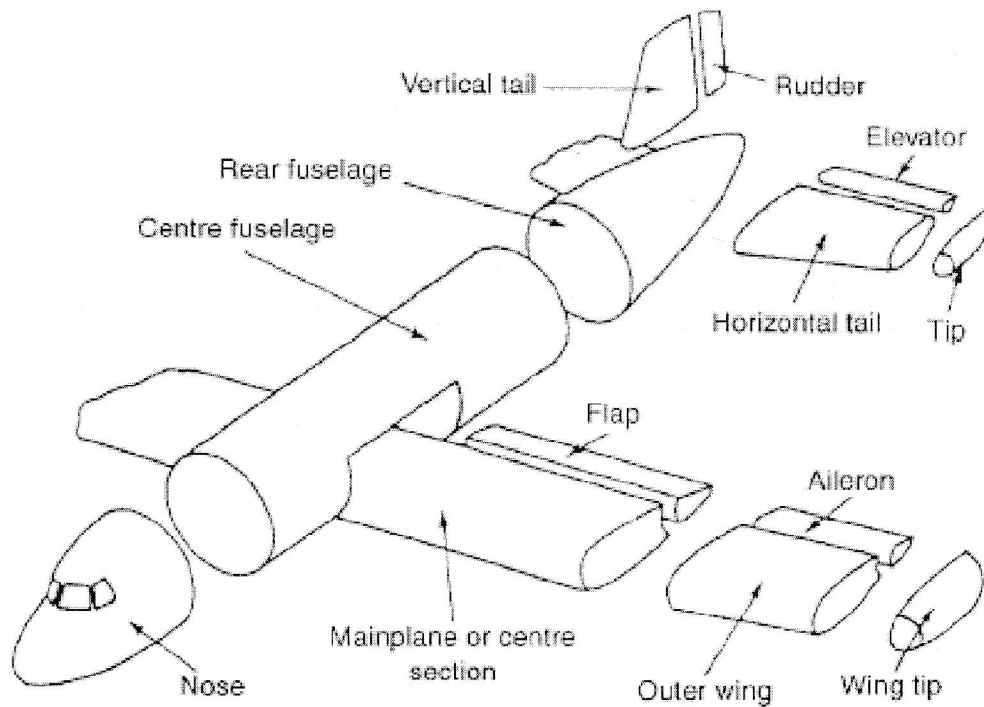
Fig. 1.1: Construction of Aircraft

The basic functions of an aircraft's structure

- Transmit and resist loads
- Provide aerodynamic shape.
- Protect passengers, payloads, and systems from environmental conditions during flight.

1.1 Loads on structural components

The structure of an aircraft is required to support two distinct classes of load:

The ground loads: includes all loads encountered by the aircraft during movement or transportation on the ground such as taxiing and landing loads, towing and hoisting.

The air loads: comprises loading imposed on the structure during flight by manoeuvres and gusts.

Aircraft must be capable of landing on water and aircraft designed to fly at high speed at low altitude, e.g. the Tornado, require a structure of above average strength to withstand the effects of flight in extremely turbulent air.

The **surface forces** which act upon the surface of the structure, e.g. aerodynamic and hydrostatic pressure, and body forces which act over the volume of the structure and are produced by gravitational and inertial effects.

Generally, these resultants cause direct loads, bending, shear and torsion in all parts of the structure in addition to local, normal pressure loads imposed on the skin.

Conventional aircraft usually consist of fuselage, wings and tail plane.

    a. The fuselage contains crew and payload, the latter being passengers, cargo, weapons plus fuel, depending on the type of aircraft and its function;

    b. The wings provide the lift and the tail plane is the main contributor to directional control. In addition, ailerons, elevators and the rudder enable the pilot to manoeuvre the aircraft and maintain its stability in flight, while wing flaps provide the necessary increase of lift for take-off and landing.

Figure 1.2 shows typical aerodynamic force resultants experienced by an aircraft in steady flight.
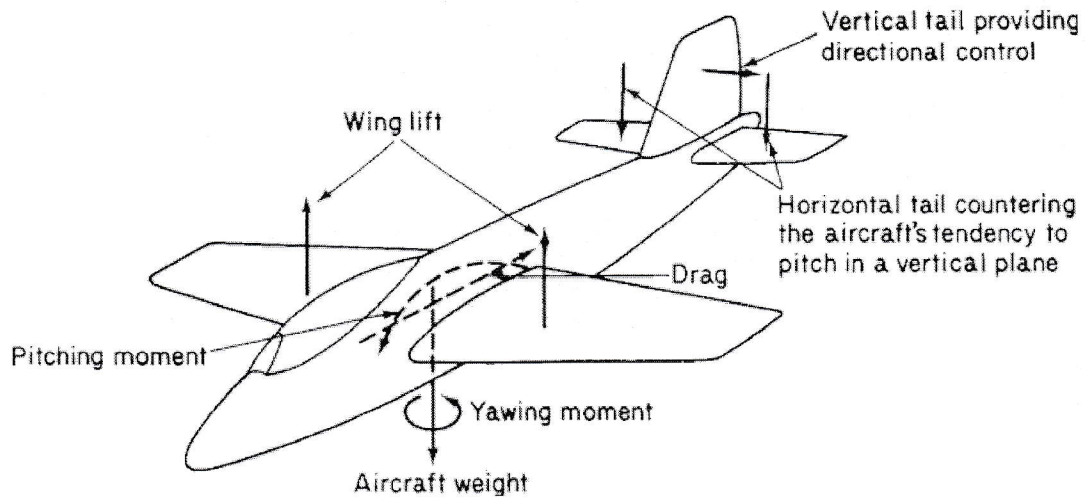
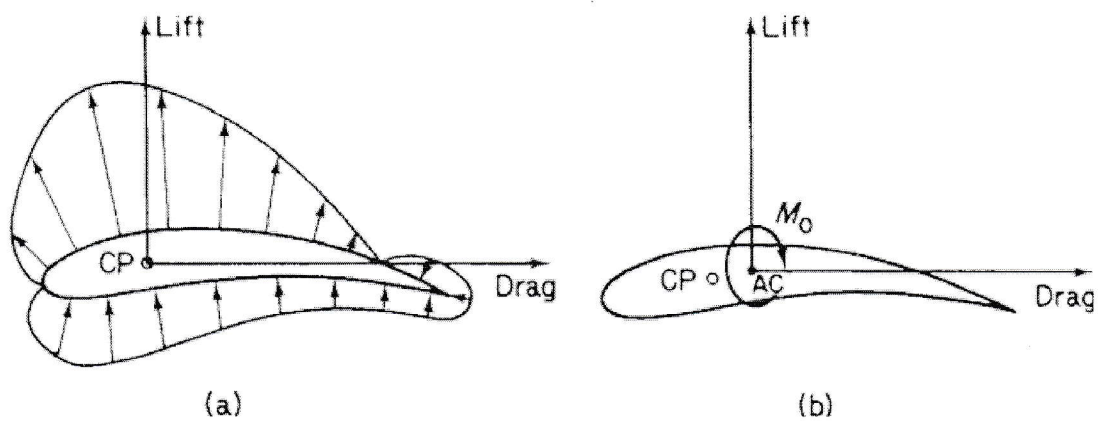**Fig.1.2: Principal aerodynamic forces on an aircraft during light**

Fig. 1.3: a) Pressure distribution around an aerofoil. (b) Transference of lift and drag load to AC.

The pressure distribution, shown in Fig. 1.3(a), has vertical (lift) and horizontal

(drag) resultants acting at a centre of pressure (CP). The position of the CP changes as the pressure distribution varies with speed or wing incidence.
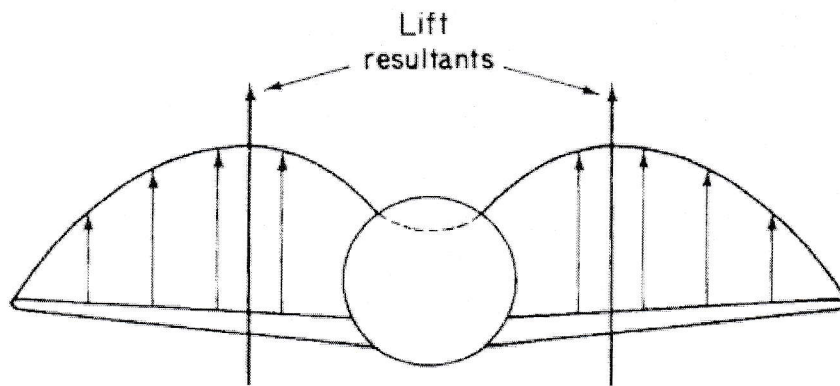
Fig. 1.4: Typical lift distribution for a wing/fuselage combination

We replace the lift and drag forces acting at the CP by lift and drag forces acting at the aerodynamic centre (AC) plus a constant moment M0 as shown in Fig. 1.3(b).

A typical distribution for a wing/fuselage combination is shown in Fig. 1.4.

1.2 Types of Aircraft structures

1. **Monocoque** (a skin structure): It is a thin shell structure, which relies entirely on its skin to resist different loads and can be defined as:
   A structure that supports loads through an objects external skin, similar to an egg shell. The term is also used to indicate a structure in which the skin provides the main structural support (Fig. 1.5).
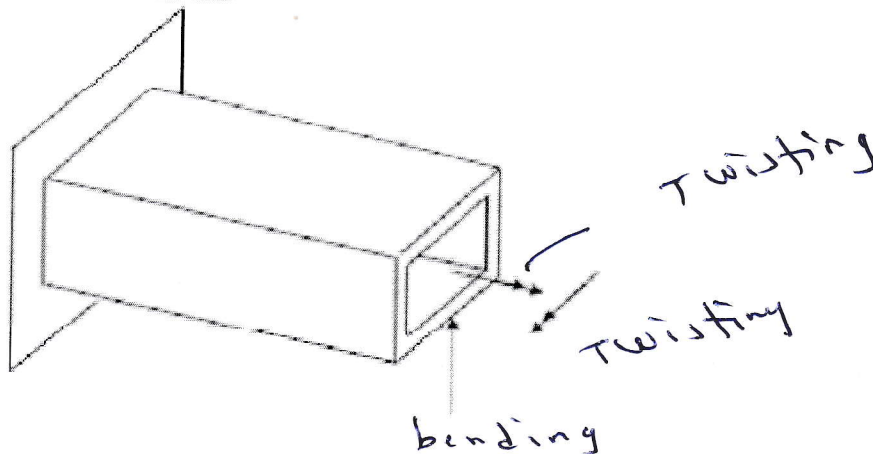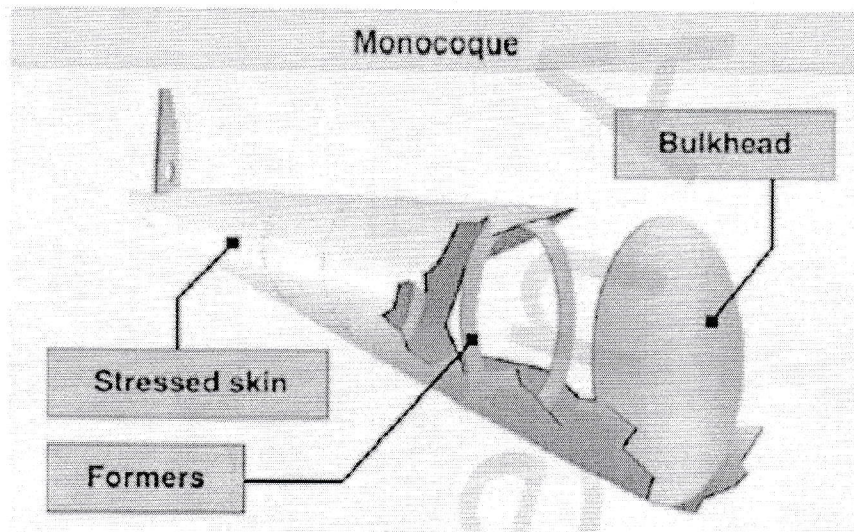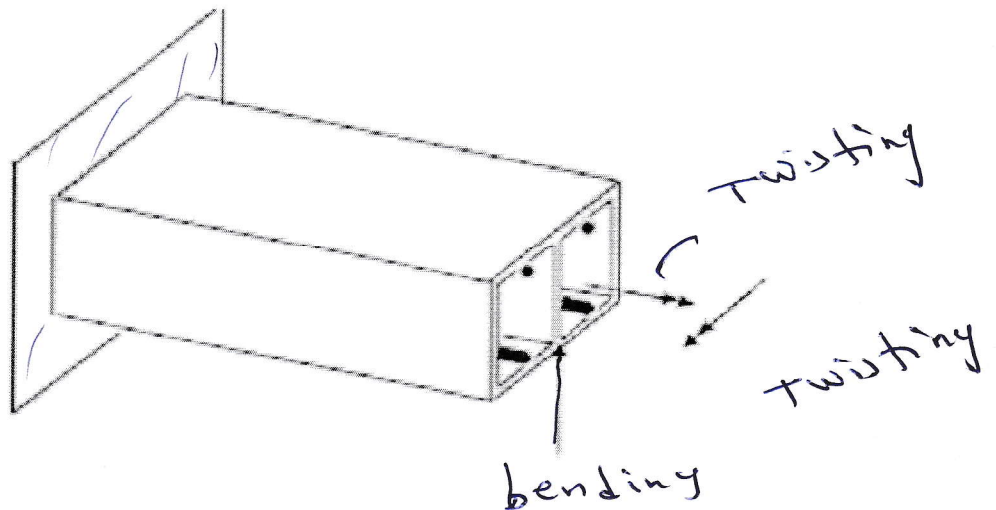
Fig. 1.5: Monocoque structure

2. **Semi-Monocoque:** Thin shell structure where the outer surface is usually supported by longitudinal stiffening members, and transverse frames to enable the structure to resist bending, compressive and twisting loads (Fig. 1.7).
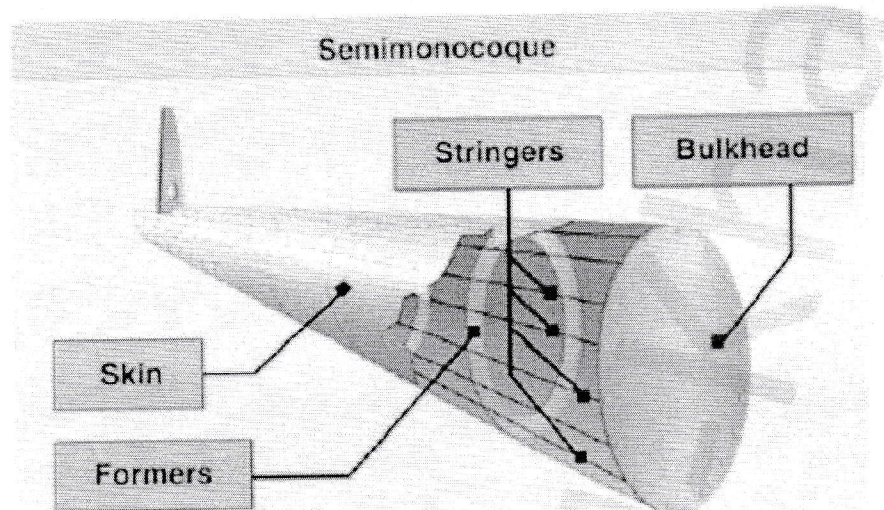
Fig. 1.6: Semi-Monocoque structure

1.3 Functions of Aircraft structural components

- **For Wings**

Skin

- . Resists the applied torsion and shear forces by transmitting aerodynamic forces to the longitudinal and transverse supporting members.
- Supports the longitudinal members in resisting the applied bending and axial loads.
- Supports the transverse members in resisting the hoop, or circumferential, load when the structure is pressurized.

Ribs and Frames : It is usually made of Aluminum alloys and used to maintain the shape of the wing cross section as it is governed by aerodynamic consideration and:

- Structural integration of the wing and fuselage.
- Keep the wing in its aerodynamic profile.
- To distribute concentrated loads from engine, fuel, fuel tanks…etc into structure.
- To support longitudinal stiffeners (stringers) at their ends and to increase their resistance to column buckling stress.
- To increase plate buckling stress o skin panels.
- Re-distribute stresses round discontinuities such as (under carriage wells, inspection panels, fuel tanks, …etc.
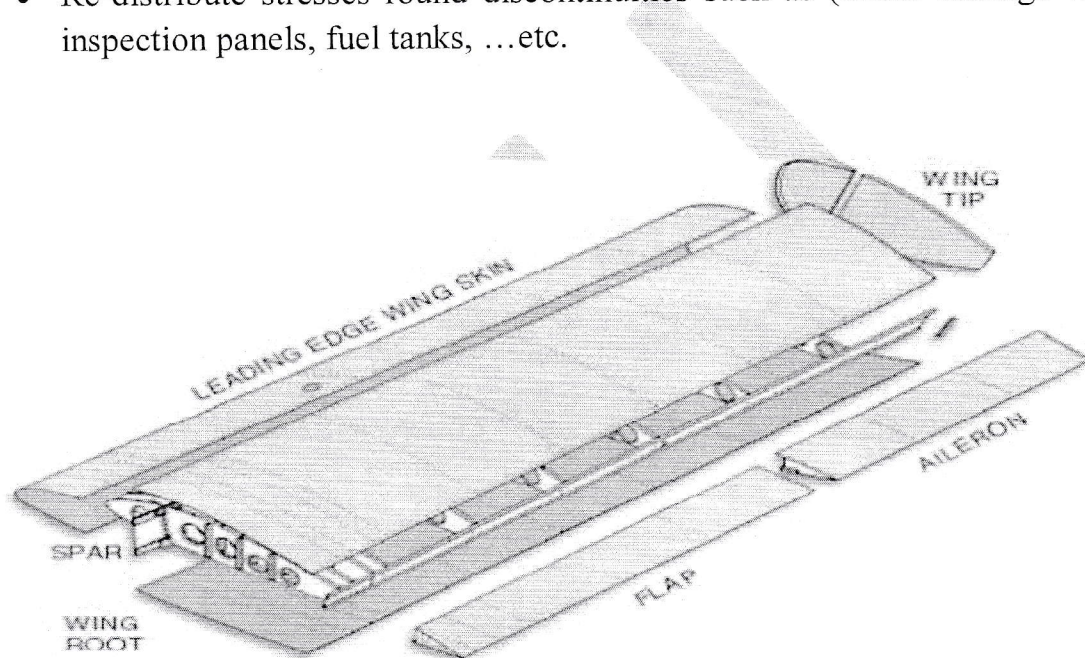
Fig. 1.7 The Wing structure
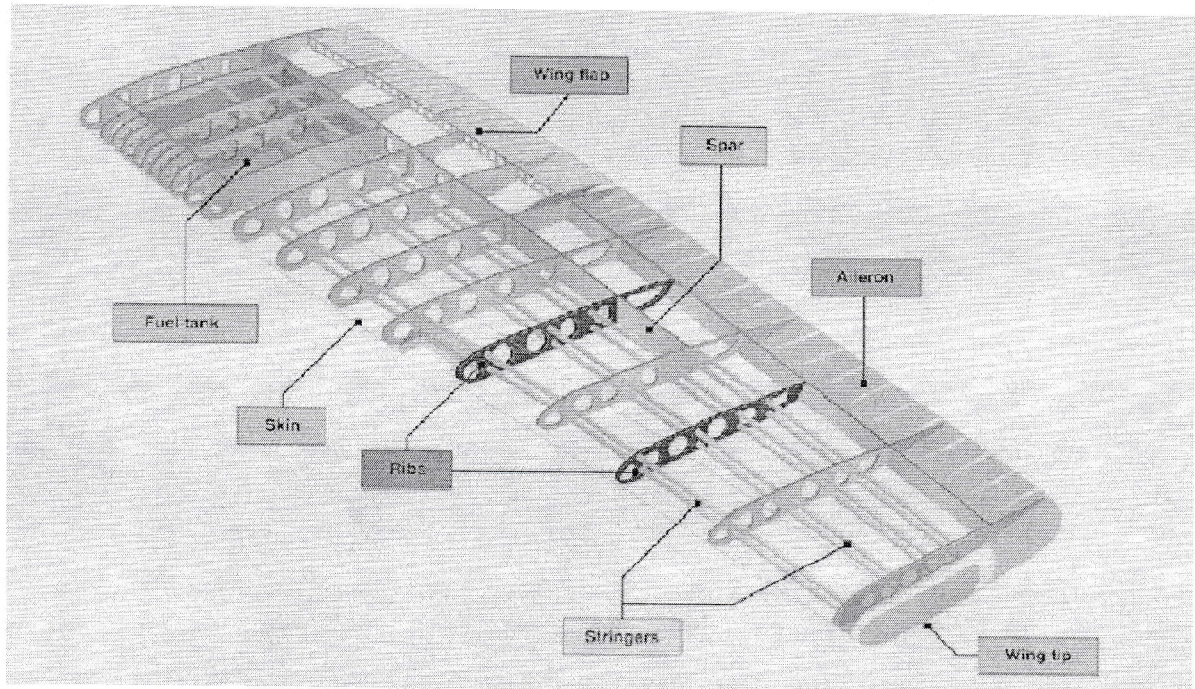
Fig. 1.8: A detailed wing structure

Spar It is used to transmit loads from wing structure to fuselage structure and it has other secondary jobs:

- Spar flanges hold axial and bending loads.
- Spar webs hold shear and torsion loads.
- Support the wing skin.
- To hold loads due to engine, fuel tanks, ...etc that attached to the wing, usually spars are made of Aluminum Alloys.
- Form the wing box for stable torsion resistance
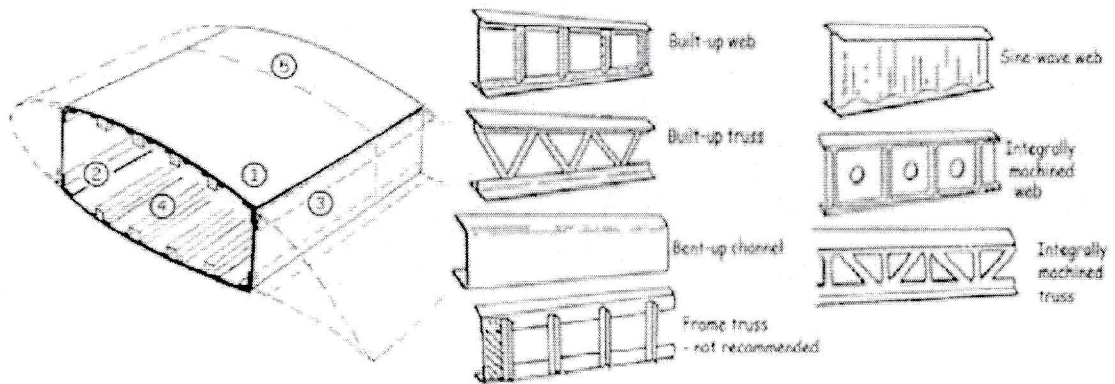
Fig. 1.9: A simplified wing strucure

Stiffener or Stringers

- Resist bending and axial loading along with the skin.
- Divide the skin into small panels and thereby increase its Buckling and failing stresses.
- Act with the skin in resisting axial loads caused by pressurization.

skin

stringers

Actual skin and web
carries axial and
shear stresses

(a)

Effective longitudinals
(axial stress only)

Idealized webs
(shear stress only)

Ribs

Rear spar

Stringer

Nose rib

Front spar

Ribs
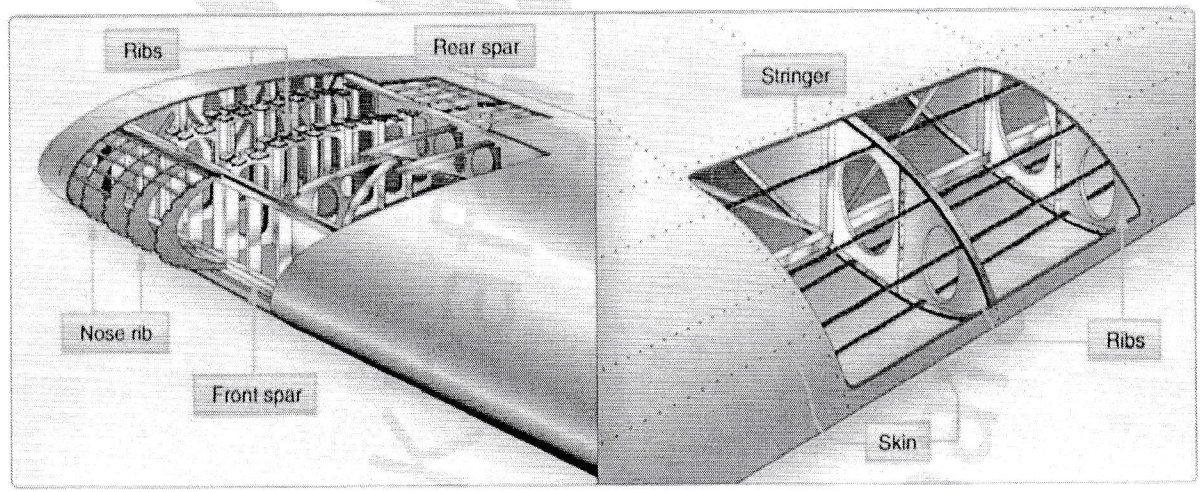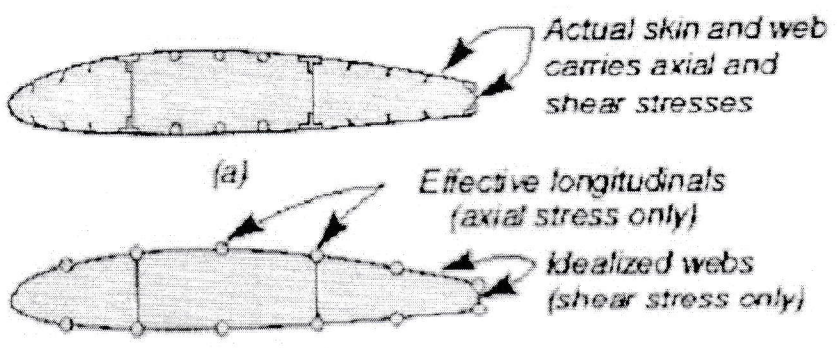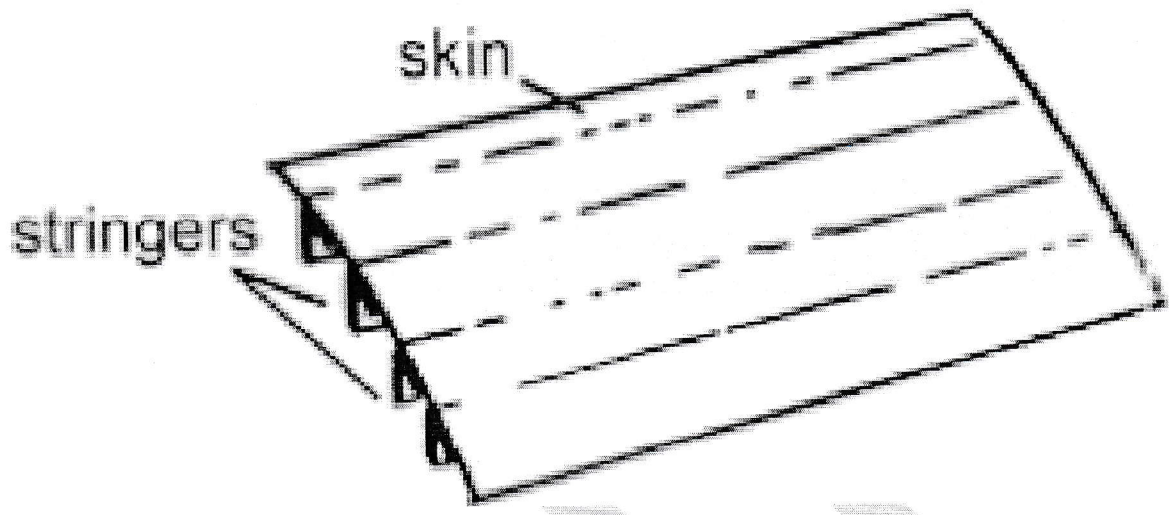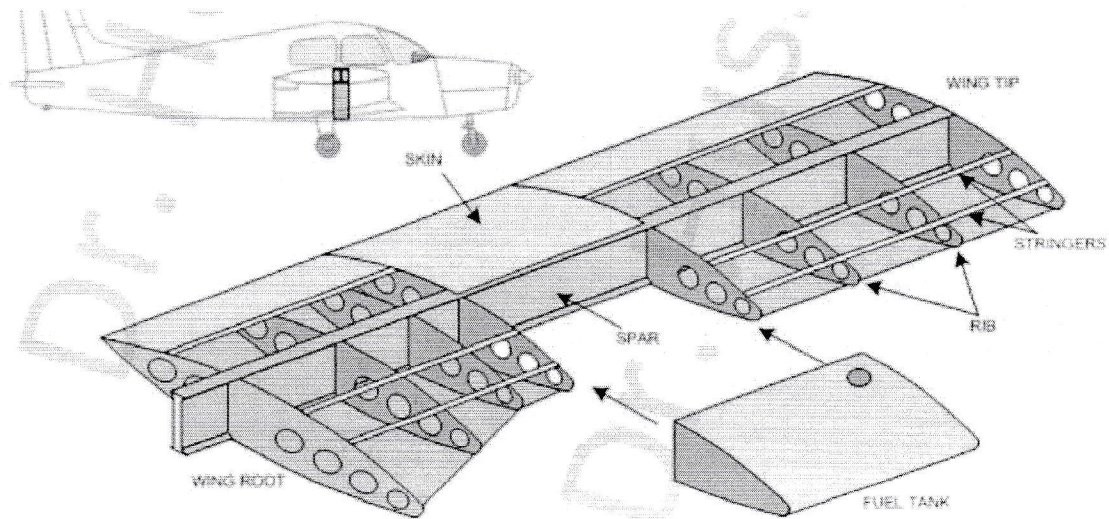
Skin

Modeling:

1. The behavior of these structural elements is often idealized to simplify the analysis of the assembled component

2. The webs (skin and spar webs) carry only shearing stresses.

3. The longitudinal elements carry only axial stress.

4. The transverse frames and ribs are rigid within their own.

5. The cross section is maintained unchanged during loading.

- ## For Fuselage

Skin: It is used to cover aircraft structure which is used to provide an aerodynamic shape and to protect passengers, pay load, systems, ..etc from environmental conditions encountered in flight skin. It is usually made of Aluminum alloys.

Frames (Rings): It is the transverse members in fuselage and I it extends across the complete cross section, it named **Bulkheads**.

It is unction is similar to wing ribs. It has a circular or semi-circular cross section. The most important differences arises in the case of pressurized aircraft where the

skin combines with frames and stringers to react the hoop and circumferential stresses respectively.

Longerons: They are longitudinal members reinforce the skin support primary bending loads. They are typically made o aluminum alloy either o a single and longerons together prevent tension and compression from bending the fuselage.

Stringers: They are used in the Semi-monocoque fuselage. Theses longitudinal members are typically more numerous and lighter in weight than the Longerons.

Stringers and Longerons together prevent tension and compression rom bending the fuselage. The fuselage section is bolted together through flanges round periphery, while wings and tail plane are attached to pick-up points on the relevant fuselage frames.

Frame   Longeron

Skin

Stringer   Bulkhead
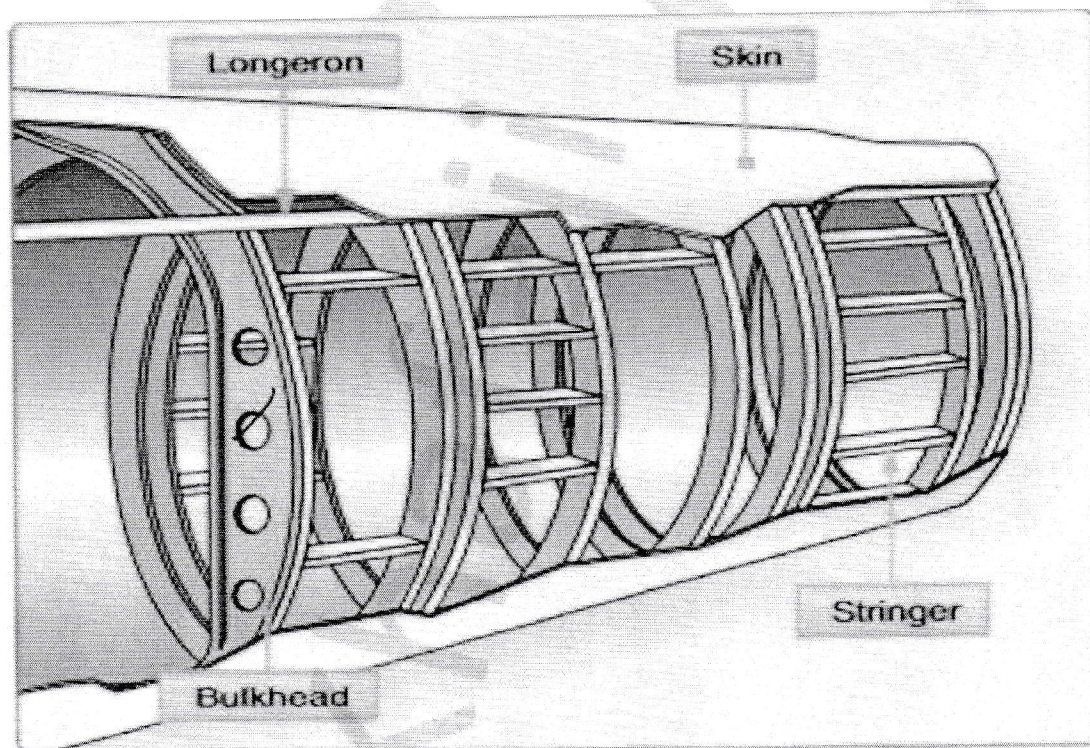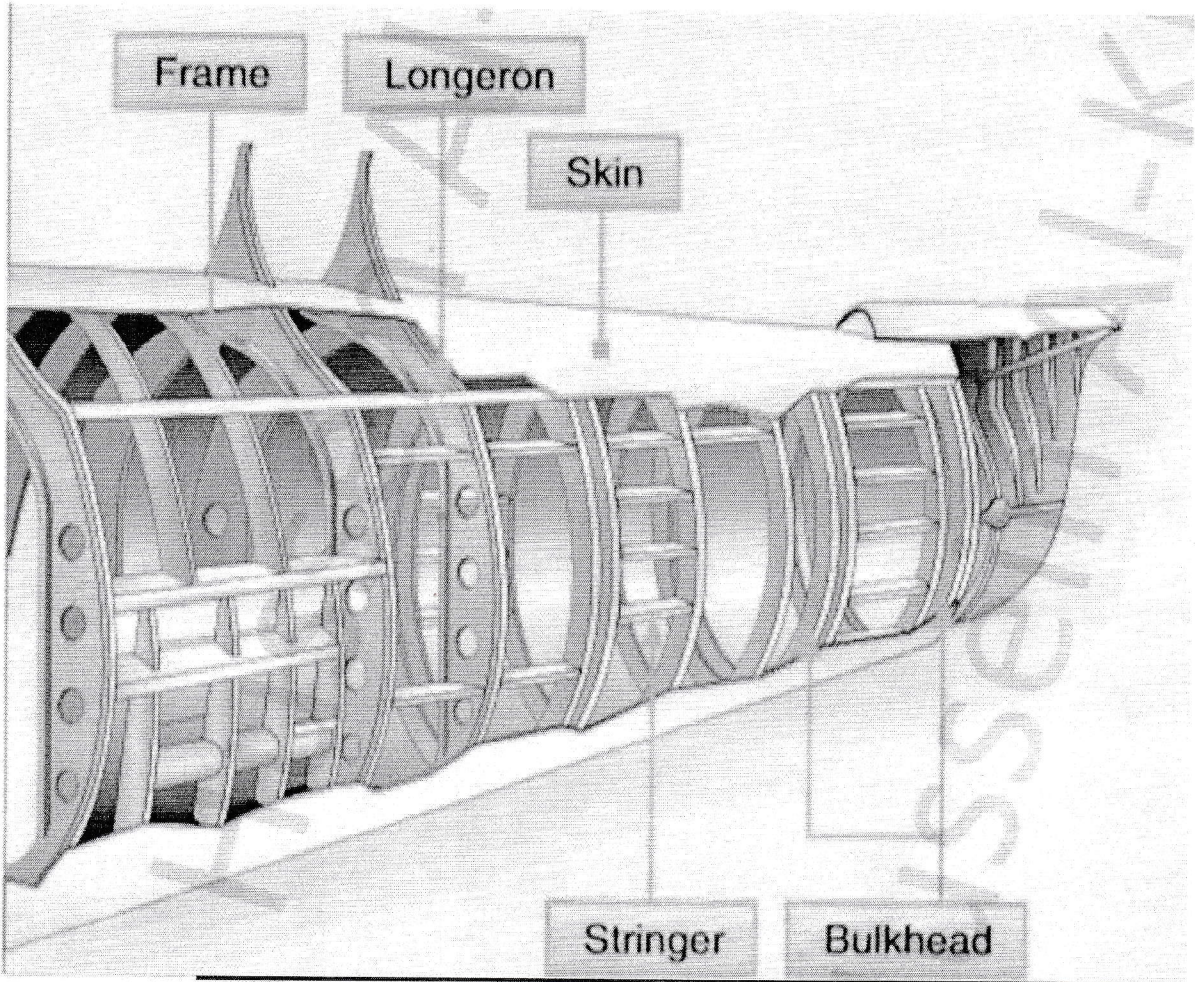
AL-Farahidi University /College of Technical Eng.
Aircraft Structure/ 4th Year
Chapter Two: Materials Used in A/C Structure

We shall discuss the materials used in aircraft construction. Several factors influence the selection of the structural material for an aircraft, but amongst these strength allied to lightness is probably the most important. **The   selection of the most suitable material for a given aircraft and engine parts will be governed by**:

- The function , size and shape of the part
- Required mechanical properties, strength, stiffness or rigidity, hardness and ductility, with particular consideration of the extreme temperature conditions liquid engines.
- Required physical and chemical properties, density, thermal conductivity, specific heat, and coefficient of expansion, poisons ratio, strength to weight ratio, corrosion resistance, and compatibility with propellants as function of temperature.
- Consideration to fabrication , such as forgeability, castability, weldability, machinability and formability
- Cost and availability
- Existing industry and government standards

Alloys

An alloy is composed of two or more metals. The metal present in the alloy in the largest amount is called the ***base metal***. All other metals added to the base metal are called ***alloying elements***. Adding the alloying elements may result in a change in the properties of the base metal. For example, **pure aluminum** is relatively **soft and weak**. However, adding small amounts or **copper, manganese, and magnesium** will increase aluminum's strength many times. **Alloys** are important to the aircraft industry. They provide materials with properties that pure metals do not possess
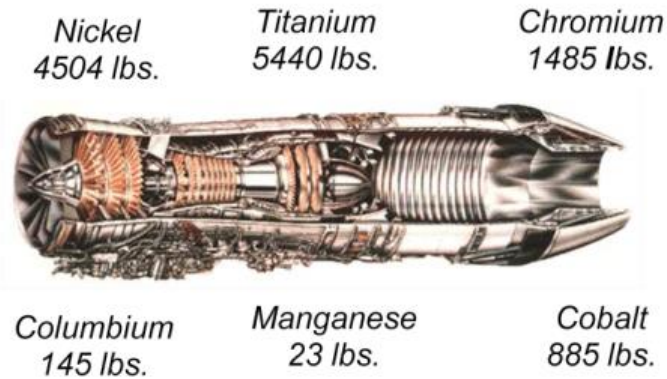
Nickel
4504 lbs.

Titanium
5440 lbs.

Chromium
1485 lbs.

Columbium
145 lbs.

Manganese
23 lbs.

Cobalt
885 lbs.

Figure -Whitney F-100 engine cutaway listing metallic elements required for manufacturing.

Aluminium Alloys

Pure aluminum is a relatively **low strength** extremely flexible metal with virtually no structural applications. However, when alloyed with other metals its properties are improved significantly. **Three groups of aluminum alloy** have been used in the aircraft industry for many years and still play a major role in aircraft construction.

In the first of this aluminum is alloyed with copper, magnesium, manganese, silicon and iron, and has a typical composition of 4% copper, 0.5% magnesium, 0.5% manganese, 0.3% silicon and 0.2% iron with the remainder being aluminum.

The second group of alloys contains, in addition to the above, 1–2% of nickel, a higher content of magnesium and possible variations in the amounts of copper, silicon and iron. The most important property of these alloys is their retention of strength at high temperatures which makes them particularly suitable for aero engine manufacture. A development of these alloys by **Rolls-Royce and High Duty** Alloys Ltd replaced some of the nickel by iron and reduced the copper content; were used in aero engines and airframes **The third group** of alloys depends upon the inclusion of zinc and magnesium for their high strength and has a typical composition of 2.5% copper, 5% zinc, 3% magnesium and up to 1% nickel with mechanical properties of 0.1% **proof stress** 510 N/mm2.

Alloys from each of the above groups have been used extensively for **airframes, skins and other stressed components**, the choice of alloy being influenced by factors such as **strength, ductility**, **ease of manufacture** (e.g. in extrusion and forging), **resistance to corrosion, fatigue strength, and resistance to fast crack propagation under load.**

The latest aluminum alloys to find general use in the aerospace industry are the aluminum–lithium alloys. Of these, the aluminum–lithium–copper–manganese alloy, developed in the UK, is extensively used in the main fuselage structure of Helicopters' design. **Aluminum–lithium alloys** can be successfully welded, possess high fracture toughness and exhibit a high resistance to crack propagation.

Steel

The use of **steel** for the manufacture of thin-walled, box-section spars in the 1930s has been superseded by the aluminum alloys described in section above. Clearly, its **high specific gravity** prevents its widespread use in aircraft construction, but it has retained some value as a material for **castings** for small components demanding high tensile strengths, high stiffness and high resistance to wear. Such components include **undercarriage pivot brackets, wing-root attachments**.

- High tensile strengths
- High stiffness
- High resistance to wear

Maraging Steels were developed in 1961, from which carbon is either eliminated entirely or present only in very small amounts. **The hardening** of maraging steels is achieved by the addition of other elements such as **nickel**, **cobalt** and **molybdenum**. Typical **Maraging Steel** would have these elements present in the proportions: nickel 17–19 per cent, cobalt 8–9 percent, molybdenum 3–3.5 per cent, with titanium 0.15–0.25 per cent. The **carbon content** would be a maximum of 0.03 per cent. It is 0.2 per cent **proof stress** would be nominally **1400N/mm2** and its **Modulus of Elasticity 180000N/mm2**. The main advantages of **Maraging** steels:

- Higher fracture toughness
- Simpler heat treatment
- Much lower volume change and distortion during hardening
- Very much simpler to weld and easier to machine
- Better resistance to stress corrosion/hydrogen embrittlement.

Maraging Steels have been used in: aircraft arrester hooks, rocket motor cases, helicopter undercarriages, gears, ejector seats and various structural forgings.

The use of **titanium alloys** increased significantly in the 1980s, particularly in the construction of **combat aircraft** as opposed to transport aircraft. **Titanium alloys** possess high specific properties, have a **good fatigue strength/tensile strength ratio with a distinct fatigue limit, and some retain considerable strength at temperatures up to 400–500∘C.** Generally, there is also a good resistance to corrosion and corrosion fatigue although properties are adversely affected by exposure to temperature and stress in a salt environment. **The disadvantages** are a relatively high density so that weight penalties are imposed if the alloy is extensively used, coupled with high primary and high fabrication costs, approximately seven times those of aluminum and steel. **Titanium alloys** were used in the airframe and engines of Concorde, while the Tornado wing carry-through box is fabricated from a wieldable medium strength titanium alloy. **Titanium alloys** are also used extensively in the F15 and F22 American fighter aircraft and are incorporated in the tail assembly of the Boeing 777 civil airliner. Other uses include forged components such as flap and undercarriage parts.

Composite Materials

Composite is material consisting of two or more materials, which have different physical and chemical properties combined together in a proper content and fashion to produce a new material properties that are different from the properties of those individual martials. **The main of the aircraft industries is to reduce weight keeping the same or more strength.**

Different types of composite materials are available in these days such as **fiber glass, Kevlar, and boron fibers** which is used in many industrial applications.

The fibres may be continuous or discontinuous but possess a strength very much greater than that of the same bulk materials. For example, carbon fibres have a tensile strength of the order of 2400 N/mm2 and a modulus of elasticity of 400 000 N/mm2. In the early stages of the development of composite materials glass fibres were used in a matrix of epoxy resin. This **glass-reinforced plastic** (**GRP**) was used for helicopter blades but found limited use in components of fixed wing aircraft due to its low stiffness.

In the 1960s, new fibrous reinforcements were introduced: **Kevlar** composites are tough but **poor in compression** and difficult to machine, so they were used in secondary structures. Another composite, using **Boron fiber** and developed in the USA, was the first to possess sufficient strength and stiffness for primary structures. These composites have now been replaced by carbon-fiber reinforced plastics (**CFRP**)

Typically; CFRP has a modulus of the order of three times that of **GRP**, one and a half times that of a Kevlar composite and twice that of aluminum alloy. Its strength is three times that of aluminum alloy, approximately the same as that of **GRP**, and slightly less than that of Kevlar composites. **CFRP** is included in the **wing, tail plane and forward fuselage** of the latest Harrier development, is used in **Jaguar wing**. The use of **CFRP** in the fabrication of **helicopter blades** has led to significant increases in their service life, where fatigue resistance rather than stiffness is of primary importance.
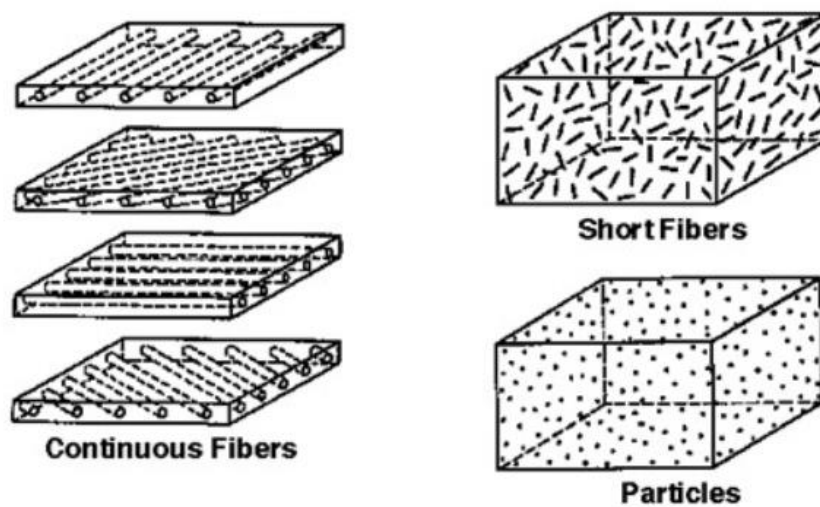
Figure. Composite Materials

Advantages of Composite Material
- High strength to weight ratio
- Fiber-to-fiber transfer of stress allowed by chemical bonding
- Modulus (stiffness to density ratio) 3.5 to 5 times that of steel or aluminum
- Longer life than metals
- Higher corrosion resistance
- Tensile strength 4 to 6 times that of steel or aluminum
- Greater design flexibility
- Bonded construction eliminates joints and fasteners
- Easily repairable

- It is a brittle material
- Does not yield plastically in regions of high stress concentration.
- Its strength is reduced by impact damage which may not be visible.
- Further, the properties of CFRP are subject to more random variation than those of metals.
- Delamination of layers
- High cost

Application of Composite in Aircraft

- Fuselage (bulkhead)
- Wing flap
- Rudder
- Elevator
- Spoilers
- Floor beams and panels

Figure. Materials used in 787 body

Properties of Metals

This section was used to describe various properties and characteristics of metals used in the aircraft industry

Hardness

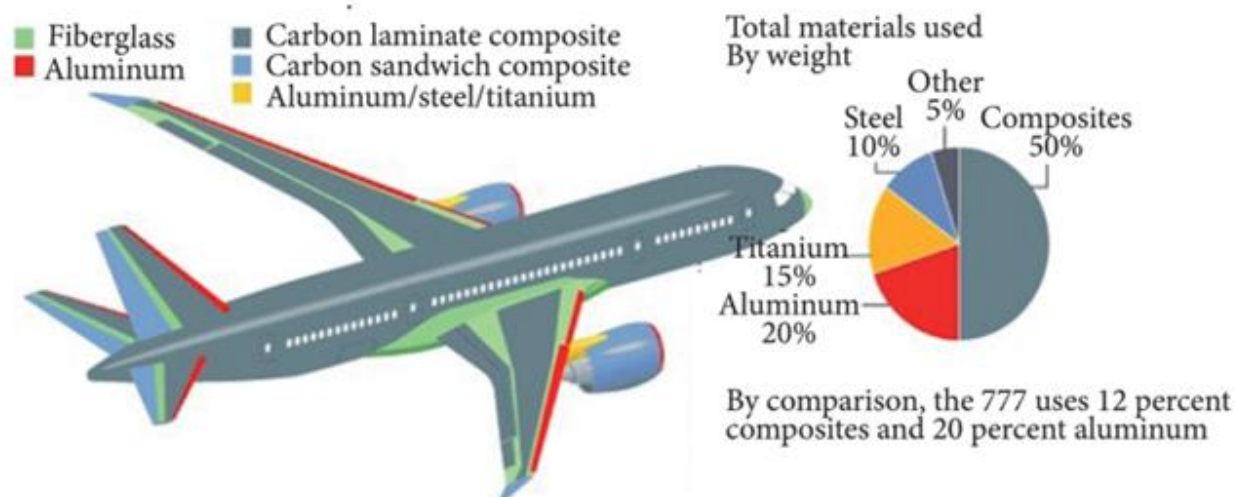**Hardnes**s refers to the ability of a material to resist abrasion, penetration, cutting action, or permanent distortion. **Hardness** may be increased by cold working the metal and, in the case of steel and certain aluminum alloys, by **heat treatment. Hardness and strength** are closely associated properties of metals.

Strength

One of the most important properties of a material is **strength**. Strength is the ability of a material to resist deformation. **Strength** is also the ability of a material to resist stress without breaking.

Density

Density is the weight of a unit volume of a material. In aircraft work, the specified weight of a material per cubic inch is preferred. **Density** is an important consideration when choosing a material to be used in the design of a part in order to maintain the proper weight and balance of the aircraft.

Malleability

A metal which can be **hammered, rolled, or pressed** into various shapes without cracking, breaking, or leaving some other detrimental effect, is said to be **malleable**. This property is necessary in sheet metal that is worked into curved shapes, such as cowlings, fairings, or wingtips. **Copper** is an example of a **malleable** metal.

Ductility

Ductility is the property of a metal which permits it to be permanently **drawn, bent, or twisted** into various shapes without breaking. This property is essential for metals used in making wire and tubing. **Ductile** metals are greatly preferred for aircraft use because of their ease of forming and resistance to failure under shock loads. For this reason, **aluminum alloys** are used for cowlings; fuselage and wing skin, and formed or extruded parts, such as ribs, spars, and bulkheads. **Chrome molybdenum steel** is also easily formed into desired shapes.

Elasticity

Elasticity is that property that enables a metal to return to its original **size and shape** when the force which causes the change of shape is removed. This property is extremely valuable because it would be highly undesirable to have a part permanently distorted after an applied load was removed. Each metal has a point known as the **elastic limit**, beyond which it cannot be loaded without causing permanent distortion. **In aircraft** construction, members and parts are so designed that the maximum loads to which they are subjected will not stress them beyond their **elastic limits**.

Toughness

A material which possesses **toughness** will withstand **tearing or shearing** and may be stretched or otherwise deformed without breaking. **Toughness** is a desirable property in aircraft metals.

Brittleness

Brittleness is the property of a metal which allows little **bending or deformation** without shattering. A **brittle** metal is apt to break or crack without change of shape. Because structural metals are often subjected to shock loads, **brittleness** is not a very desirable property. **Cast iron, cast aluminum**, and very hard steel are examples of **brittle metals**.

Conductivity

Conductivity is the property which enables a metal to carry **heat or electricity**. The heat conductivity of a metal is especially important in **welding** because it governs the amount of heat that will be required for proper fusion. **In aircraft**, electrical **conductivity** must also be considered in conjunction with bonding, to eliminate radio interference.

Thermal Expansion

Thermal expansion refers to **contraction and expansion** that are reactions produced in metals as the result of heating or cooling. Heat applied to a metal will cause it to expand or become larger. **Cooling and heating** affect the design of welding, castings, and tolerances necessary for hot rolled material.

Isotropic Material

In many materials the **elastic properties** are the same in all directions at each point in the material although they may vary from point to point, such a material is

known as **isotropic**. An isotropic material having the same properties at all points is known as **homogeneous**.

<mark>Anisotropic Materials</mark>

Materials having varying **elastic properties** in different directions are known as **anisotropic**

<mark>Orthotropic Materials</mark>

Orthotropic materials mean **different elastic properties** in different directions. A material whose elastic properties are limited to **three different** values in three mutually perpendicular directions is known as **orthotropic.**

Bending of Open and Closed Thin-Walled Beams

Bending is the combination of **compressive and tensile stresses**. When an A/C is in Flight, when will generate the **lift force** which will cause **bending** effect in the **wing.**

If the **bending** is taking place in the plane of loading it is called a **symmetrical bending**. Other than plane of loading it is called **unsymmetrical bending**. Two cases for unsymmetrical bending;

- Unsymmetrical section will always have unsymmetrical bending.
- Symmetrical section when subjected loading other than in the line of symmetry.
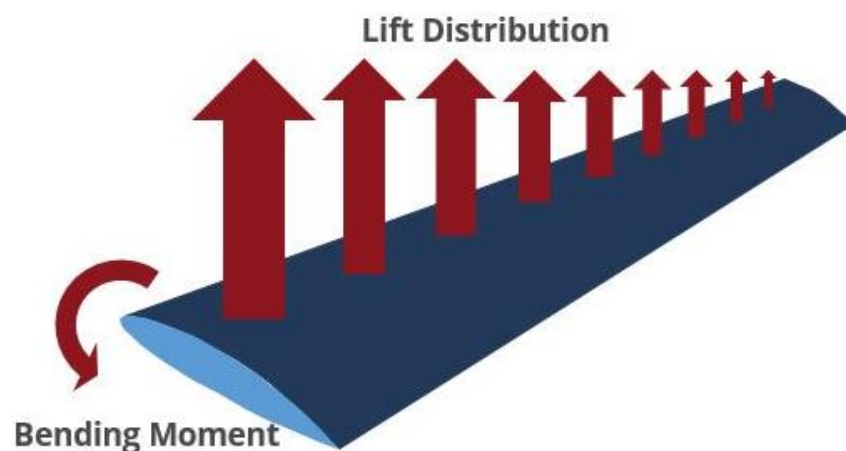
Assumptions made in the theory of pure bending;

- Beam is assumed to be initially **straight**
- Material is **homogenous and isotropic**
- The stress induced is proportional to the strain and at no place, the stress exceed the **elastic limit**

- The value of **modulus of elasticity** is same for the fibers of the beam under **compression or under tension**
- The transverse section of the beam which is plane before bending **remains plane after bending**
- Elongation above particular axis is **proportional to distance** from particular axis.

3.1 Calculation of A/C Section Properties

Center of gravity (centroid of):

It is a point in a body where the resultant gravity force is acted through. This resultant force is equal to the sum of weights (w_i) of all elements of the body, then:

$$\bar{x} = \frac{\sum x.w}{\sum w} \qquad \qquad \bar{y} = \frac{\sum y.w}{\sum w}$$

Centroid of area:

For plate of uniform thickness and density lies in xy plane:

$$\bar{x} = \frac{\sum x.A_i}{\sum A_i} \qquad \qquad \bar{y} = \frac{\sum y.A_i}{\sum A_i}$$

Where; A_i is the area of each element.

Centroid of wing cross section

It is the centroid of this cross section area and it is evaluated after accomplishment of structural idealization for this cross section.

Second moments of area of standard sections

- Second Moment of area

$$I_{xx} = \int y^2 \, dA \qquad \text{Moment of inertia of cross section about x- axis.}$$
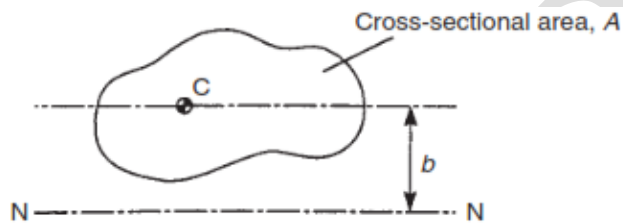
$$I_{yy} = \int x^2 \, dA \qquad \text{Moment of inertia of cross section about y-axis.}$$

$I_{xy} = \int x.y \, dA$ Product moment of inertia of cross section.

- Parallel axes theorem:

Suppose that the second moment of area, I_c , about an axis through its centroid C is known. The second moment of area, I_N , about a parallel axis, NN, a distance b from the centroidal axis is then given by

$$I_N = I_c + Ab^2$$

Cross-sectional area, A

Neutral axis:

It is an axis passing through the centroid of cross section. The bending moments Mx and M$_y$ about it produce zero direct stress in all the points on it.

Principle axes:

Two perpendicular axes a bout which product moment of area is zero ($I_{xy} = 0$), and the two other moments, I_{xx} and I_{yy} , are either maximum or minimum for example it I_{xx} is maximum about one axis , I_{yy} is minimum about this axis, and I_{xx} will be minimum about the other axis, while I_{yy} become maximum. If either x-axis or y-axis is coincided with principle axis then $I_{xy} = 0$ also.

Elastic axis:

It is an axis for the wing about which rotation will occur when the wing is loaded in pure torsion. It is important for flutter analysis of the wing.

Shear center:

It is a point in the wing cross section at which the resultant shear load must act to produce a wing deflection with no rotation (twist).

Shear centers for all wing sections must lie on the elastic axis of the wing, about this is not true because skin wrinkles and becomes ineffective in resisting compression loads. For

practical purpose the elastic axis may be assumed to coincide with line joining the shear centers for all wing sections.

3.2 Bending moments and bending stresses

Resolution of bending moments:

A bending moment M applied in any longitudinal plane parallel to the z- axis may be resolved into components M_x and M_y by the normal rules of vectors.

M_x and M_y are positive when the induced tension in the positive xy quadrant of the beam cross-section.
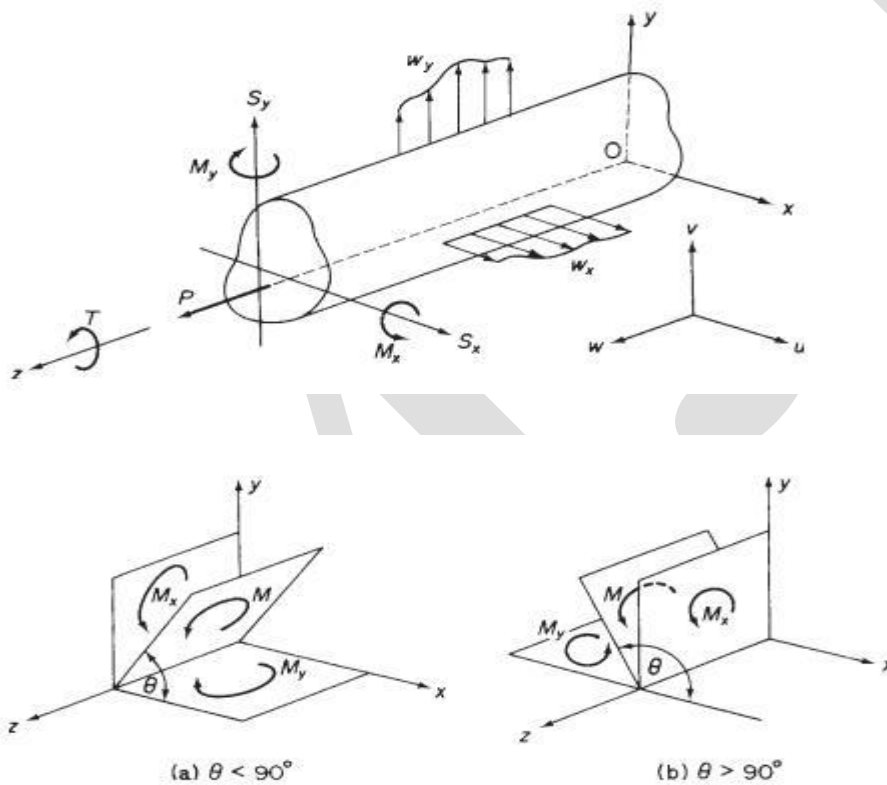
(a) $\theta < 90°$ (b) $\theta > 90°$

Bending moment M applied in any longitudinal plane parallel to the z-axis may be resolved into components M_x and M_y.

$$M_x = M \sin \theta \qquad \text{and} \qquad M_y = M \cos \theta$$

For positive M,

if $\theta < \pi/2$ M_x is +ve and M_y is +ve

33

If $\theta > \pi/2$ $\qquad\qquad$ M_x is +ve $\quad$ and $\quad$ M_y is -ve

Direct stress distribution due to bending:
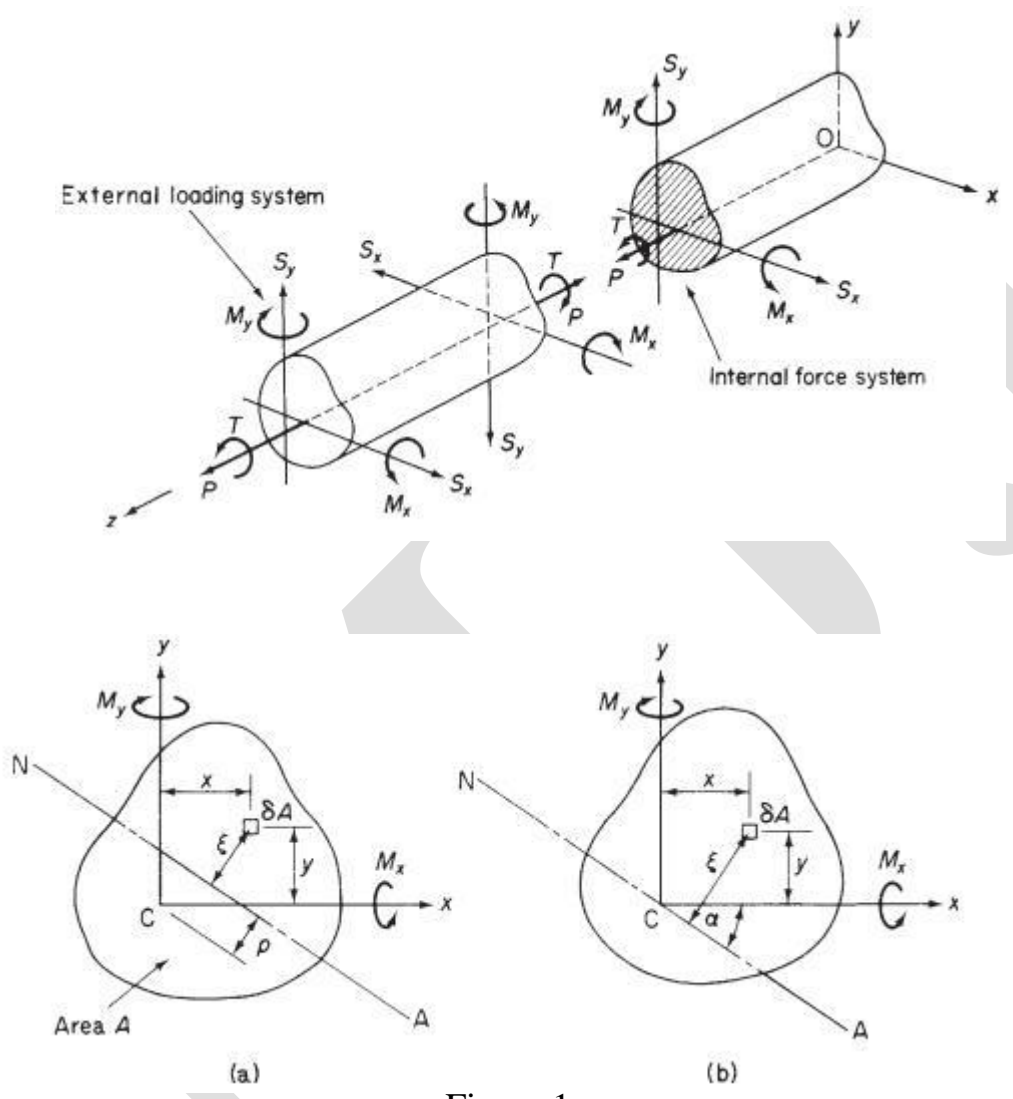

Figure 1

C is the centroid, N.A. is neutral axes.

Origin of axes is coincide with the centroid C, (ξ) is the distance from element (δA) to N.A.

From Hooke's low

$\sigma_z = E\varepsilon_z$

If the beam is bent to a radius of curvature ρ about neutral axis at this particular section and since plane sections are assumed to remain plane after bending, then:

$$\varepsilon_z = \frac{Change\ in\ length}{orginal\ length}$$

$$\varepsilon_z = \frac{(\rho+\xi)\theta-\rho\theta}{\rho\theta} \qquad \Rightarrow \qquad \varepsilon_z = \frac{\xi}{\rho}$$

$$\sigma_z = E\varepsilon_z \qquad \Rightarrow \qquad \sigma_z = \frac{E\,\xi}{\rho}$$
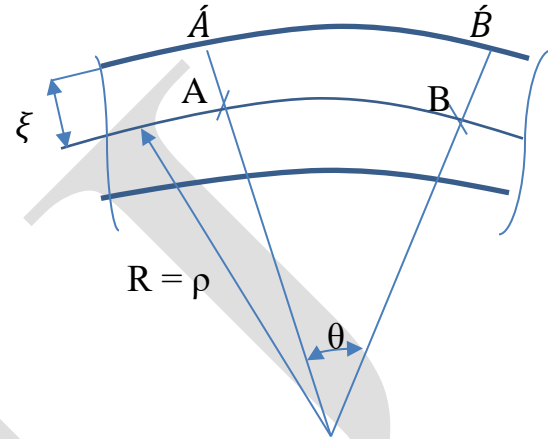
The beam supports pure bending moments so that the resultant end load on any section must be zero.

$$\int_A \sigma_z\, dA = 0$$

$$\int_A \frac{E\xi}{\rho}\, dA = 0 \qquad \rightarrow \qquad \int_A \zeta\, dA = 0$$

(E/ ρ) is constant and has been canceled. It follows that the N.A. passes through the centroid see figure b.

Suppose that N.A. is inclined to C_x by angle α, then

$$\xi = x \sin\alpha + y \cos\alpha$$

$$\sigma_z = \frac{E\,\xi}{\rho} \qquad \rightarrow \qquad \sigma_z = \frac{E}{\rho}(x \sin\alpha + y \cos\alpha) \tag{3.1}$$

The moment resultants of the internal direct stress distributions have the same sense as the applied moments (M_x) and (M_y). Thus

$$M_x = \int_A \sigma_z \, y \; dA \qquad \text{and} \qquad M_y = \int_A \sigma_z \, x \; dA$$

Substitute for σ_z from Equation (i)

$$M_x = \int_A \frac{E}{\rho} (x\,y\,sinx + y^2 cosx) \; dA$$

$$I_{xx} = \int_A y^2 \, dA, \quad I_{yy} = \int_A x^2 \, dA, \quad I_{xy} = \int_A xy \, dA$$

$$M_x = \frac{E}{\rho} \sin\alpha \; I_{xy} + \frac{E}{\rho} \cos\alpha \; I_{xx} \qquad M_y = \frac{E}{\rho} \sin\alpha \; I_{yy} + \frac{E}{\rho} \cos\alpha \; I_{xy}$$

$$Now \text{ let } \quad A = \frac{E}{\rho} \sin\alpha \qquad \text{and} \qquad B = \frac{E}{\rho} \cos\alpha$$

$$M_x = A\, I_{xy} + B\, I_{xx} \tag{3,2}$$

$$M_y = A\, I_{yy} + B\, I_{xy} \tag{3.3}$$

Solving these two equations (3.2) and (3.3) gives:

$$A = \frac{M_y\, I_{xx} - M_x\, I_{xy}}{I_{xx}\, I_{yy} - I^2_{xy}} \qquad\qquad B = \frac{M_x\, I_{yy} - M_y\, I_{xy}}{I_{xx}\, I_{yy} - I^2_{xy}}$$

Then $\quad \sigma_z = A.x + B.y$

$$\boxed{\sigma_z = \left(\frac{M_y\, I_{xx} - M_x\, I_{xy}}{I_{xx}\, I_{yy} - I^2_{xy}} \right).x + \left(\frac{M_x\, I_{yy} - M_y\, I_{xy}}{I_{xx}\, I_{yy} - I^2_{xy}} \right).y}$$

$$\boxed{\sigma_z = \frac{\overline{M_x}}{I_{xx}}y + \frac{\overline{M_y}}{I_{yy}}x}$$

Where $\overline{M_x}$ and $\overline{M_y}$ are effective bending moment,

$$\boxed{\overline{M}_x = \left(\frac{M_x - M_y\, I_{xy}/\,I_{yy}}{1 - I^2_{xy}/\,I_{xx}\,I_{yy}}\right) \qquad \overline{M}_y = \left(\frac{M_y - M_x\, I_{xy}/\,I_{xx}}{1 - I^2_{xy}/\,I_{xx}\,I_{yy}}\right)}$$

Note: if either C_x or C_y is axis of symmetry or both, then $\mathbf{I_{xy}}$ **is zero** and that axis is principal axis and

$$\overline{M}_x = M_x \qquad \text{and} \qquad \overline{M}_y = M_y$$

$$\boxed{\sigma_z = \frac{M_x}{I_{xx}} . y + \frac{M_y}{I_{yy}} . x}$$

Further if either **M_x or M_y is zero** then $\quad \sigma = \frac{M_x}{I_{xx}} . y \qquad$ or $\qquad \sigma = \frac{M_y}{I_{yy}} . x$

Which is the result of simple engineering theory of bending for beams having at least singly symmetrical cross section.

M_x and M_y are pure bending moment about x-axis and y-axis respectively.{if shear loads S_x and S_y are acted on any section then they will produce bending moment on the next section.

Position of the neutral axis

At all points on the neutral axis the direct stress is zero by definition.

Therefore:

$$\sigma_z = \frac{\overline{M_x}}{I_{xx}}y + \frac{\overline{M_y}}{I_{vv}}x \quad \Longrightarrow \quad 0 = \frac{\overline{M_x}}{I_{xx}}y + \frac{\overline{M_y}}{I_{vv}}x$$

$$0 = \left(\frac{M_y I_{xx} - M_x I_{xy}}{I_{xx} I_{yy} - I_{xy}^2} \right) x_{NA} + \left(\frac{M_x I_{yy} - M_y I_{xy}}{I_{xx} I_{yy} - I_{xy}^2} \right) y_{NA}$$

Where $x_{N.A.}$ and $y_{N.A.}$ are coordinates of points on the neutral axis. Hence
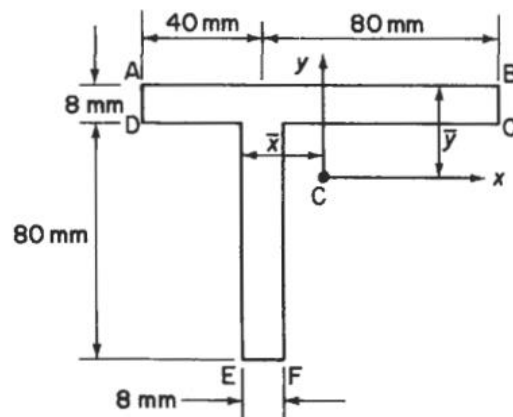
$$\boxed{\frac{y_{NA}}{x_{NA}} = -\frac{M_y I_{xx} - M_x I_{xy}}{M_x I_{yy} - M_y I_{xy}}}$$

Or from figure 1 (b)

$$\boxed{\tan \alpha = \frac{M_y I_{xx} - M_x I_{xy}}{M_x I_{yy} - M_y I_{xy}}}$$

Example:

A beam having the cross-section   is subjected to a bending moment of 1500 N m in a vertical plane. Calculate the maximum direct stress due to bending stating the point at which it acts.

The position of the centroid of the section may be found by taking moments of   areas about some convenient point. Thus

$$(120 \times 8 + 80 \times 8)\bar{y} = 120 \times 8 \times 4 + 80 \times 8 \times 48$$

 Giving $\qquad\qquad\qquad \bar{y} = 21.6\ mm$

And

$$(120 \times 8 + 80 \times 8)\bar{x} = 80 \times 8 \times 4 + 120 \times 8 \times 24$$

Giving $\qquad \bar{x} = 16 \; mm$

The next step is to calculate the section properties referred to axes Cxy. Hence

$$I_{xx} = \frac{120 \times (8)^3}{12} + 120 \times 8 \times (17.6)^2 + \frac{8 \times (80)^3}{12} + 80 \times 8 \times (26.4)^2$$

$$= 1.09 \times 10^6 \; mm^4$$

$$I_{yy} = \frac{8 \times (120)^3}{12} + 120 \times 8 \times (8)^2 + \frac{80 \times (8)^3}{12} + 80 \times 8 \times (12)^2$$

$$= 1.31 \times 10^6 \; mm^4$$

$$I_{xy} = 120 \times 8 \times 8 \times 17.6 + 80 \times 8 \times (-12) \times (-26.4)$$

$$= 0.34 \times 10^6 \; mm^4$$

By inspection of Eq. (i) the σ_z will be a maximum at point F where

$$x = \quad 8mm \quad , y = -66.4 \; mm$$

Since $M_x = 1500 \, \text{N m}$ and $M_y = 0$

$$\sigma_z = 1.5y - 0.39x \qquad\qquad\qquad (i)$$

Thus $\qquad\qquad \sigma_{z,max} = -96 \; N/mm^2 \qquad$ (compressive)

. **A** horizontal **cantilever 2m long** is constructed from the **Z-section** shown in Figure below **A** load of **10** kN is applied to the end of the cantilever at an angle of **60°** to the horizontal as shown. Assuming that no twisting moment is applied to the section, determine the **stresses at points** *A* and *B*. ($I_{xx} = 48.3 * 10^6 m^4$, $I_{yy} = 4.4 * 10^6 m^4$. **All dimensions are in mm)**
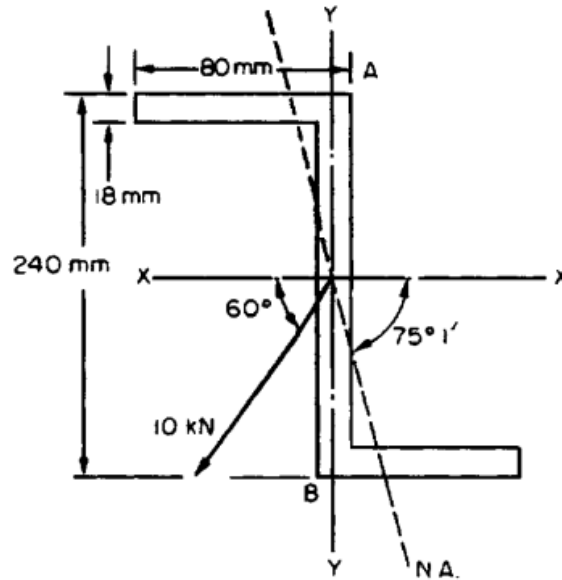
Solution

For this section I_{xy} for the web is zero since its centroid lies on both axes and hence $\bar{x}$ and $\bar{y}$ are both zero. The contributions to I_{xy} of the other two portions will be negative since in both cases either $\bar{x}$ or $\bar{y}$ is negative.

∴
$$I_{xy} = -2(80 \times 18)(40 - 9)(120 - 9)10^{-12}$$
$$= -9.91 \times 10^{-6} \ m^4$$

Now, at the built-in end,

$$M_x = +10\,000 \sin 60° \times 2 = +17\,320 \ \text{Nm}$$
$$M_y = -10\,000 \cos 60° \times 2 = -10\,000 \ \text{Nm}$$

$$17\,320 = AI_{xy} + \hat{B}I_{xx} = (-9.91A + 48.3B)10^{-6}$$
$$-10\,000 = -AI_{yy} - BI_{xy} = (-4.4A + 9.91B)10^{-6}$$

∴
$$1.732 \times 10^{10} = -9.91A + 48.3B \tag{1}$$
$$-1 \times 10^{10} = -4.4A + 9.91B \tag{2}$$

40

$$1.769 \times 10^{10} = 11.54\textsf{\scriptsize(}$$

$$\therefore \qquad\qquad B = 1533 \times 10^6$$

and substituting in (2) gives

$$A = 5725 \times 10^6$$

The inclination of the N.A. relative to the X axis is then given by

$$\tan \alpha_{N.A.} = -\frac{A}{B} = -\frac{5725}{1533} = -3.735$$

$$\alpha_{N.A.} = \mathbf{-75°1'}$$

This has been added and indicates that the points A and B are on either side of the N.A. and equidistant from it. Stresses at A and B are therefore of equal magnitude but opposite sign.

Now

$$\sigma = Ax + By$$

$\therefore \qquad$ stress at $A = 5725 \times 10^6 \times 9 \times 10^{-3} + 1533 \times 10^6 \times 120 \times 10^{-3}$

$$= \mathbf{235 \ MN/m^2 \ (tensile)}$$

Similarly,

$$\text{stress at } B = \mathbf{235 \ MN/m^2 \ (compressive)}$$

The section of a **thick beam** has the dimensions shown in Figure below. Calculate the **section properties I_{xx}, I_{yy} and I_{xy}** referred to horizontal and vertical axes through the **centroid of the section**. Determine also the **direct stress** at the point **A** due to a bending moment $M\ y= 55$ N m.
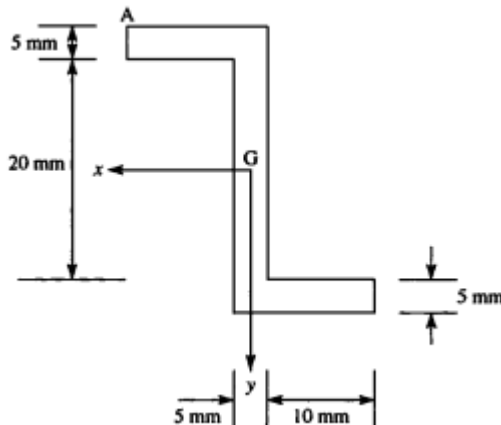
The maximum bending moment experienced by the T-section is 30 kNm The beam is arranged as a cantilever of 3 m long (see Figure) You are required to

1 Calculate I_{xx}, I_{yy} and I_{xy},

2 Determine the values of the maximum tensile and compressive stresses,

3 Determine the location of the maximum bending stress, and The thickness is the same for the flange and the web, t = 10 mm

Dimensions are in millimetres

3.3 General case of loading

Consider the element shown, where

δz : element of length in z-direction.

S_y : shear load in y-direction.

M_x : bending moment about x-axis.

w_y : distributed load of varying intensity.

As the element length is small, then the intensity is assumed constant.

(M_x) and S_y are +ve in the direction shown.

There for, for equilibrium of the element in the y direction

$$\left(S_y + \frac{\partial S_y}{\partial z}\delta z\right) + w_y\delta z - S_y = 0$$

From which,

$$w_y = -\frac{\partial S_y}{\partial z}$$

Taking moments about A

$$\left(M_x + \frac{\partial M_x}{\partial z}\delta z\right) - \left(S_y + \frac{\partial S_y}{\partial z}\delta z\right)\delta z - w_y\frac{(\delta z)^2}{2} - M_x = 0$$

Or , when second order terms are neglected,

$$S_y = \frac{\partial M_x}{\partial z}$$

Combine these results into a single expression

$$-w_y = \frac{\partial S_y}{\partial z} = \frac{\partial^2 M_x}{\partial z^2}$$

Similarly for loads in the xz plane

$$-w_x = \frac{\partial S_x}{\partial z} = \frac{\partial^2 M_y}{\partial z^2}$$

If it assumed that a parameter $\bar{S}_y$ bears the same relationship to $\bar{M}_x$ as S_y does to M_x then

$$\overline{S_y} = \frac{\partial \overline{M_x}}{\partial z} = \frac{\partial M_x/\partial z - (\partial M_y/\partial z)I_{xy}/I_{yy}}{1 - I_{xy}^2/I_{xx}I_{yy}}$$

$$\boxed{\overline{S_y} = \frac{S_y - S_x I_{xy}/I_{yy}}{1 - I_{xy}^2/I_{xx}I_{yy}}}$$

In similar fashion

$$\boxed{\overline{S_x} = \frac{S_x - S_y I_{xy}/I_{xx}}{1 - I_{xy}^2/I_{xx}I_{yy}}}$$

Parameters $\bar{w}_y$ and $\bar{w}_x$ are related to load intensities $\bar{w}_y$ and $\bar{w}_x$.

$$\boxed{\overline{w_x} = \frac{w_x - w_y I_{xy}/I_{xx}}{1 - I_{xy}^2/I_{xx}I_{yy}} \quad \text{and} \quad \overline{w_y} = \frac{w_y - w_x I_{xy}/I_{yy}}{1 - I_{xy}^2/I_{xx}I_{yy}}}$$

The parameters $\bar{M}_x, \bar{M}_y, \bar{S}_x, \bar{S}_y, \bar{w}_x, \bar{w}_y$ are often termed "effective" bending moments, shear forces and load intensities.

3.4 Approximations for thin-walled sections

We may exploit the thin-walled nature of aircraft structures to make simplifying **assumptions** in the determination of stresses and deflections produced by bending. Thus, the **thickness t of thin-walled** sections is assumed to be small compared with their cross-sectional dimensions so that **stresses** may be regarded as being constant across the thickness. Furthermore, **neglect squares** and higher powers of **t** in the computation of sectional properties and take the section to be represented by the **mid-line of its wall.**

Moment of inertia

Moment of inertia is the one of the important sectional properties which gives the details about resistance to **Bending** of a section. Thin walled section is used in airframe structure to withstand the **Torsion as wall as Bending Loads**. Thin walled section also provides weight advantages for airframe designers. As an illustration of the procedure, consider the **channel section** as shown in figure below.

(a)   (b)
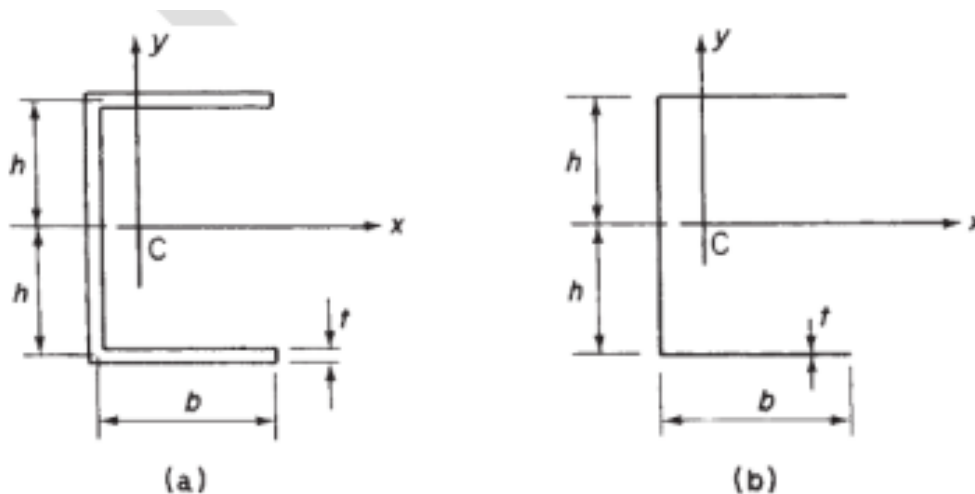
The section is singly symmetric about the x **axis** so that:

$$I_{xy} = 0$$

The second moment of area is $I_{xx} =$ then given by:

$$I_{xx} = 2\left[\frac{(b+t/2)t^3}{12} + \left(b + \frac{t}{2}\right)th^2\right] + t\frac{[2(h-t/2)]^3}{12}$$

Expanding the cubed term to be
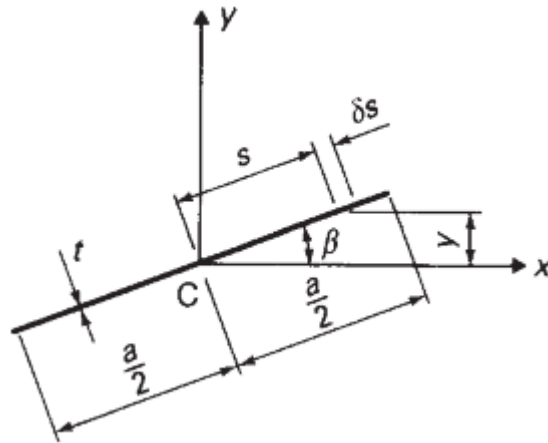
$$I_{xx} = 2\left[\frac{(b+t/2)t^3}{12} + \left(b + \frac{t}{2}\right)th^2\right] + \frac{t}{12}\left[(2)^3\left(h^3 - 3h^2\frac{t}{2} + 3h\frac{t^2}{4} - \frac{t^3}{8}\right)\right]$$

Which reduces, after powers of **t²** and **upwards** are **ignored** to

$$I_{xx} = 2bth^2 + t\frac{(2h)^3}{12}$$

The second moment of area of the section about C_y is obtained in a similar manner.

Thin- walled sections frequently have inclined or curved walls which complicated the calculation of section properties.

Consider the inclined thin section of figure below. Its second moment of area about a horizontal axis through its centroid is given by

$$I_{xx} = 2\int_0^{a/2} t\,y^2\,ds \;=\; 2\int_0^{a/2} t(\,s\,\sin\beta)^2\,ds$$

From which
$$I_{xx} = \frac{a^3 t \sin^2\beta}{12}$$

Similarly
$$I_{yy} = \frac{a^3 t \cos^2\beta}{12}$$

The product second moment of area is:

$$I_{xy} = 2\int_0^{a/2} t\,xy\,ds \;=\; 2\int_0^{a/2} t(\,s\,\cos\beta)\,(\,s\,\sin\beta)\,ds$$

Which gives
$$I_{xy} = \frac{a^3 t\,\sin 2\beta}{24}$$

It could be note here that expressions are approximate in that their derivation neglects power of t^2 and upwards by ignoring the second moments of area of the element δs about axes through its own centroid.

Properties of thin-walled curved sections are found in a similar manner. Thus, I_{xx} for semicircular section of figure below.
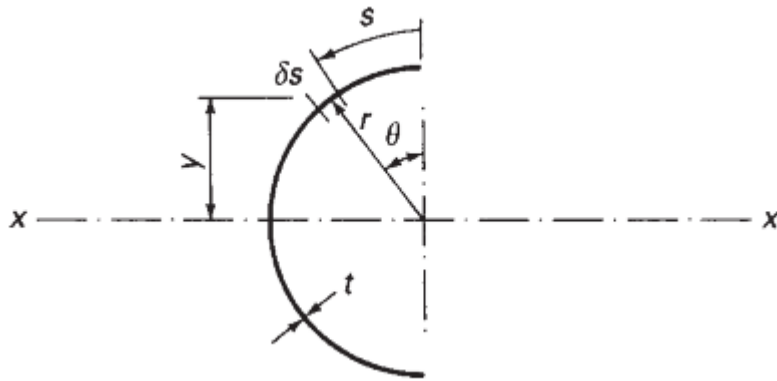
$$I_{xx} = \int\limits_{0}^{\pi r} t\, y^2\, ds$$

Expressing y and s terms of a single variable θ simplifies the integration, hence

$$I_{xx} = \int\limits_{0}^{\pi} t\,(r \cos \theta)^2\, r\, d\theta$$

From which

$$I_{xx} = \frac{\pi r^3 t}{2}$$

Example:

Determine the direct stress distribution in the thin-walled Z-section shown produced by a positive bending moment M_x.
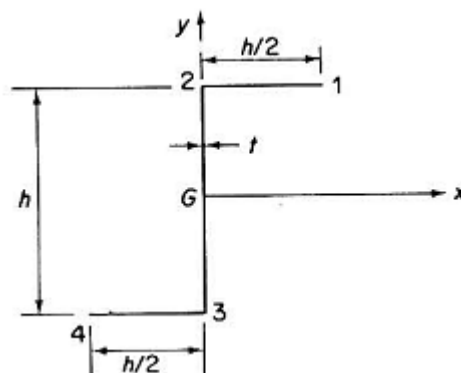
$M_x = 1000$ Kg.mm, h = 40 mm, t = 1mm

$M_y = 0$

Solution:

48

The section is anti-symmetrical with its centroid at the mid-point of the vertical web. Therefore, the direct stress distribution is given by

$$\sigma_z = \frac{M_x(I_{yy}y - I_{xy}x)}{I_{xx}I_{yy} - I_{xy}^2} \qquad \text{(i)}$$

Where, for this problem

$$\overline{M_x} = \frac{M_x}{1 - I_{xy}^2/I_{xx}I_{yy}}, \quad \overline{M_y} = \frac{-M_x I_{xy}/I_{xx}}{1 - I_{xy}^2/I_{xx}I_{yy}} \qquad \text{(ii)}$$

The section properties are calculated as follows

$$I_{xx} = 2\frac{ht}{2}\left(\frac{h}{2}\right)^2 + \frac{th^3}{12} = \frac{h^3 t}{3}$$

$$I_{yy} = 2\frac{t}{3}\left(\frac{h}{2}\right)^3 = \frac{h^3 t}{12}$$

$$I_{xy} = \frac{ht}{2}\left(\frac{h}{4}\right)\left(\frac{h}{2}\right) + \frac{ht}{2}\left(-\frac{h}{4}\right)\left(-\frac{h}{2}\right) = \frac{h^3 t}{8}$$

Substituting these values in Eqs. (ii) give,

$$\overline{M_x} = 2{\cdot}29 M_x, \quad \overline{M_y} = -0{\cdot}86 M_x$$

$$\overline{M_x} = 2286 \text{ kg mm} \quad , \qquad \overline{M_y} = -857 \text{ kg mm}$$

These expression when substituted in Eq. (i) give

$$\sigma_z = \frac{M_x}{h^3 t}(6{\cdot}86y - 10{\cdot}30x) \qquad \text{(iii)}$$

$$\sigma_z = 0.107y - 0.161x$$

On the top flange y= 20 , $0 \leq x \leq$ 20 (y=h/2 $0 \leq x \leq h/2$)   and the distribution of direct stress is given by

$$\sigma_z = \frac{M_x}{h^3 t}(3 \cdot 43h - 10 \cdot 30x)$$

$$\sigma_{z1} = 1.08 \text{ kg/mm}^2$$

At point (1) $x = 20$ mm,   y = 20 mm

$$\sigma_{z,1} = -\frac{1 \cdot 72 M_x}{h^3 t} \text{ (compressive)} \qquad \sigma_z = 0.107 * 20 - 0.161 * 20$$

$$\sigma_{z1} = -1.08 \text{ kg/mm}^2 \quad \text{(Compressive)}$$

At point (2) $x = 0$ mm,   y=20 mm

$$\sigma_z = 0.107 * 20 - 0.161 * 0$$

$$\sigma_{z2} = +2.14 \text{ kg/mm}^2 \quad \text{(Tensile)}$$

In the web $h/2 \leqslant y \leqslant -h/2$ and $x = 0$. Again the distribution is of linear form and is given by the equation

$$\sigma_z = \frac{M_x}{h^3 t} 6 \cdot 86 y \qquad \sigma_z = 0.107 * y$$

At point (3) $x = 0$ mm,   y = -20 mm

$$\sigma_{z3} = 0.107 * (-20)$$

$$\sigma_{z3} = -2.14 \text{ kg/mm}^2 \text{ (Compression)}$$

At point (4)   x= -20 mm,   y = -20 mm

$$\sigma_{z4} = 0.107 * (-20) - 0.161 * (-20)$$

$$\sigma_{z4} = +1.08 \ kg/mm^2 \quad \text{(Tensile)}$$

The distribution in the lower flange may be deduced from anti-symmetry , the complete distribution is then as shown.
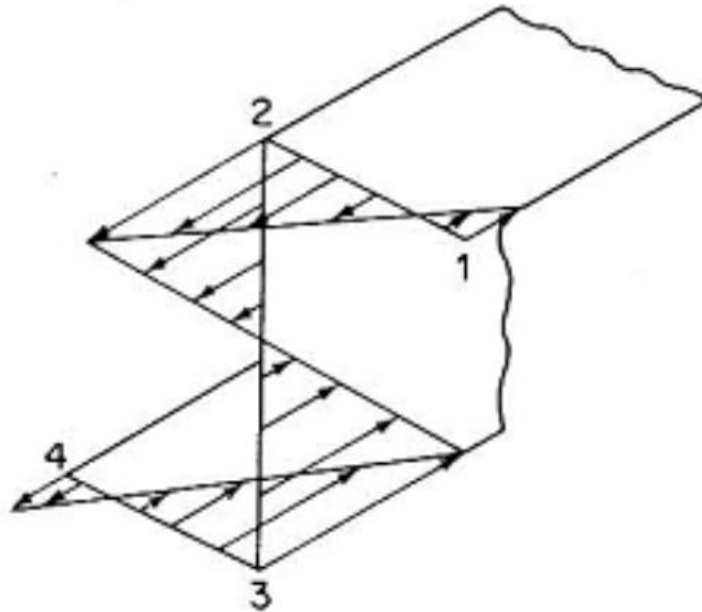
A thin-walled, cantilever beam of unsymmetrical cross-section supports shear loads at its free end as shown in   Figure   . Calculate the value of direct stress at the extremity of the lower flange (point A) at a section half-way along the beam if the position of the shear loads is such that no twisting of the beam occurs.
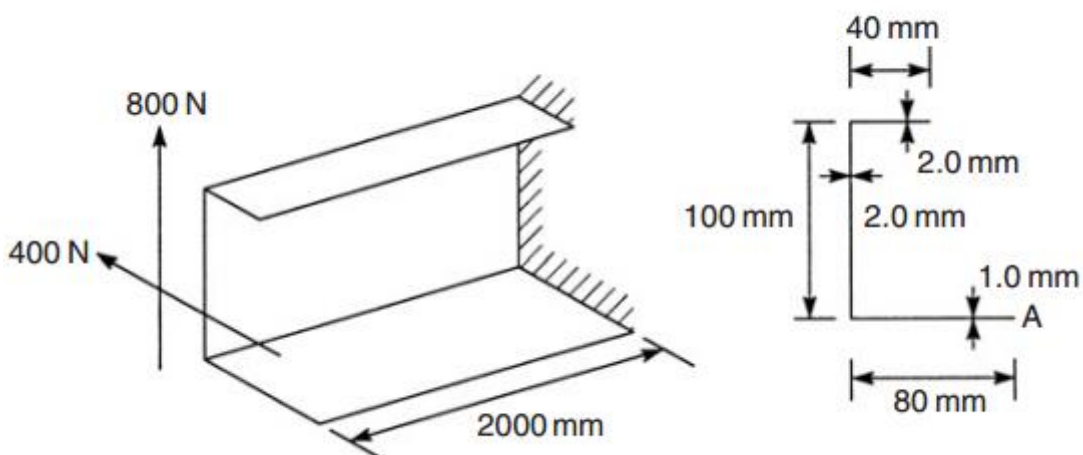
Ans. 194.7 N/mm2 (tension).

Chapter Four

General case of loading

Consider the element shown, where

δz : element of length in z-direction.

S_y : shear load in y-direction.

M_x : bending moment about x-axis.

w_y : distributed load of varying intensity.

As the element length is small, then the intensity is assumed constant.

(M_x) and S_y are +ve in the direction shown.

There for, for equilibrium of the element in the y direction

$$\left(S_y + \frac{\partial S_y}{\partial z} \delta z \right) + w_y \delta z - S_y = 0$$

From which,

$$w_y = -\frac{\partial S_y}{\partial z}$$

Taking moments about A

$$\left(M_x + \frac{\partial M_x}{\partial z} \delta z \right) - \left(S_y + \frac{\partial S_y}{\partial z} \delta z \right) \delta z - w_y \frac{(\delta z)^2}{2} - M_x = 0$$

Or , when second order terms are neglected,

$$S_y = \frac{\partial M_x}{\partial z}$$

Combine these results into a single expression

$$-w_y = \frac{\partial S_y}{\partial z} = \frac{\partial^2 M_x}{\partial z^2}$$

Similarly for loads in the xz plane

$$-w_x = \frac{\partial S_x}{\partial z} = \frac{\partial^2 M_y}{\partial z^2}$$

If it assumed that a parameter $\bar{S}_y$ bears the same relationship to $\bar{M}_x$ as S_y does to M_x then

$$\overline{S_y} = \frac{\partial \overline{M_x}}{\partial z} = \frac{\partial M_x/\partial z - (\partial M_y/\partial z)I_{xy}/I_{yy}}{1 - I_{xy}^2/I_{xx}I_{yy}}$$

$$\boxed{\overline{S_y} = \frac{S_y - S_x I_{xy}/I_{yy}}{1 - I_{xy}^2/I_{xx}I_{yy}}}$$

In similar fashion

$$\boxed{\overline{S_x} = \frac{S_x - S_y I_{xy}/I_{xx}}{1 - I_{xy}^2/I_{xx}I_{yy}}}$$

Parameters $\bar{w}_y$ and $\bar{w}_x$ are related to load intensities $\bar{w}_y$ and $\bar{w}_x$.

$$\boxed{\overline{w_x} = \frac{w_x - w_y I_{xy}/I_{xx}}{1 - I_{xy}^2/I_{xx}I_{yy}} \qquad \text{and} \qquad \overline{w_y} = \frac{w_y - w_x I_{xy}/I_{yy}}{1 - I_{xy}^2/I_{xx}I_{yy}}}$$

The parameters $\bar{M}_x, \bar{M}_y, \bar{S}_x, \bar{S}_y, \bar{w}_x, \bar{w}_y$ are often termed "effective" bending moments, shear forces and load intensities.

Deflections due to bending

In this chapter, the deflections and stresses in thin open and closed tubes will be determined due to bending. The relations to determine the deflections and stresses are similar to those developed in bending of beams.

General beam deflection are caused primarily by the bending action of applied loads, where a beam's cross section dimensions are not small compared with its length.

The following relationships exist between loading, shearing force, and bending moment, slope and deflection of a symmetrical section beam for:
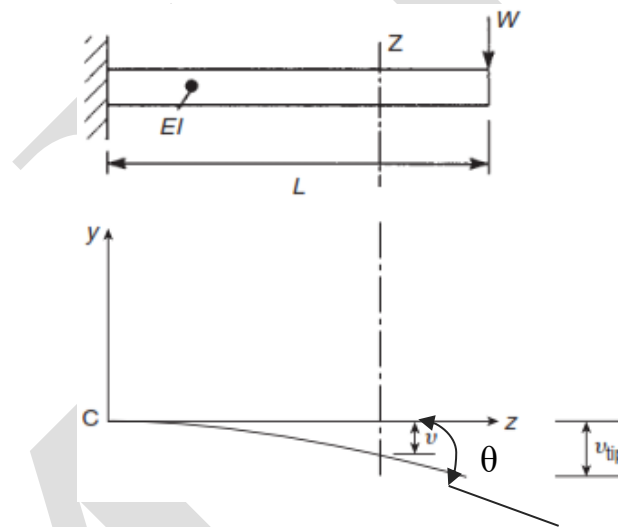
$v = Deflection\ in\ y\ dirction$

$$\frac{dv}{dz} = \theta = Slope$$

$$M = EI\frac{d^2v}{dz^2} = Bending\ moment$$

$$S = EI\frac{d^3v}{dz^3} = Shearing\ force$$

$$w = EI\frac{d^4v}{dz^4} = Loading$$

54

Deflection by Method of Singularity Function

In cases where a beam is subjected to a combination of distributed loads, concentrated loads, and moments, using the method of double integration to determine the deflections of such beams is really involving, since various segments of the beam are represented by several moment functions, and much computational efforts are required to find the constants of integration. Using the **method of singularity function** in such cases to determine deflections is comparatively easier and relatively quick. This method of analysis was first introduced by Macaulay in 1919, and it entails the use of one equation that contains a singularity or half-range function to describe the entire beam deflection curve. A singularity or half-range function is defined as follows:

$$(z -)^n = \begin{cases} 0 & \text{for } (z - a) \ < 0 \text{ or } z < a \\ (z - a)^n & \text{for } z - a \geq 0 \text{ or } z \geq a \end{cases}$$

Where;
z - Coordinate position of a point along the beam.
a - Any location along the beam where discontinuity due to bending occurs.
n- The exponential values of the functions; this must always be greater than or equal to zero for the functions to be valid.

The above outlined definition implies that the quantity **(z - a) equals zero** or **vanishes** if it is negative, but it is equal to **(z - a) if it is positive.** Integration of the Macaulay function follows the same rules as for ordinary functions**;**

$$\int (z - a)^n \, dz = \frac{(z - a)^{n+1}}{n + 1} + C$$

Note; That the square brackets must be retained during the integration. The arbitrary constants are found using the boundary conditions.

Example

Determine the position and magnitude of the maximum upward and downward deflections of the beam shown in Figure below.
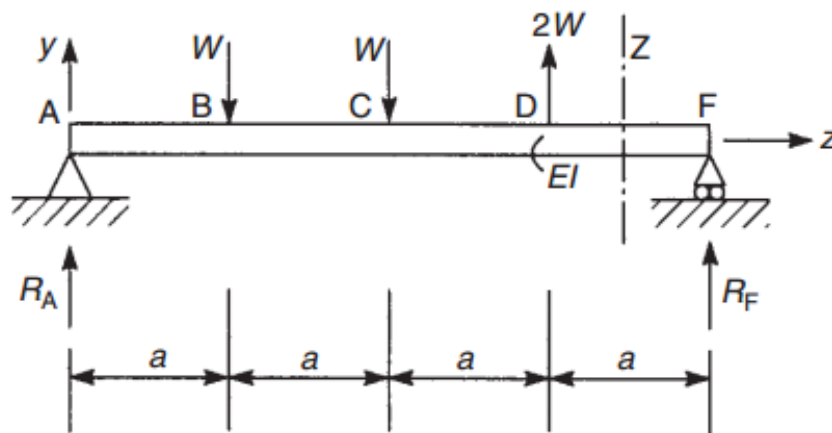
A consideration of the overall equilibrium of the beam gives the support reactions; thus

$$RA = \frac{3}{4}W \text{ (upward)} \quad RF = \frac{3}{4}W \text{ (downward)}$$

Using the method of singularity functions and taking the origin of axes at the left-hand support, we write down an expression for the bending moment, M, at any section Z between D and F, *the region of the beam furthest from the origin*

$$M = -R_A z + W[z - a] + W[z - 2a] - 2W[z - 3a] \tag{i}$$

Substituting for M in the second we have

$$EIv'' = \frac{3}{4}Wz - W[z - a] - W[z - 2a] + 2W[z - 3a] \tag{ii}$$

Integrating Eq. (ii) and retaining the square brackets we obtain

$$EIv' = \frac{3}{8}Wz^2 - \frac{W}{2}[z - a]^2 - \frac{W}{2}[z - 2a]^2 + W[z - 3a]^2 + C_1 \tag{iii}$$

and

$$EIv = \frac{1}{8}Wz^3 - \frac{W}{6}[z - a]^3 - \frac{W}{6}[z - 2a]^3 + \frac{W}{3}[z - 3a]^3 + C_1 z + C_2 \tag{iv}$$

56

in which C_1 and C_2 are arbitrary constants. When $z = 0$ (at A), $v = 0$ and hence $C_2 = 0$. Note that the second, third and fourth terms on the right-hand side of Eq. (iv) disappear for $z < a$. Also $v = 0$ at $z = 4a$ (F) so that, from Eq. (iv), we have

$$0 = \frac{W}{8}64a^3 - \frac{W}{6}27a^3 - \frac{W}{6}8a^3 + \frac{W}{3}a^3 + 4aC_1$$

which gives

$$C_1 = -\frac{5}{8}Wa^2$$

Equations (iii) and (iv) now become

$$EIv' = \frac{3}{8}Wz^2 - \frac{W}{2}[z-a]^2 - \frac{W}{2}[z-2a]^2 + W[z-3a]^2 - \frac{5}{8}Wa^2 \qquad \text{(v)}$$

and

$$EIv = \frac{1}{8}Wz^3 - \frac{W}{6}[z-a]^3 - \frac{W}{6}[z-2a]^3 + \frac{W}{3}[z-3a]^3 - \frac{5}{8}Wa^2z \qquad \text{(vi)}$$

By inspection of the figure above it seems likely that the maximum downward deflection will occur in BC. At B, using Eq. (v)

$$EIv' = \frac{3}{8}Wa^2 - \frac{5}{8}Wa^2$$

which is clearly negative. At C

$$EIv' = \frac{3}{8}W4a^2 - \frac{W}{2}a^2 - \frac{5}{8}Wa^2$$

which is positive. Therefore, the maximum downward deflection does occur in BC and its exact position is located by equating v to zero for any section in BC. Thus, from Eq. (v)

$$0 = \frac{3}{8}Wz^2 - \frac{W}{2}[z-a]^2 - \frac{5}{8}Wa^2$$

or, simplifying,

$$0 = z^2 - 8az + 9a^2 \tag{vii}$$

Solution of Eq. (vii) gives

$$z = 1.35a$$

so that the maximum downward deflection is, from Eq. (vi)

$$EIv = \frac{1}{8}W(1.35a)^3 - \frac{W}{6}(0.35a)^3 - \frac{5}{8}Wa^2(1.35a)$$

i.e.

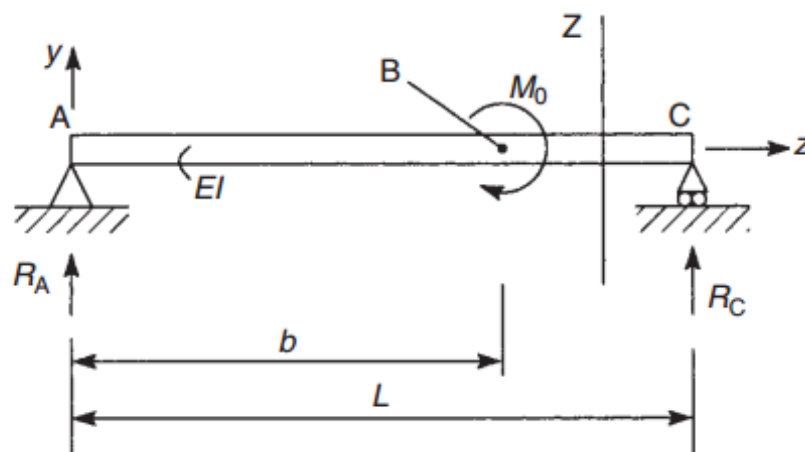$$v_{max}(\text{downward}) = -\frac{0.54Wa^3}{EI}$$

In a similar manner it can be shown that the maximum upward deflection lies between **D** and **F** at $z = 3.42a$ and that its magnitude is

Example
Determine the deflected shape of the beam shown in Figure below

In this problem an external moment $M0$ is applied to the beam at B. The support reactions are found in the normal way and are

58

$$R_A = -\frac{M_0}{L} \text{(downwards)} \quad R_C = \frac{M_0}{L} \text{(upwards)}$$

The bending moment at any section Z between B and C is then given by

$$M = -R_A z - M_0 \quad \text{(i)}$$

Equation (i) is valid only for the region BC and clearly does not contain a singularity function which would cause M_0 to vanish for $z \le b$. We overcome this difficulty by writing

$$M = -R_A z - M_0[z-b]^0 \quad \text{(Note: } [z-b]^0 = 1) \quad \text{(ii)}$$

Equation (ii) has the same value as Eq. (i) but is now applicable to all sections of the beam since $[z-b]^0$ disappears when $z \le b$. Substituting for M from Eq. (ii) in the second of Eq. we obtain

$$EIv'' = R_A z + M_0[z-b]^0 \quad \text{(iii)}$$

Integration of Eq. (iii) yields

$$EIv' = R_A \frac{z^2}{2} + M_0[z-b] + C_1 \quad \text{(vi)}$$

and

$$EIv = R_A \frac{z^3}{6} + \frac{M_0}{2}[z-b]^2 + C_1 z + C_2 \quad \text{(v)}$$

where C_1 and C_2 are arbitrary constants. The boundary conditions are $v = 0$ when $z = 0$ and $z = L$. From the first of these we have $C_2 = 0$ while the second gives

$$0 = -\frac{M_0}{L}\frac{L^3}{6} + \frac{M_0}{2}[L - b]^2 + C_1 L$$

from which

$$C_1 = -\frac{M_0}{6L}(2L^2 - 6Lb + 3b^2)$$

The equation of the deflection curve of the beam is then

$$v = \frac{M_0}{6EIL}\{z^3 + 3L[z - b]^2 - (2L^2 - 6Lb + 3b^2)z\} \tag{vi}$$

Deflections due to unsymmetrical bending

We noted that a beam bends about its neutral axis whose inclination to arbitrary centroid axes is determined. Beam deflections, therefore, are always perpendicular in direction to the neutral axis

For unsymmetrical section with load acting in x and y directions the relationships will be:

$u = Deflection\ in\ x\ dirction$ $\qquad\qquad v = Deflection\ in\ y\ dirction$

$$\bar{M}_x = EI_{xx}\frac{d^2v}{dz^2} = EIv'' \qquad\qquad \bar{M}_y = EI_{yy}\frac{d^2u}{dz^2} = EIu''$$

$$\bar{S}_x = EI_{yy}\frac{d^3u}{dz^3} \qquad\qquad\qquad \bar{S}_y = EI_{xx}\frac{d^3v}{dz^3}$$

Where, $\bar{M}_x$, $\bar{M}_y$, $\bar{S}_x$ and $\bar{S}_y$ are effective moments and effective shear forces, respectively.

$$\begin{Bmatrix} u'' \\ v'' \end{Bmatrix} = \frac{-1}{E\left(I_{xx}I_{yy} - I_{xy}{}^2\right)}\begin{bmatrix} -I_{xy} & I_{xx} \\ I_{yy} & -I_{xy} \end{bmatrix}\begin{Bmatrix} M_x \\ M_y \end{Bmatrix}$$

$$\begin{Bmatrix} M_x \\ M_y \end{Bmatrix} = -E\begin{bmatrix} I_{xy} & I_{xx} \\ I_{yy} & I_{xy} \end{bmatrix}\begin{Bmatrix} u'' \\ v'' \end{Bmatrix}$$

$$\boxed{M_x = -EI_{xy}u'' - EI_{xx}v''} \qquad\qquad \boxed{M_y = -EI_{yy}u'' - EI_{xy}v''}$$

$$\boxed{u'' = \frac{M_x I_{xy} - M_y I_{xx}}{E\left(I_{xx}I_{yy} - I_{xy}{}^2\right)} \qquad\qquad v'' = \frac{M_y I_{xy} - M_x I_{yy}}{E\left(I_{xx}I_{yy} - I_{xy}{}^2\right)}}$$

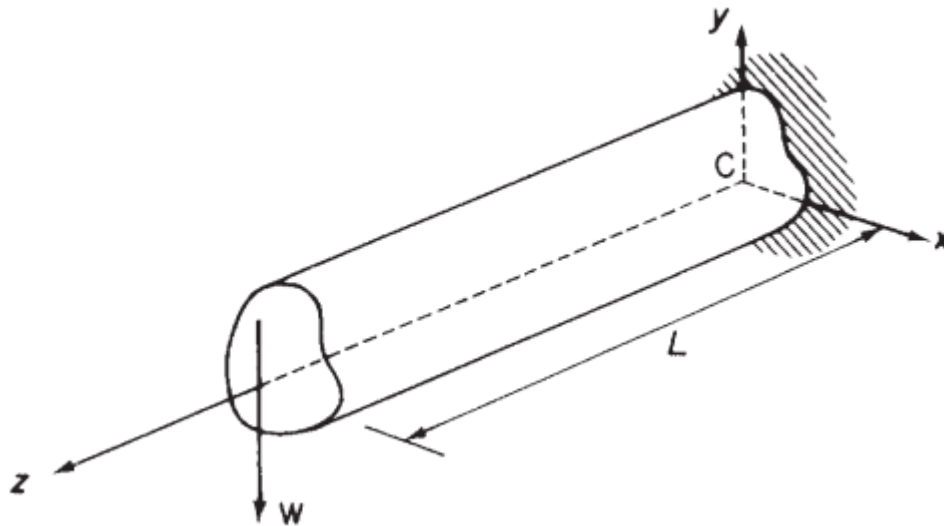$$\boxed{\bar{M}_x = \frac{M_x - M_y I_{xy}/I_{yy}}{\left(1 - I_{xy}{}^2/I_{xx}I_{yy}\right)} \qquad\qquad \bar{M}_x = \frac{M_y - M_x I_{xy}/I_{xx}}{\left(1 - I_{xy}{}^2/I_{xx}I_{yy}\right)}}$$

$$\boxed{\bar{S_x} = \frac{S_x - S_y I_{xy}/I_{xx}}{1 - I_{xy}^2/I_{xx}I_{yy}} \qquad\qquad \bar{S_y} = \frac{S_y - S_x I_{xy}/I_{yy}}{1 - I_{xy}^2/I_{xx}I_{yy}}}$$

61

Example

Determine the horizontal and vertical components of the tip deflection of the cantilever shown in Figure. The second moments of area of its unsymmetrical section are *Ixx*, *Iyy* and *Ixy*

From Equations;

$$u'' = \frac{M_x I_{xy} - M_y I_{xx}}{E(I_{xx}I_{yy} - I_{xy}^2)} \qquad (i)$$

In this case $M_x = W(L - z)$, $M_y = 0$ so that Eq. (i) simplifies to

$$u'' = \frac{WI_{xy}}{E(I_{xx}I_{yy} - I_{xy}^2)}(L - z) \qquad (ii)$$

Integrating Eq. (ii) with respect to z

$$u' = \frac{WI_{xy}}{E(I_{xx}I_{yy} - I_{xy}^2)}\left(Lz - \frac{z^2}{2} + A\right) \qquad (iii)$$

and

$$u = \frac{WI_{xy}}{E(I_{xx}I_{yy} - I_{xy}^2)}\left(L\frac{z^2}{2} - \frac{z^3}{6} + Az + B\right) \qquad (iv)$$

in which u' denotes du/dz and the constants of integration A and B are found from the boundary conditions, viz. $u' = 0$ and $u = 0$ when $z = 0$. From the first of these and Eq. (iii), $A = 0$, while from the second and Eq. (iv), $B = 0$. Hence the deflected shape of the beam in the xz plane is given by

$$u = \frac{WI_{xy}}{E(I_{xx}I_{yy} - I_{xy}^2)} \left(L\frac{z^2}{2} - \frac{z^3}{6}\right) \tag{v}$$

At the free end of the cantilever $(z = L)$ the horizontal component of deflection is

$$u_{\text{f.e.}} = \frac{WI_{xy}L^3}{3E(I_{xx}I_{yy} - I_{xy}^2)} \tag{vi}$$

Similarly, the vertical component of the deflection at the free end of the cantilever is

$$v_{\text{f.e.}} = \frac{-WI_{yy}L^3}{3E(I_{xx}I_{yy} - I_{xy}^2)} \tag{vii}$$

The actual deflection $\delta_{\text{f.e.}}$ at the free end is then given by

$$\delta_{\text{f.e.}} = (u_{\text{f.e.}}^2 + v_{\text{f.e.}}^2)^{\frac{1}{2}}$$

at an angle of $\tan^{-1} u_{\text{f.e.}}/v_{\text{f.e.}}$ to the vertical.

Note that if either Cx or Cy were an axis of symmetry, $I_{xy} = 0$ and Eqs (vi) and (vii) reduce to

$$u_{\text{f.e.}} = 0 \quad v_{\text{f.e.}} = \frac{-WL^3}{3EI_{xx}}$$

the well-known results for the bending of a cantilever having a symmetrical cross-section and carrying a concentrated vertical load at its free end

Example

Determine the deflection of the free end of the cantilever beam shown in Fig. The second moments of area of its cross-section about a horizontal and vertical system of centroidal axes are I_x, I_y and I_{xy}.
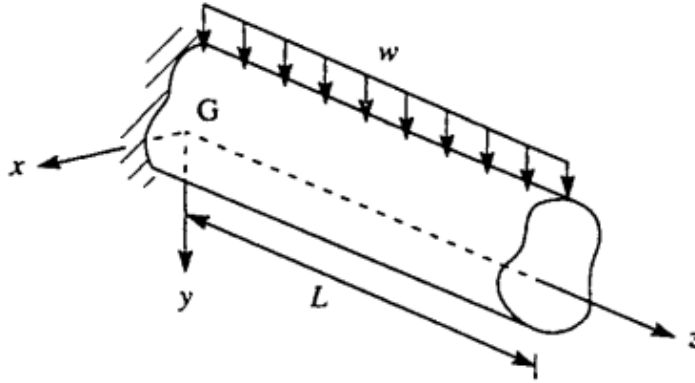
In this problem S_y, and therefore $\bar{S}_y$ and $\bar{S}_x$, are functions of z. We therefore use the relationships

$$\frac{\partial^2 \bar{M}_x}{\partial z^2} = -\bar{w}_y, \qquad \frac{\partial^2 \bar{M}_y}{\partial z^2} = -\bar{w}_x \qquad \text{(i)}$$

to determine the variation of $\bar{M}_x$ and $\bar{M}_y$ with z. Integrating the first of Eqs (i) we obtain

$$\frac{\partial \bar{M}_x}{\partial z} = -\bar{w}_y z + C_1 \qquad \text{(ii)}$$

When $z = L$, $\dfrac{\partial \bar{M}_x}{\partial z} = \bar{S}_y = 0$, hence $C_1 = \bar{w}_y L$ and

$$\frac{\partial \bar{M}_x}{\partial z} = \bar{w}_y (L - z) \qquad \text{(iii)}$$

Integrating Eq. (iii) we have

$$\bar{M}_x = \bar{w}_y\left(Lz - \frac{z^2}{2}\right) + C_2 \qquad \text{(iv)}$$

When $z = L$, $\bar{M}_x = 0$ so that $C_2 = -\bar{w}_y L^2/2$. Thus Eq. (iv) becomes

$$\bar{M}_x = \bar{w}_y\left(Lz - \frac{z^2}{2} - \frac{L^2}{2}\right) \qquad \text{(v)}$$

64

The remainder of the solution is identical and yield

$$v_{tip} = \frac{\bar{w}_y L^4}{8EI_x}, \qquad u_{tip} = \frac{\bar{w}_x L^4}{8EI_y}$$

in which
$$\bar{w}_y = \frac{w}{1 - I_{xy}^2/I_x I_y}, \qquad \bar{w}_x = \frac{-wI_{xy}/I_x}{1 - I_{xy}^2/I_x I_y}.$$

4.1 Shear of open tubes (section beams)

In considering the shear stress distribution in thin-walled open section beams we shall make identical **assumptions r**egarding the calculation of beam section;

- Shear stresses in the plane of the cross-section and parallel to the tangent at any point on the beam wall are constant across the thickness whereas shear stresses normal to the tangent are negligible as shown in Fig.4.1.
- The wall thickness can vary round the section but is constant along the length of the member
- Generally in the analysis, the axial constraint effects are negligible.
- The squares and higher powers of the thickness **t** are neglected in the calculation of section constants.
- The hoop stress (σ_s) is usually zero for open tube, while for closed tube, if there is an internal pressure, the hoop stress (σ_s) will be not equal to zero.
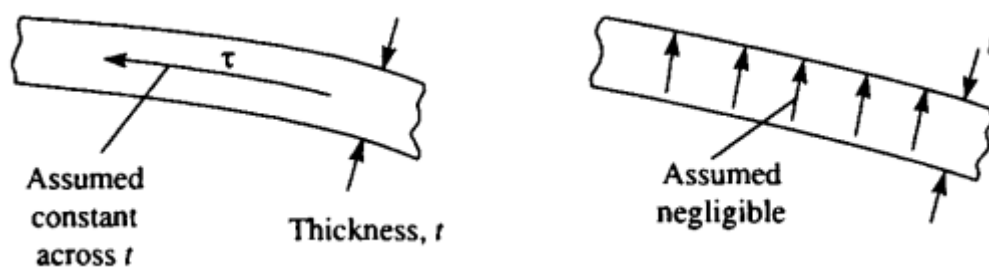
Fig.4.1. Assumption in thin walled open section beam

Fig.4.2 shows a length of a thin-walled beam of arbitrary section subjected to shear loads S_x and S_y which are applied such that no twisting of the beam occurs.
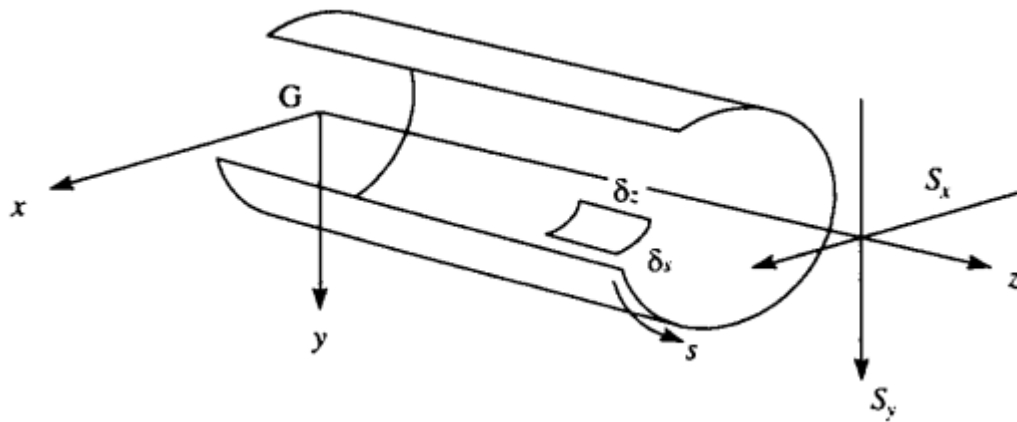
Fig.4.2. shear of a thin walled open section beam

In addition to shear stresses, direct stresses due to the bending action of the shear loads are present so that an element **δs x δz** of the beam wall is in equilibrium under the stress system shown in Fig.4.3.The shear stress **τ** is assumed to be positive in the positive direction of **s**, the distance round the profile of the section measured from an open edge. Although we have specified that the thickness **t** may vary with s, this variation is small for most thin-walled sections so that we may reasonably make the approximation that t is constant over the length **δ**s.

Fig.4.3. Equilibrium of beam element

To work in terms of shear flow to which we assign the symbol $(\mathbf{q} = \tau \mathbf{t})$ the shear stress system represented in terms of $\boldsymbol{q}$. Thus for equilibrium of the element in the $\boldsymbol{z}-$ direction
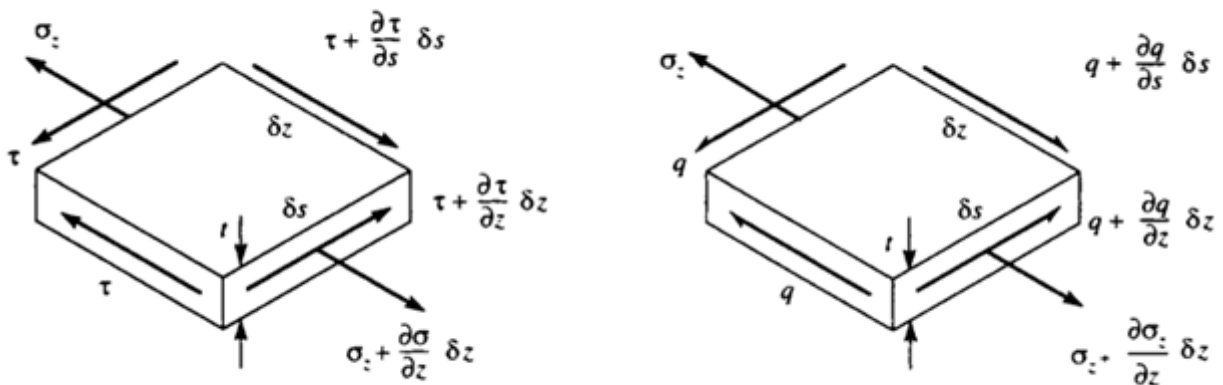
$$\left(\sigma_z + \frac{\partial \sigma_z}{\partial z}\, \delta z\right) t\, \delta s - \sigma_z t\, \delta s + \left(q + \frac{\partial q}{\partial s}\, \delta s\right) \delta z - q\, \delta z = 0$$

Which gives

$$\frac{\partial q}{\partial s} + t\, \frac{\partial \sigma_z}{\partial z} = 0$$

Again we assume that the direct stresses are given so that

$$\frac{\partial \sigma_z}{\partial z} = \frac{\partial \overline{M}_x}{\partial z}\, \frac{y}{I_x} + \frac{\partial \overline{M}_y}{\partial z}\, \frac{x}{I_y}$$

which becomes

$$\frac{\partial \sigma_z}{\partial z} = \frac{\overline{S}_y}{I_x}\, y + \frac{\overline{S}_x}{I_y}\, x$$

we obtain

$$\frac{\partial q}{\partial s} = -\frac{\overline{S}_y}{I_x}\, ty - \frac{\overline{S}_x}{I_y}\, tx$$

Integrating this expression from $\boldsymbol{s} = \boldsymbol{0}$ (where $\boldsymbol{q} = \boldsymbol{0}$ on the open edge of the section) to any point $\boldsymbol{s}$ we have

$$q_s = -\frac{\overline{S}_y}{I_x} \int_0^s ty\, ds - \frac{\overline{S}_x}{I_y} \int_0^s tx\, ds$$

The shear stress at any point in the beam section wall is obtained by dividing the shear flow **q**, by the appropriate wall thickness. Thus

$$\tau_s = - \frac{\bar{S}_y}{t_s I_x} \int_0^s ty \, ds - \frac{\bar{S}_x}{t_s I_y} \int_0^s tx \, ds$$

Example. Determine the shear flow distribution in the thin-walled Z-section beam shown in Fig.4.4 produced by a shear load S_y, applied in the plane of the web
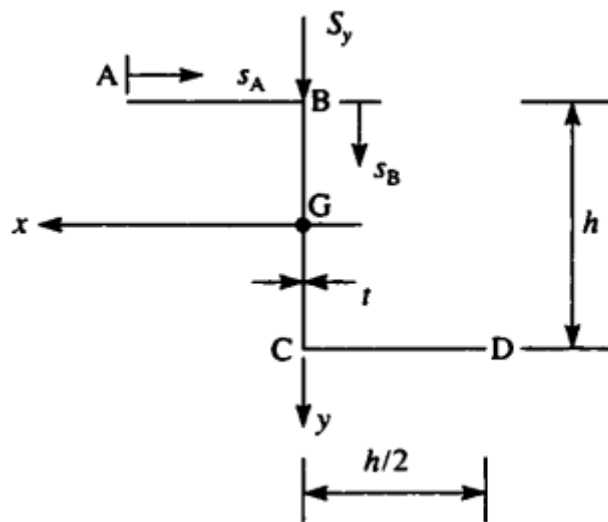
Fig.4.4. beam section

The origin for our system of reference axes coincides with the centroid of the section at the mid-point of the web. The centroid is also the center of antisymmetry of the section so that the shear load, applied through this point, causes no twisting of the section and the shear flow distribution is given by;

$$\bar{S}_y = \frac{S_y}{1 - I_{xy}^2/I_x I_y}, \qquad \bar{S}_x = \frac{-S_y I_{xy}/I_x}{1 - I_{xy}^2/I_x I_y} \tag{i}$$

The second moments of area of the section about the x and y axes have previously been calculated

$$I_x = \frac{h^3 t}{3}, \qquad I_y = \frac{h^3 t}{12}, \qquad I_{xy} = -\frac{h^3 t}{8}$$

69

Substituting these values in **Eqn.** (i) we obtain

$$\bar{S}_y = 2 \cdot 28 \ S_y, \quad \bar{S}_x = 0 \cdot 86 \ S_y$$

From eqn. $\quad q_s = - \dfrac{\bar{S}_y}{I_x} \int_0^s ty \ ds - \dfrac{\bar{S}_x}{I_y} \int_0^s tx \ ds$

$$q_s = - \dfrac{S_y}{h^3} \int_0^s (6 \cdot 84 \ y + 10 \cdot 32 \ x) \ ds$$

On the upper flange AB, $y = -h/2$ and $x = h/2 - s_A$ where $0 \leqslant s_A \leqslant h/2$. Therefore

$$q_{AB} = \dfrac{S_y}{h^3} \int_0^{s_A} (10 \cdot 32 \ s_A - 1 \cdot 74h) \ ds_A$$

which gives $\qquad q_{AB} = \dfrac{S_y}{h^3} (5 \cdot 16 s_A^2 - 1 \cdot 74 h s_A)$ $\qquad\qquad$ (ii)

Thus at $A(s_A = 0)$, $q_A = 0$ and at $B(s_A = h/2)$, $q_B = 0 \cdot 42 S_y/h$.

An examination of Eq. (ii) shows that the shear flow distribution on the upper flange is parabolic with a change of sign at $s_A = 0 \cdot 34h$. For values of $s_A < 0 \cdot 34h$, q_{AB} is negative and is therefore in the opposite direction to s_A. Furthermore, q_{AB} has a turning value between $s_A = 0$ and $s_A = 0 \cdot 34h$ at a value of s_A given by

$$\dfrac{dq_{AB}}{ds_A} = 10 \cdot 32 s_A - 1 \cdot 74h = 0$$

at $s_A = 0 \cdot 17h$. The corresponding value of q_{AB} is then, $q_{AB} = -0 \cdot 15 S_y/h$.

In the web BC, $y = -h/2 + s_B$ where $0 \leq s_B \leq h$ and $x = 0$. Thus

$$q_{BC} = -\frac{S_y}{h^3} \int_0^{s_B} (6 \cdot 84 s_B - 3 \cdot 42 h)\, ds_B + q_B \qquad \text{(iii)}$$

Note that in Eq. (iii), q_{BC} is not zero when $s_B = 0$ but equal to the value obtained by inserting $s_A = h/2$ in Eq. (ii), i.e. $q_B = 0 \cdot 42 S_y / h$. Integrating the first two terms on the right-hand side of Eq. (iii) we obtain

$$q_{BC} = -\frac{S_y}{h^3} (3 \cdot 42 s_B^2 - 3 \cdot 42 h s_B - 0 \cdot 42 h^2) \qquad \text{(iv)}$$

Equation (iv) gives a parabolic shear flow distribution in the web, symmetrical about Gx and with a maximum value at $s_B = h/2$ equal to $1 \cdot 28 S_y / h$; q_{AB} is positive at all points in the web.

The shear flow distribution in the lower flange may be deduced from antisymmetry; the complete distribution
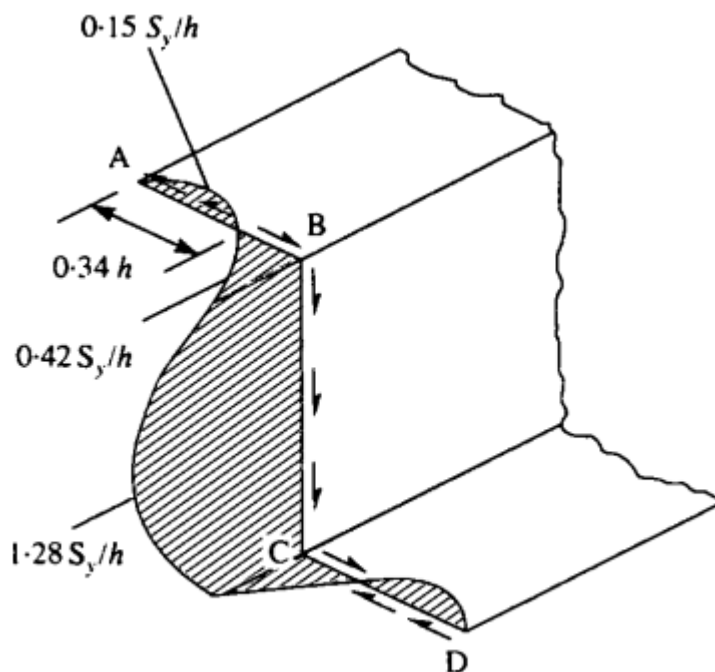

Fig.4.5. Shear flow distribution in beam section

71

4.2 Shear center of open section

The shear center is that point in the cross section through which the shear loads produce **no twisting**. It is also the center of twist when torsional loads are applied. As a rule, if a cross - section has an axis of symmetry, then the shear center must lie on that axis and in cruciform or angle sections show in Fig.4.6, **the shear center is located at the intersections.** It is important to define the position of the shear center because although most wings are not loaded at this point, if we know its location, we can represent the shear loads applied as combinations of shear loads through the shear center and a torque.
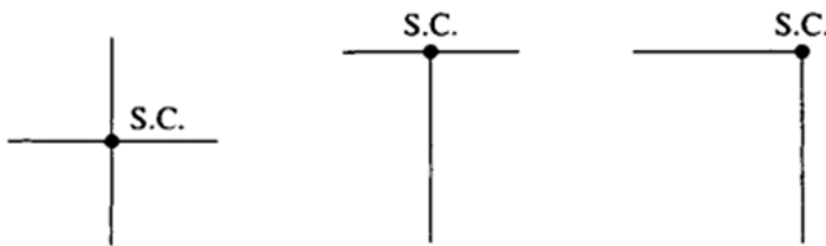

Fig.4.6. Special cases of shear center position

To calculate the shear center, determine the moment generated by the shear flow about an appropriate point in the cross section. This moment is equal to the moment generated by the applied shear force about this same point.

$$\sum M_{Applied} = \sum M_{Shear\ flow}$$

Note: In the case of unsymmetrical sections, the coordinates (sc_x, sc_y) of the shear center have to be found. This is best achieved by first applying a vertical shear force S_y, determining $\mathbf{sc_x}$, then applying a horizontal force S_x determining $\boldsymbol{sc_y}$.

Example . Determine the position of the shear center of the thin-walled channel section shown in Fig. 4.7.
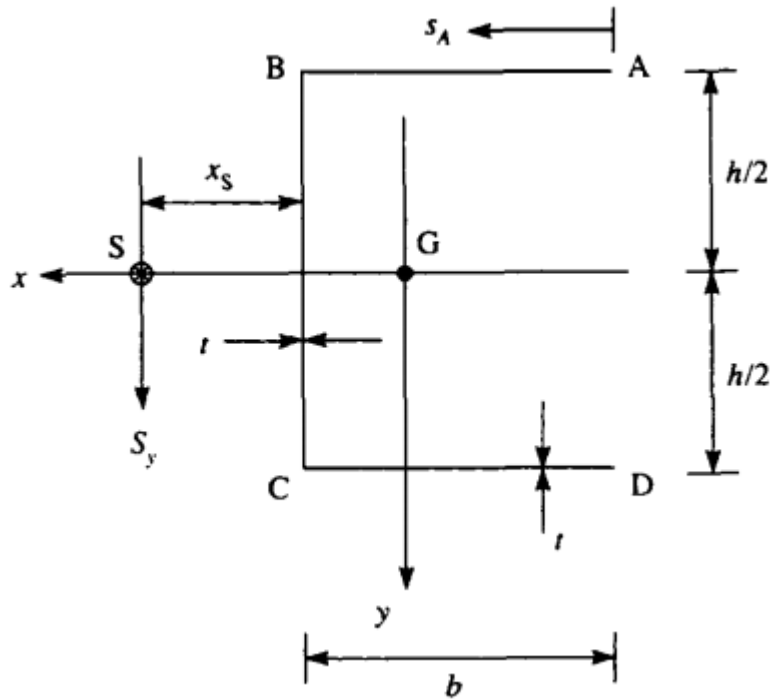
Fig.4.7. Channel section beam

The shear center S lies on the horizontal axis of symmetry at some distance x_s say, from the web. If an arbitrary shear load, S_y is applied through the shear center, then the shear flow distribution is given and the moment about any point in the cross-section produced by these shear flows is equivalent to the moment of the applied shear load about the same point.

For the channel section, Gx is an axis of symmetry so that $I_{xy} = 0$, giving $S_y = \bar{S}_y$ and $\bar{S}_x = S_x = 0$. therefore simplifies to

$$q_s = -\frac{S_y}{I_x}\int_0^s ty\, ds$$

where

$$I_x = \frac{th^3}{12} + 2bt\left(\frac{h}{2}\right)^2 = \frac{th^3}{12}\left(1 + 6\frac{b}{h}\right)$$

Substituting for I_x and noting that t is constant round the section, we have

$$q_s = -\frac{12S_y}{h^3(1 + 6b/h)}\int_0^s y\, ds \tag{i}$$

The solution of this type of problem may be reduced in length by giving some thought to what is required. We are asked, in this case, to obtain the position of the shear center and not a complete shear flow distribution. From symmetry it can be seen that the moments of the resultant shear forces on the upper and lower flanges about the mid-point of the web are numerically equal and act in the same sense. Furthermore, the moment of the web shear about the same point is zero. Therefore it is only necessary to obtain the shear flow distribution on either the upper or lower flange for a solution.

On the upper flange, $y = -h/2$ so that from Eq. (i) we obtain

$$q_{AB} = \frac{6S_y}{h^2(1 + 6b/h)} s_A \qquad \text{(ii)}$$

Of the web to the anticlockwise moment of the applied shear load about the same point gives

$$S_y x_S = 2 \int_0^b q_{AB} \frac{h}{2} ds_A$$

Substituting for q_{AB} from Eq. (ii) we have

$$S_y x_S = 2 \int_0^b \frac{6S_y}{h^2(1 + 6b/h)} \frac{h}{2} s_A ds_A$$

from which

$$x_S = \frac{3b^2}{h(1 + 6b/h)}$$

In the case of an unsymmetrical section, the coordinates (x_s, y_s) of the shear center referred to some convenient point in the cross-section are obtained by first determining x_s in a similar manner to that described above and then calculating y_s by applying a shear load S_x through the shear center.

4.3 Shear of closed tubes (section beams)

The solution for a shear loaded closed section beam follows a similar pattern to that described in section of shear of open tube but with two important differences;

- The shear loads may be applied through points in the cross-section other than the shear center(shear loads may be applied through any point in cross-section)
- The origin for **s** does not generally coincide with a known value of shear flow (at the origin of **'s'**, the value of shear flow $q_{s,0}$ is unknown).
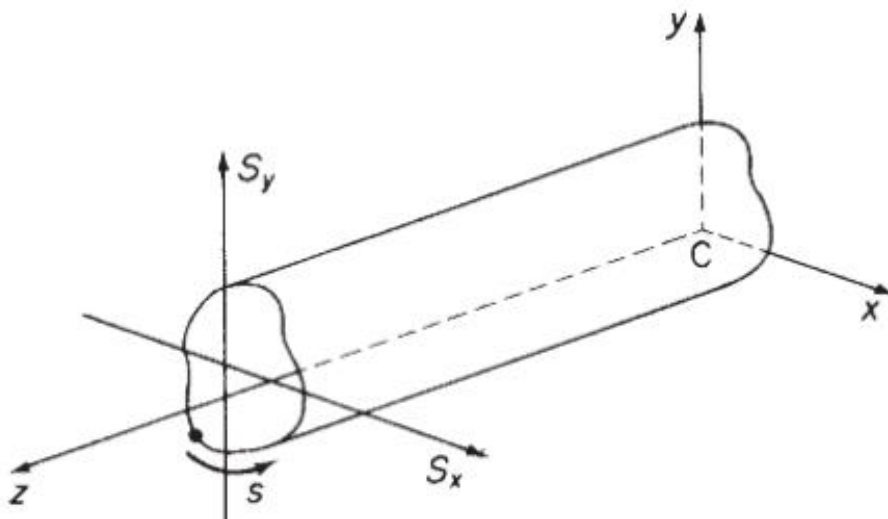

Fig.4.8. Shear of a thin-walled closed section beam

Look at arbitrary closed beam Fig.4.8, with applied shear forces S_x and S_y. In general, cause direct bending stresses and shear flows, which are related by the equilibrium equation;

If hoop stresses and body forces are absent, it is necessary to use equation

$$\frac{\partial q}{\partial s} + t\frac{\partial \sigma_z}{\partial z} = 0$$

and as for the analysis of open beam sections, when substituting for σ_z, we obtained:

$$\int_0^s \frac{\partial q}{\partial s} = -\frac{\bar{S}_y}{I_{xx}}\int_0^s ty\,ds - \frac{\bar{S}_x}{I_{yy}}\int_0^s tx\,ds$$

However unlike for open beams, at s = 0, $q_{s0} \neq 0$, so when integrating we get:

$$q_s = -\frac{\bar{S}_y}{I_{xx}} \int_0^s ty\,ds - \frac{\bar{S}_x}{I_{yy}} \int_0^s tx\,ds + q_{s,0}$$

The first two terms are identical to the equation of shear flow of open tube loaded through shear centre. If we let this terms be 'q_b' then:

$$q_s = q_b + q_{s,0}$$

To obtain q_b we assume the beam section is cut at some point to produce an open tube, and the shear flow distribution is then given by the following equation

$$q_b = -\frac{\bar{S}_y}{I_{xx}} \int_0^s ty\,ds - \frac{\bar{S}_x}{I_{yy}} \int_0^s tx\,ds$$

where at s = 0 , $q_s = 0$.

What is now required, is a way of determining the value of the shear stress at the point where the beam was cut. To do this, look at beam cross section loaded at some point:

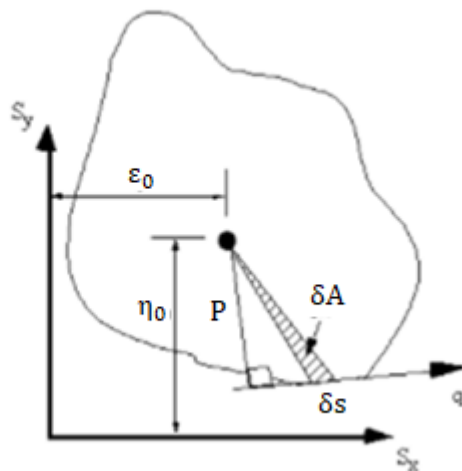To do this, look at beam cross section loaded at some point:

Fig.4.9. Resolving moments due to applied loads and shear flow

Take moments about a convenient point inside the beam. *The moment equation will look like this*

$$S_x \eta_0 - S_y \varepsilon_0 = \oint p q \, ds$$

but the shear flow term is given by equation , so substituting for q gives:

$$S_x \eta_0 - S_y \varepsilon_0 = \oint p q_b \, ds + q_{s,0} \oint p \, ds$$

The term $\oint$ is the integral around the cross section.

By looking at the area enclosed by the elemental distance s and the point where moments are taken, then:

$$dA = \frac{1}{2} \, ds \, p$$

Integrating this over the cross section as the element $\delta_s \to 0$, gives:

Which means that:

$$\oint p \, ds = 2A$$

where :

$\qquad$ A = Area enclosed by the mid-line of the beam section wall

Giving that:

$$S_x \eta_0 - S_y \varepsilon_0 = \oint p q_b \, ds + 2 q_{s,0} A$$

But if we take moments about the points where the shear forces are applied, then this equation becomes:

$$0 = \oint p q_b \, ds + 2 q_{s,0} A$$

which can easily be used to determine the value of $q_{s,0}$.

4.4. Twist and warping of shear loaded

If a shear load is not applied at the shear center, the closed beam section will both twist and have an out of plane axial displacement (warp). From equation; shear flow is define by ; $q_s = \tau t$

and from elasticity: $\tau = G\gamma$

with the term for shear strain given by equation

$$\gamma = \frac{\partial w}{\partial s} + \frac{\partial v_t}{\partial z}$$

Combining all three equations gives:

$$q_s = Gt\left(\frac{\partial w}{\partial s} + \frac{\partial v_t}{\partial z}\right)$$

Integrating this equation around the cross-section wrt 's' gives:

$$\frac{d\theta}{dz} = \frac{1}{2A}\oint \frac{q_s}{Gt}ds$$

Which is the rate of twist of the beam wrt z.

4.5. Shear center of close section

The position of the shear center for a beam loaded as shown in Fig.4.10 , can be found by using equation ;

$$S_y \varepsilon_0 - S_x \eta_0 = \oint p q_b ds + 2q_{s,0}A$$

Where:

η_0 = vertical distance from x-axis to shear centre from reference axis

ε_0 = horizontal distance from y-axis to shear center from reference axis
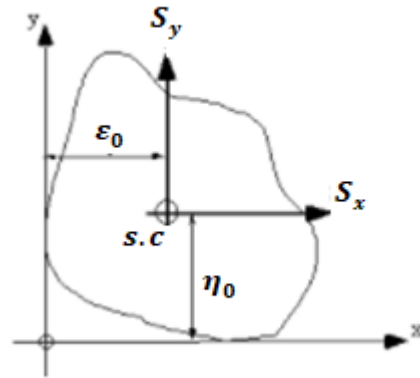
Fig.4.10 determining location of shear center for closed beam section

In order to determine the shear centre we need to determine $q_{s,0}$. From the definition for shear centre, if a shear load is applied here, it produces no twist, so by using equation:

$$\frac{1}{2A}\oint\frac{q_s}{Gt}ds = 0$$

and substituting for $q_{s,0}$ it gives:

$$\frac{1}{2A}\oint\frac{1}{Gt}(q_b + q_{s,o})ds = 0$$

which gives that:

$$q_{s,0} = -\frac{\oint\dfrac{q_b}{Gt}ds}{\oint\dfrac{1}{Gt}ds}$$

and if Gt is constant:

$$q_{s,0} = -\frac{\oint q_b ds}{\oint ds}$$

With these equations the shear flow , shear center, the rate of twist, and warping in a closed beam section can now be determined.

Example. A thin-walled, closed section beam has the singly symmetrical, trapezoidal cross-section shown in Figure below. Calculate the distance of the shear center from the wall AD. The shear modulus **G is** constant throughout the section
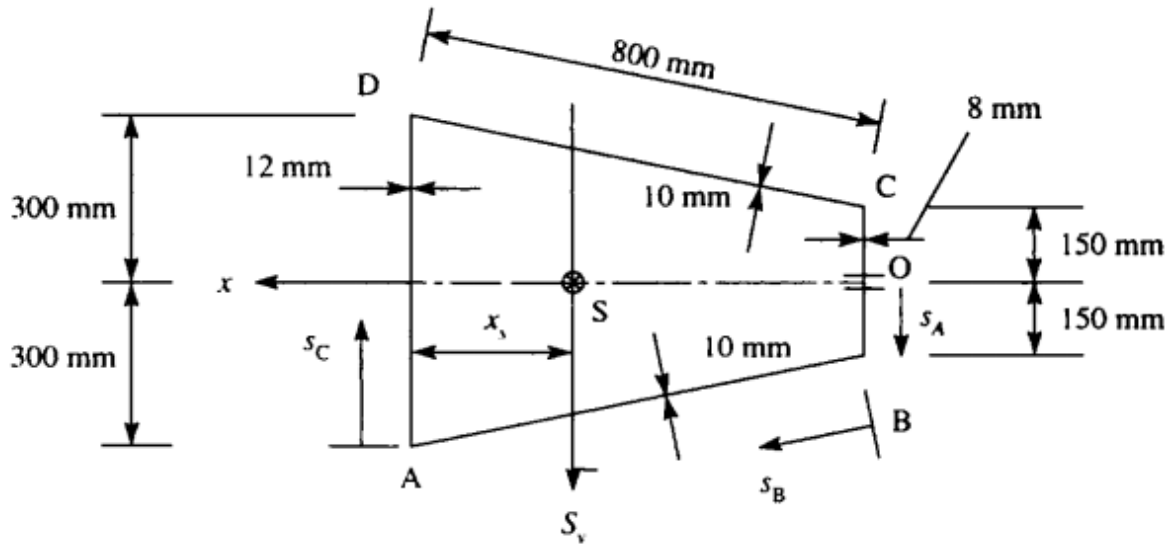
The shear centre lies on the horizontal axis of symmetry so that it is only necessary to apply a shear load S_y through S to determine x_S. Furthermore the axis of symmetry coincides with the centroidal reference axis Gx so that $I_{xy} = 0$, $\bar{S}_y = S_y$ and $\bar{S}_x = S_x = 0$. therefore simplifies to

$$q_s = - \frac{S_y}{I_x} \int_0^s ty \, ds + q_{s,0} \qquad (i)$$

Note that in Eq. (i) only the second moment of area about the x axis and coordinates of points referred to the x axis are required so that it is unnecessary to calculate the position of the centroid on the x axis. It will not, in general, and in this case in particular, coincide with S.

The second moment of area of the section about the x axis is given by

$$I_x = \frac{12 \times 600^3}{12} + \frac{8 \times 300^3}{12} + 2\left[\int_0^{800} 10\left(150 + \frac{150}{800} s\right)^2 ds\right]$$

from which $I_x = 1074 \times 10^6$ mm^4. Alternatively, the second moment of area of each inclined wall about an axis through its own centroid may be found using the method described and then transferred to the x axis by the parallel axes theorem.

We now obtain the q_b shear flow distribution by 'cutting' the beam section at the mid-point O of the wall CB. Thus, since $y = s_A$ we have

$$q_{b,OB} = - \frac{S_y}{I_x} \int_0^{s_A} 8 s_A \, ds_A$$

which gives

$$q_{b,OB} = - \frac{S_y}{I_x} 4 s_A^2 \qquad \text{(ii)}$$

Thus

$$q_{b,B} = - \frac{S_y}{I_x} \times 9 \times 10^4$$

For the wall BA where $y = 150 + 150 s_B / 800$

$$q_{b,BA} = - \frac{S_y}{I_x} \left[\int_0^{s_B} 10 \left(150 + \frac{150}{800} s_B \right) ds_B + 9 \times 10^4 \right]$$

from which

$$q_{b,BA} = - \frac{S_y}{I_x} \left(1500 s_B + \frac{15}{16} s_B^2 + 9 \times 10^4 \right) \qquad \text{(iii)}$$

whence

$$q_{b,A} = - \frac{S_y}{I_x} \times 189 \times 10^4$$

In the wall AD, $y = 300 - s_C$ so that

$$q_{b,AD} = - \frac{S_y}{I_x} \left[\int_0^{s_C} 12(300 - s_C) \, ds_C + 189 \times 10^4 \right]$$

which gives

$$q_{b,AD} = - \frac{S_y}{I_x} (3600 s_C - 6 s_C^2 + 189 \times 10^4) \qquad \text{(iv)}$$

The remainder of the q_b distribution follows from symmetry.

The shear load S_y is applied through the shear centre of the section so that we must determine $q_{s,0}$. Now

$$\oint \frac{ds}{t} = \frac{600}{12} + \frac{2 \times 800}{10} + \frac{300}{8} = 247.5$$

Hence

$$q_{s,0} = -\frac{2}{247.5} \left(\int_0^{150} \frac{q_{b,OB}}{8} \, ds_A + \int_0^{800} \frac{q_{b,BA}}{10} \, ds_B + \int_0^{300} \frac{q_{b,AD}}{12} \, ds_C \right) \quad \text{(v)}$$

Substituting for $q_{b,OB}$, $q_{b,BA}$ and $q_{b,AD}$ in Eq. (v) from Eqs (ii), (iii) and (iv), respectively, we obtain

$$q_{s,0} = \frac{2s_y}{247.5I_x} \left[\int_0^{150} \frac{s_A^2}{2} \, ds_A + \int_0^{800} \left(150s_B + \frac{15}{160} s_B^2 + 9 \times 10^3 \right) ds_B \right.$$

$$\left. + \int_0^{300} \left(300s_C - \frac{1}{2} s_C^2 + \frac{189 \times 10^4}{12} \right) ds_C \right]$$

from which

$$q_{s,0} = \frac{S_y}{I_x} \times 1.04 \times 10^6$$

Taking moments about the mid-point of the wall AD we have

$$S_y x_s = 2 \left(\int_0^{150} 786 q_{OB} \, ds_A + \int_0^{800} 294 q_{BA} \, ds_B \right) \quad \text{(vi)}$$

Noting that $q_{OB} = q_{b,OB} + q_{s,0}$ and $q_{BA} = q_{b,BA} + q_{s,0}$ we rewrite Eq. (vi) as

$$S_y x_s = \frac{2S_y}{I_x} \left[\int_0^{150} 786(-4s_A^2 + 1.04 \times 10^6) \, ds_A \right.$$

$$\left. + \int_0^{800} 294(-1500s_B - \frac{15}{16} s_B^2 + 0.95 \times 10^6) \, ds_B \right] \quad \text{(vii)}$$

Integrating Eq. (vii) and eliminating S_y gives

$$x_S = 282 \text{ mm.}$$

<mark>STRUCTURAL IDEALISATION</mark>

In the work done so far, the aircraft structural components analyzed have been relatively simple. However an aircraft wing (for example) can be made up of many cell compartments. Each section of the wing would be covered by a thin skin, and the skins would be reinforced by many stringers of Z, C or T section. The analysis of such a structure would be extremely complex and time consuming. In order to simplify this, structural idealisation should be carried out.

1. The longitudinal stiffeners and spar flanges carry only axial stresses
2. The web, skin and spars webs carry only shear stresses
3. The axial stress is constant over the cross section of each longitudinal stiffener
4. The shearing stress is uniform through the thickness of the webs
5. Transverse frames and ribs are rigid within their own planes

In idealising a structural component by following these **Five Points** the new simpler structure looks something like this:
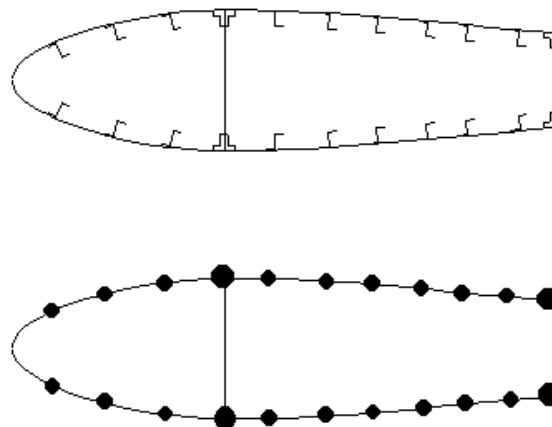

Figure 6.1: Original and Idealised wing sections

For which:

- The stiffeners are represented by **circles called booms**, which have a concentrated mass in the plane of the skin.
- The direct stresses are calculated at the centroid of these booms and are assumed to have constant stress through their cross-section.
- Shear stresses are assumed uniform through the thickness of the skins and webs.
- The direct stress carrying capability of skin is represented as an addition to existing booms or as additional separate booms.

Because the skin can carry some direct load, usually tensile (although some can be carried in compression but this is determined by the buckling load of the skin).

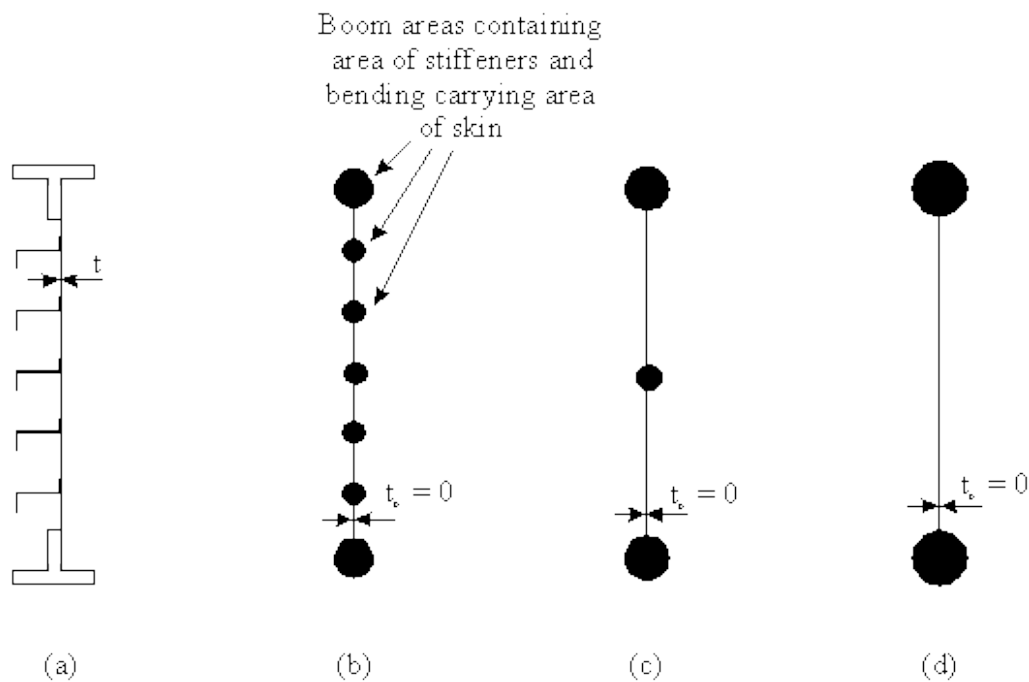*We now need to look at how these idealisation techniques can be applied:*

Figure 6.2: Typical stiffened panel. a) Actual panel, b) Idealised panel with same number of stiffeners and booms, c) Idealized panel with reduced boom number, d) Further Idealised panel with all stiffener and bending carrying areas lumped into two booms.

To idealize a structure you can:

- Replace the spar web by replacing its area to the major booms
- Reduce the number of stiffeners or booms by combining the stiffener mass with that of the skin into one boom

84

**REMEMBER:** When idealising a structure, the **Elastic Characteristics** of the idealised structure must be the same as for the original structure.
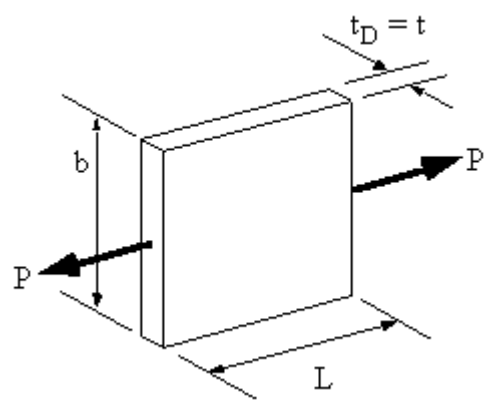
Idealised Sheet to Support Tensile Load

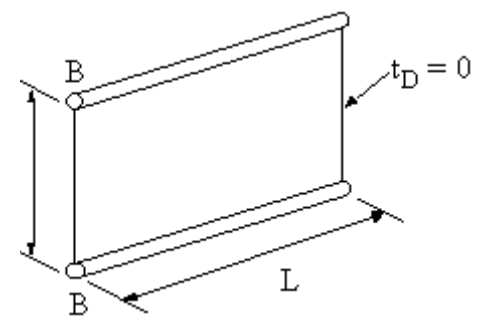**Figure 6.3:** Actual sheet to be Idealised.

Figure 6.4: Idealised structure.

Let; the thickness of the skin is defined as:

t_D = Actual skin thickness **t,** if skin resists totally direct load

t_D = Percentage of **t**, if partially resists applied load

t_D = **0** if skin only able to resist shear load

In order to idealise the structure of Figure 6.3 into that of Figure 6.4. Two things should be considered, Force (stress) equilibrium and Compatibility (displacement).

In the real structure the **direct stress** is determined using:

$$\sigma_z = \frac{P}{bt_D}$$

and its elongation is given by :

$$\delta = \frac{FL}{EA} = \frac{PL}{Ebt_D} \qquad (6.2)$$

In the idealised structure, however, the direct stress is given by:

$$\sigma_{z(in\ the\ booms)} = \frac{P}{2B} \qquad (6.3)$$

85

And its elongation is given by:

$$\delta = \frac{PL}{2BE} \qquad (6.4)$$

Since equations (6.2) and (6.4) should give the same elongation, and then we can define the relationship:

$$B = \frac{bt_D}{2} \qquad (i)$$

If you look at the stress in the booms they are the same as those of the original structure.

Idealised Sheet to Support Bending Moment
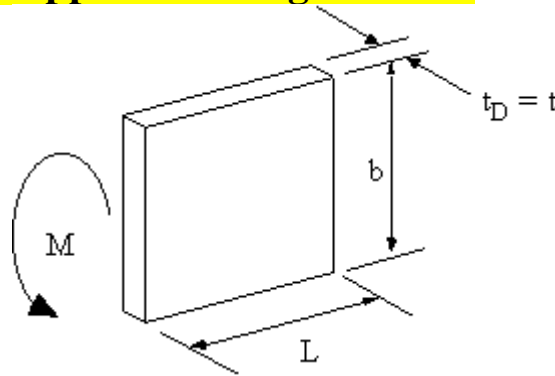
Figure 6.5: Actual sheet to be idealised with applied bending moment

The stress in this sheet is given by:

$$\sigma_z = \frac{My}{I} = \frac{6M}{b^2 t_D} \qquad (6.6)$$

The second moment of area for the idealised booms is (using parallel axis theorem) is given by:

$$I = 2B\left(\frac{b^2}{4}\right) = \frac{Bb^2}{2}$$

and its stress is given by :

$$\sigma_{z(booms)} = \frac{M}{Bb} \qquad (6.8)$$

Since equations 6.6 and 6.8 should give the same maximum stresses then:

$$B = \frac{bt_D}{6} \qquad \text{(ii)}$$

As can be seen by this equation (i) and (ii), a different idealised boom area equation is required for a different loading condition.

Idealised Sheet to Support Direct Load and Bending Moment

The stress distribution for a combined loading case with a direct load and a bending moment looks like Figure 6.6.

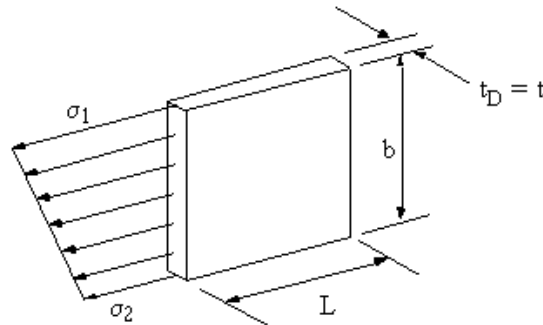**Figure 6.6:** Actual sheet supporting direct load and bending moment

In the idealised structure, the maximum and minimum stresses need to be carried by the booms as actual direct stresses as shown in Figure 6.7.
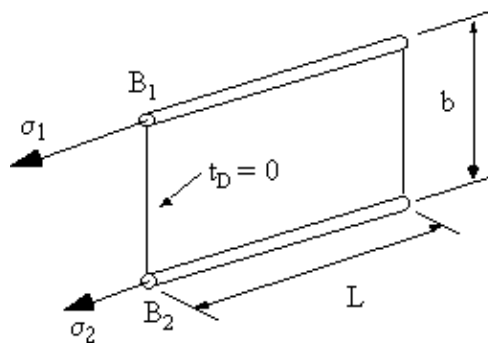

Figure 6.7: Idealised sheet supporting maximum stresses in booms.

Equating the direct loads along the z-axis gives that:

$$B_1 \sigma_1 + B_2 \sigma_2 = \frac{1}{2} bt_D (\sigma_1 + \sigma_2)$$

87

If the neutral axis in the idealised structure is in the same position as in the original sheet, the bending moment carried by the idealised structure must be the same as that carried by the real structure.

Equating moments about neutral plane gives the following:

$$\sigma_1 B_1 \frac{b}{2} - \sigma_2 B_2 \frac{b}{2} = b t_D \frac{(\sigma_1 - \sigma_2)}{2} * \left(\frac{b}{6}\right) = \frac{b^2 t_D}{12}(\sigma_1 - \sigma_2)$$

multiplying by 2 gives:

$$\sigma_1 B_1 - \sigma_2 B_2 = \frac{b t_D}{6}(\sigma_1 - \sigma_2)$$

Adding these equations and simplifying, gives:

$$B_1 = \frac{b t_D}{6}\left(2 + \frac{\sigma_2}{\sigma_1}\right)$$

$$B_2 = \frac{b t_D}{6}\left(2 + \frac{\sigma_1}{\sigma_2}\right)$$

By calculating the bending stresses, the structure can then be idealised.

WARNING: There is a problem with equations above. It has to do with idealising sections of skin very close to the neutral axis of the cross section, see Figure 6.8.
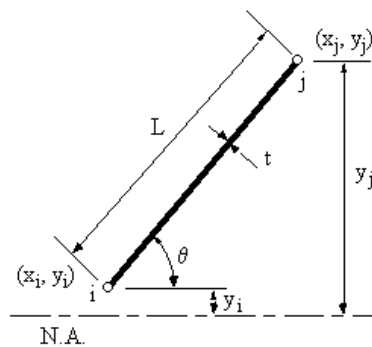

Figure 6.8: Skin segment very close to Neutral Axis to be idealised into booms i & j

he equation can be generalized in the form of:

$$B_i = \frac{L t}{6}\left(2 + \frac{\sigma_j}{\sigma_i}\right)$$

88

Idealised Sheet to Support Direct Compressive Load

When supporting a compressive load, the metal sheet is usually critical in buckling. Because of this, only a small fraction of its width '**b**' is effective in compression. Experimental research has led to the derivation of the following equations for the effective area of skin in compression.
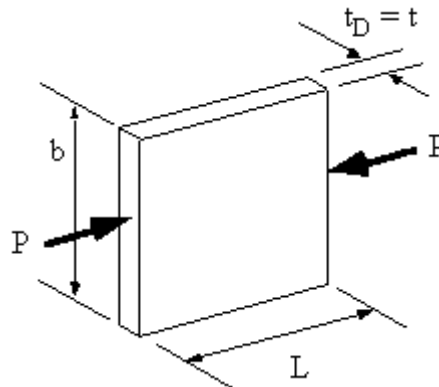
Figure 6.9: Sheet to be idealized in compression.
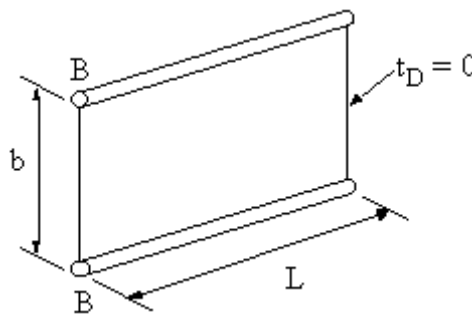
Figure 6.10: Idealised sheet.

Area of boom:

$$B = Ct$$

Where 'C' is the effective width of metal in compression, given by:

$$C = \frac{\pi t}{\sqrt{12(1 - v^2)}} \sqrt{\frac{E}{\sigma_{yield}}} = 20t$$

Note: Although the idealisation given by equations for a metal sheet in compression is valid, it is sometimes better to idealise the structure using the equations derived for the other three load cases. When the stresses on the metal skin are known we can then use critical buckling stresses for thin metal sheets to determine if they will be effective in compression.

Example: Part of a wing section is in the form of a two-cell box shown. All the vertical spar webs are connected to the skins through spar caps, all with cross - sectional areas of 300 mm^2. Idealise the section into direct stress carrying booms and shear stress only carrying skin when the wing is subjected to an applied bending moment Mx = -150 kNm. Position the booms at the spar/skin junctions.
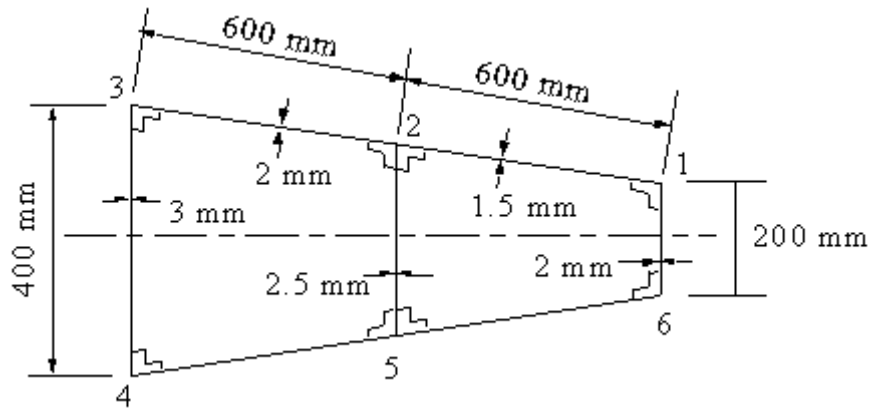
Figure 6.11: Wing section to be idealized, subject to a bending moment

Since all skin panels experience both a tensile/compressive load together with a bending moment, equation is the ones to use when idealising this section.

Now, from symmetry: $B_1 = B_6$, $B_2 = B_5$ and $B_3 = B_4$, saving us some calculations.

Lets start with determining the area of boom 1.This boom must have first of all the area of spar cap 1, which is 300 mm^2, together with the area contributions of the two adjacent skins. Therefore:

$$B_1 = 300 + \frac{1.5 \times 600}{6}\left(2 + \frac{\sigma_2}{\sigma_1}\right) + \frac{2 \times 200}{6}\left(2 + \frac{\sigma_6}{\sigma_1}\right)$$

Since the equation for stress for a beam with symmetrical cross section is:

$$\sigma = \frac{\overline{M}_x}{I_{xx}}y + \frac{\overline{M}_y}{I_{yy}}x$$

Then by substituting this equation for the different stresses, their rations simplifies to just the rations of their vertical distances.

$$B_1 = 300 + \frac{1.5 \times 600}{6}\left(2 + \frac{150}{100}\right) + \frac{2 \times 200}{6}(2 - 1)$$

Which gives:

So $B_1 = B_6 = 891.67$ mm^2

For boom 2 we have to consider the contribution of the two spar caps, and the three adjacent skins. Giving:

$$B_2 = 2x300 + \frac{2x600}{6}\left(2 + \frac{\sigma_3}{\sigma_2}\right) + \frac{2.5x300}{6}\left(2 + \frac{\sigma_5}{\sigma_2}\right) + \frac{1.5x600}{6}\left(2 + \frac{\sigma_1}{\sigma_2}\right)$$

When substituting for the bending moment equation it becomes:

$$B_2 = 2x300 + \frac{2x600}{6}\left(2 + \frac{200}{150}\right) + \frac{2.5x300}{6}(2 - 1) + \frac{1.5x600}{6}\left(2 + \frac{100}{150}\right)$$

So $B_2 = B_5 = 1791.67 \text{ mm}^2$
And for boom 3 we only have one spar cap and two adjacent skins:

$$B_3 = 300 + \frac{2x600}{6}\left(2 + \frac{\sigma_2}{\sigma_3}\right) + \frac{3x400}{6}\left(2 + \frac{\sigma_4}{\sigma_3}\right)$$

and when substituting for the bending stress equation:

$$B_3 = 300 + \frac{2x600}{6}\left(2 + \frac{150}{200}\right) + \frac{3x400}{6}(2 - 1)$$

giving that $B_3 = B_4 = 1050 \text{ mm}^2$ So the idealised wing now looks like this:
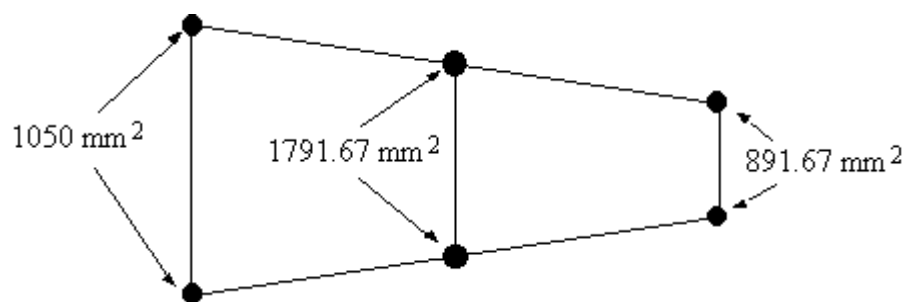
Figure 6.12: Final idealised wing with boom areas marked.

Example: The singly symmetrical fuselage cross-section is subjected to a bending moment Mx = 100 kNm. If all direct stresses are carried by the booms, determine the average direct stress in each boom.
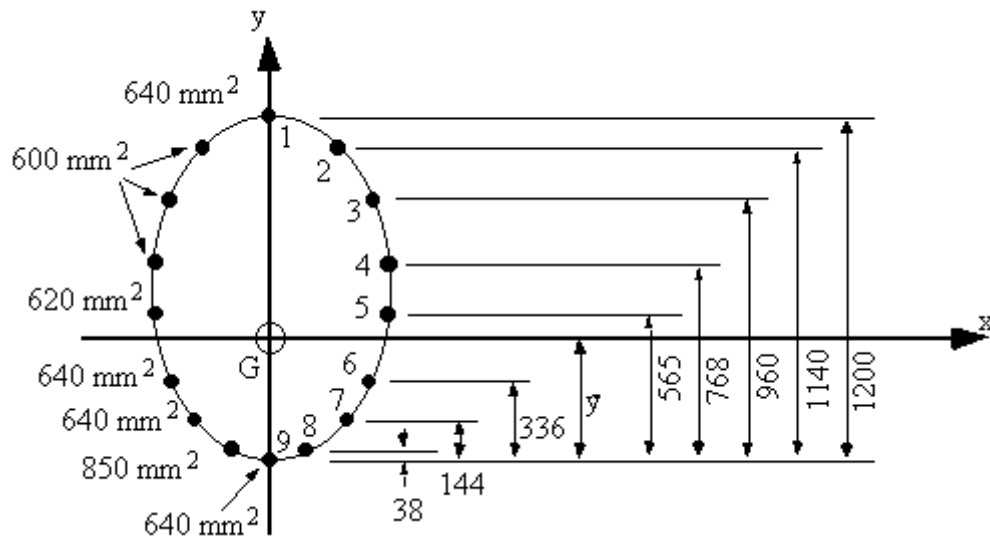
Figure 6.13: Idealised fuselage cross section.

Because the section is symmetrical about the y-axis ($I_{x,y} = 0$), and $M_y = 0$, the **effective bending moment** equations reduces to:

$$\sigma_z = \frac{M_x}{I_{xx}} y$$

a) Determine location of centroid

$$\bar{y} = \frac{1200 \times 640 + 2 \times 1140 \times 600 + 2 \times 960 \times 600 + 2 \times 768 \times 600 + 2 \times 565 \times 620 + 2 \times 336 \times 640 + 2 \times 144 \times 640 + 2 \times 38 \times 850}{640 \times 6 + 600 \times 6 + 620 \times 2 + 850 \times 2}$$

$$\bar{y} = 538.5mm$$

b) Determine sectional properties and stresses in booms
   Now that we have the position of the neutral axis, the best way to determine the stresses in each boom is by using a table

Boom	y (mm)	B (mm²)	$\Delta I_{xx} = By^2$ (mm⁴)	σ_z (MPa)
1	661.5	640	2.8005e+08	35.67
2	601.5	600	2.1708e+08	32.43

92

3	421.5	600	1.0660e+08	22.73
4	229.5	600	3.1602e+07	12.37
5	26.5	620	4.3540e+05	1.43
6	-202.5	640	2.6244e+07	-10.92
7	-394.5	640	9.9603e+07	-21.27
8	-500.5	850	2.1293e+08	-26.99
9	-538.5	640	1.8559e+08	-29.04
			I_{xx} =1.8546e+09	

Note: *Because of symmetry, this table doesn't contain values for the booms on the left hand side of the y-axis. However when calculating the second moment of area I_{xx}, the values of ΔI_{xx} for booms 2 - 8 were multiplied by 2 when doing the summation.*

Shear of Open Section Beams

The equation for shear flow for an open beam section was found by:

$$q_s = -\frac{\bar{S}_y}{I_{xx}} \int_0^s ty\,ds - \frac{\bar{S}_x}{I_{yy}} \int_0^s tx\,ds$$

From its derivation, the value of **'t'** was the direct stress carrying thickness **'t_D'** of the skin. Such that it could either be equal to:
$t_D = t$, if the skin was fully effective in carrying direct stress, Or
$t_D = 0$, if skin was assumed to carry only shear stresses.

 So:

$$q_s = -\frac{\bar{S}_y}{I_{xx}} \int_0^s t_D y\,ds - \frac{\bar{S}_x}{I_{yy}} \int_0^s t_D x\,ds$$

So that if we are idealising the beam's cross section, based on our idealisation technique, the value of 't_D' may or may not be equal to zero.

This equation, however does not consider the effect of the idealised booms to the overall shear flow. To account for this, we need to consider the equilibrium of one such boom.
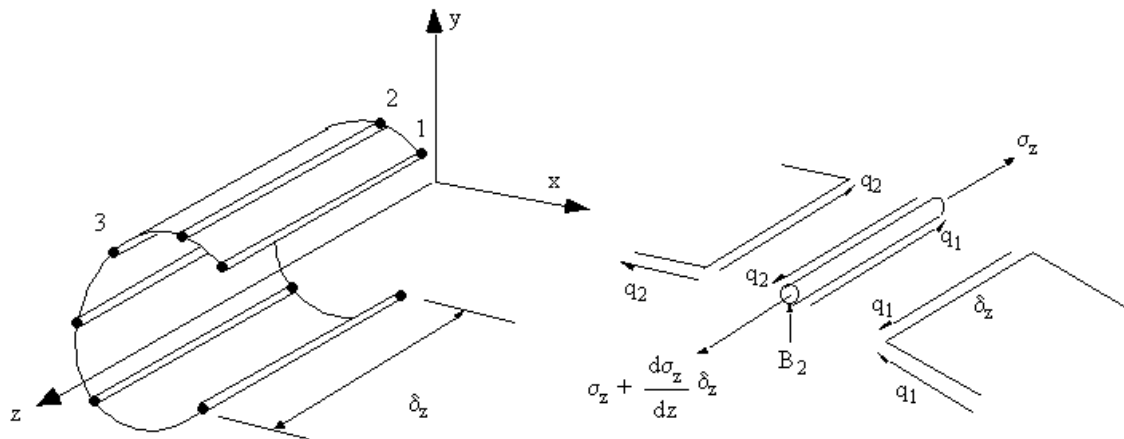
Figure 6.14: Shear loaded open beam with booms, and equilibrium of ith boom.

Summing the forces along the length of the elemental length of the boom gives:

$$\sum F_z = \left(\sigma_z + \frac{\partial \sigma_z}{\partial z}\delta_z\right)B_2 - \sigma_z B_2 + q_2\,\delta_z - q_1\delta_z = 0$$

this equation simplifies to :

$$q_2 - q_1 = -\frac{\partial \sigma_z}{\partial z}B_2$$

but since the direct stress is given by:

$$\sigma_z = \frac{\overline{M}_x}{I_{xx}}y + \frac{\overline{M}_y}{I_{yy}}x$$

then substituting for it gives:

$$\Delta q_{1-2} = q_2 - q_1 = -\frac{\overline{S}_y}{I_{xx}}B_2 y_2 - \frac{\overline{S}_x}{I_{yy}}B_2 x_2$$

Giving the change in shear flow induced in the skin by the presence of a boom. If several booms were present, their presence becomes an additive one, such that for a beam with 'n' booms becomes:

$$q_s = -\frac{\bar{S}_y}{I_{xx}}\left(\int_0^s t_D y \, ds + \sum_{i-1}^n B_i y_i\right) - \frac{\bar{S}_x}{I_{yy}}\left(\int_0^s t_D x \, ds + \sum_{i-1}^n B_i x_i\right)$$

But because in an idealised structure the skin only carries the shear stresses, then equation   can be simplified to have only the summation terms. To give:

$$q_s = -\frac{\bar{S}_y}{I_{xx}}\sum_{i-1}^n B_i y_i - \frac{\bar{S}_x}{I_{yy}}\sum_{i-1}^n B_i x_i$$

A simpler way of thinking of equation is by looking at the shear flow in a skin segment *i* due to the shear flow in skin segment *i-1* and the change of shear flow due to the boom *k* separating these two skin segments, Figure 7.17.
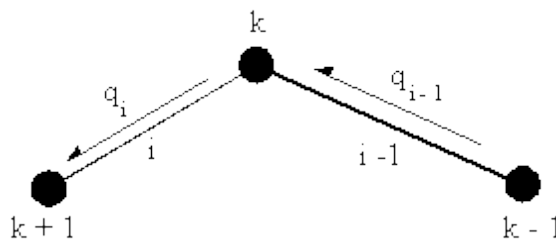
Figure 6.15: Sketch of skin segments *i* and *i-1* and boom *k* to show how the shear flow is determined.

In general terms, the change in shear flow between any two skin elements (*i* and *i-1*) due to the area of boom *k* of coordinates x_k and y_k about the structures' centroid is:

$$\Delta q_k = -\frac{\bar{S}_y}{I_{xx}}B_k y_k - \frac{\bar{S}_x}{I_{yy}}B_k x_k$$

The **shear flow** in skin segment *i* is then a function of the **shear flow** in the previous **skin segment** (*i - 1*) and the change in shear flow due to **boom** k(Δq_k),

$$q_i = q_{i-1} + \Delta q_k$$

Note: *Because of the idealisation process, the shear flow in any skin section between any two booms always has a constant value.*

95

Example 9: Calculate the shear flow in the following channel section. The skin is only effective in shear ($t_D=0$), area of all booms 1 & 4 = 250 mm^{2}, areas of booms 2& 3 = 350 mm^2.
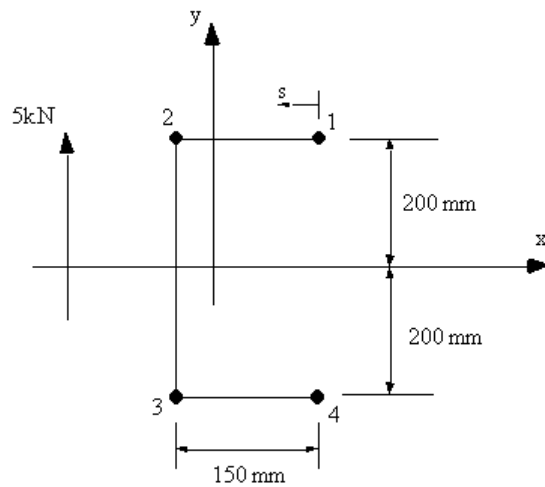
Figure 6.16: Open channel with force applied through shear center.

Because the structure is symmetrical $I_{xy} = 0$ and as we are only applying a vertical load, equation above becomes:

$$q_s = -\frac{S_y}{I_{xx}}\sum_{i-1}^{n} B_i y_i$$

The second moment of area I_{xx} is:

$$I_{xx} = 48 x 10^6 mm^4$$

On the RHS of boom 1, $q_s = 0$, so the change in shear flow due to boom 1 is:

1) $\Delta q_1 = q_{12} = -5.280 N / mm$

2) $\Delta q_1 = q_{12} = 5.208 N / mm$

3) $\Delta q_1 = q_{12} = -5.208 N / mm$

4) $\Delta q_1 = q_{12} = 5.280 N / mm$

this shear flow is constant until boom 2, where:

1) $q_{23} = q_{12} + \Delta q_2 = 12.05 N / mm$

96

2) $q_{23} = q_{12} + \Delta q_2 = -12.5 N/mm$

3) $q_{23} = q_{12} + \Delta q_2 = -12.05 N/mm$

4) $q_{23} = q_{12} + \Delta q_2 = 12.5 N/mm$

which is constant until boom 3, where:

1) $q_{34} = q_{23} + \Delta q_3 = -5.280 N/mm$

2) $q_{34} = q_{23} + \Delta q_3 = 5.208 N/mm$

3) $q_{34} = q_{23} + \Delta q_3 = 5.280 N/mm$

4) $q_{34} = q_{23} + \Delta q_3 = -5.208 N/mm$

and you can see that after boom 4, q = 0

Figure 6.17: Shear flow distribution around channel.

Shear of Closed Section Beams

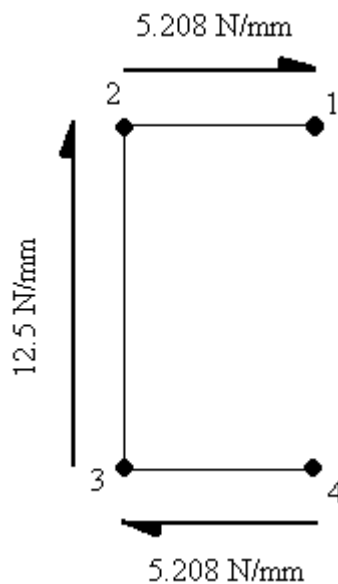The derivation of the equation to determine this shear flow is identical as the analysis for open beam sections, making equation look like this:

$$q_s = q_{s,0} - \frac{\bar{S}_y}{I_{xx}}\left(\int_0^s t_D y\, ds + \sum_{i-1}^n B_i y_i\right) - \frac{\bar{S}_x}{I_{yy}}\left(\int_0^s t_D x\, ds + \sum_{i-1}^n B_i x_i\right)$$

Since the structure has been idealised, then equation is simplified to:

$$q_{s_i} = q_{s,0} + q_{b_i}$$

Where:

q_{bi} - is the open beam shear flow of skin segment i, and which can be calculated using equation above.

$q_{s,0}$ - in the residual shear flow due to making the closed beam into an open beam section. It can be calculated if we know the location of the applied load, or if we are trying to determine the shear center.

Example: Determine shear flow in the following wing structure with an applied vertical load in the plane of booms 3 and 6. This structure has been idealised into direct stress carrying booms and shear only stress skin ($t_D = 0$). Boom areas are: $B_1 = B_8 = 200$ mm^2, $B_2 = B_7 = 300$ mm^2, $B_3 = B_6 = 400$ mm^2, $B_4 = B_5 = 150$ mm^2.
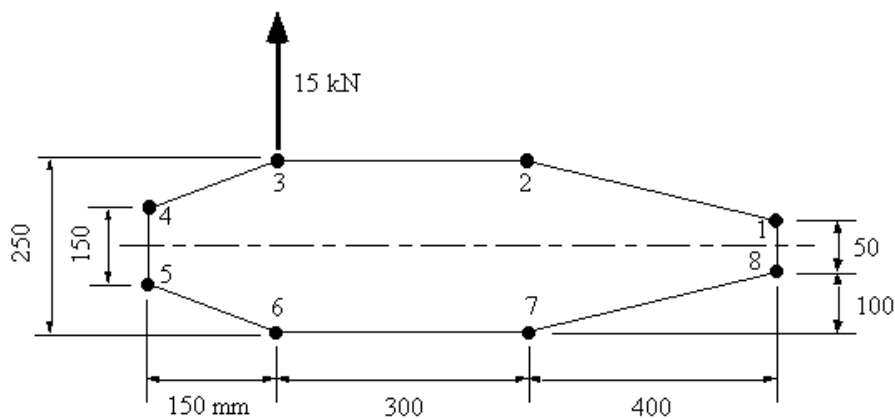
Figure 6.18: Closed wing section with applied shear force between booms 3 & 6

Because the section is symmetrical, $I_{xy} = 0$. Skin carries only shear load, $t_D = 0$ so use equation. Only a vertical load is applied, $S_x = 0$. Reducing equation to:

$$q_s = q_{s,0} - \frac{S_y}{I_{xx}} \sum_{r=1}^{n} B_r y_r \quad \text{(i)}$$

Where; $S_y = 15$ kN

$I_{xx} = 2 \times (200 \times 25^2 + 300 \times 125^2 + 400 \times 125^2 + 150 \times 75^2) = 23.813 \times 10^6$ mm^4

Substituting this into the above equation gives:

$$q_s = -6.2991 \times 10^{-4} \sum_{r-1}^{n} B_r y_r + q_{s,0} = q_b + q_{s,0} \qquad \text{(ii)}$$

Where q_b is the shear flow for an open section. Cutting the beam between sections 2 and 3 and doing the analysis in a counter clockwise sense we get:

$$q_{b_{2,3}} = 0$$

$$q_{b_{3,4}} = -6.2991 \times 10^{-4} (400 \times 125) = -31.5 N/mm$$

$$q_{b_{4,5}} = -31.5 - 6.2991 \times 10^{-4} (150 \times 75) = -38.59 N/mm$$

$$q_{b_{5,6}} = -38.59 - 6.291 \times 10^{-4} (150 \times (-75)) = -31.5 N/mm$$

$$q_{b_{6,7}} = -31.5 - 6.2991 \times 10^{-4} (400 \times (-125)) = 0 N/mm$$

$$q_{b_{7,8}} = -6.2991 \times 10^{-4} (300 \times (-125)) = 23.62 N/mm$$

$$q_{b_{8,1}} = 23.61 - 6.2991 \times 10^{-4} (200 \times (-25)) = 26.77 N/mm$$

$$q_{b_{1,2}} = 26.77 - 6.2991 \times 10^{-4} (200 \times 25) = 23.62 N/mm$$

It is now necessary to determine $q_{s,0}$. This can be done by using equation above, because we know the position of the applied force. Or we could take moments anywhere about the line of action of the applied force; both these statements mean the same thing.

Taking moments about point 3, gives:
$0 = (q_{4,5} \times 150 \times 150 + q_{5,6x} \times 158.11 \times 237.17 + q_{6,7} \times 300 \times 250 + q_{7,8} \times 412.31 \times 315.3 + q_{8,1} \times 50 \times 700 + q_{1,2} \times 412.31 \times 72.76) + 2 \times 165,000 q_{s,0}$

giving that $q_{s,0}$ = -8.08 N/mm From equation (ii) above we have that $q_s = q_b + q_{s,0}$, so:

$$q_{s12} = 23.62 - 8.08 \qquad = 15.54 \text{ N/mm}$$

$$q_{s23} = 0 - 8.08 \qquad = -8.08 \text{ N/mm}$$

$q_{s34} = -31.5 - 8.08 \quad\quad = -39.58 \text{ N/mm}$

$q_{s45} = -38.59 - 8.08 \quad\quad = -46.67 \text{ N/mm}$

$q_{s56} = -31.5 - 8.08 \quad\quad = -39.58 \text{ N/mm}$

$q_{s67} = 0 - 8.08 \quad\quad\quad = -8.08 \text{ N/mm}$

$q_{s78} = 23.62 - 8.08 \quad\quad = 15.54 \text{ N/mm}$

$q_{s81} = 26.67 - 8.08 \quad\quad = 18.59 \text{ N/mm}$
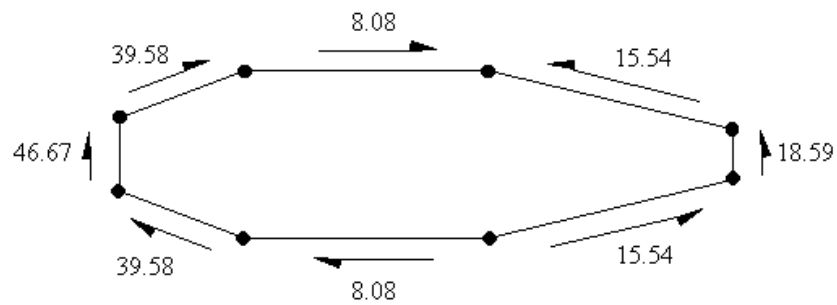
Figure 6.19: Shear flow distribution of loaded closed wing section

Aircraft fuselages consist of thin sheets of material stiffened by large numbers of longitudinal stringers together with transverse frames. Generally, they carry bending moments, shear forces and torsional loads which induce axial stresses in the stringers and skin together with shear stresses in the skin; the resistance of the stringers to shear forces is generally ignored. Also, the distance between adjacent stringers is usually small so that the variation in shear flow in the connecting panel will be small. It is therefore reasonable to assume that the shear flow is constant between adjacent stringers so that the analysis simplifies to the analysis of an idealized section in which the stringers/booms carry all the direct stresses while the skin is effective only in shear. The direct stress carrying capacity of the skin may be allowed for by increasing the stringer/boom areas. The analysis of fuselages therefore involves the calculation of direct stresses in the stringers and the shear stress distributions in the skin. The following previous Eqs. Were used previously,

$$\sigma_z = \left(\frac{M_y I_{xx} - M_x I_{xy}}{I_{xx} I_{yy} - I_{xy}^2} \right) x + \left(\frac{M_x I_{yy} - M_y I_{xy}}{I_{xx} I_{yy} - I_{xy}^2} \right) y$$

$$(7.1)$$

$$\sigma_z = \frac{M_x(I_{yy} y - I_{xy} x)}{I_{xx} I_{yy} - I_{xy}^2} + \frac{M_y(I_{xx} x - I_{xy} y)}{I_{xx} I_{yy} - I_{xy}^2}$$

$$(7.2)$$

$$B_1 = \frac{t_D b}{6} \left(2 + \frac{\sigma_2}{\sigma_1} \right)$$

$$(7.3)$$

$$q_s = -\left(\frac{S_x I_{xx} - S_y I_{xy}}{I_{xx} I_{yy} - I_{xy}^2}\right)\left(\int_0^s t_D x \, ds + \sum_{r=1}^n B_r x_r\right)$$

$$-\left(\frac{S_y I_{yy} - S_x I_{xy}}{I_{xx} I_{yy} - I_{xy}^2}\right)\left(\int_0^s t_D y \, ds + \sum_{r=1}^n B_r y_r\right) + q_{s,0}$$

<div align="right">(7.4)</div>

$$S_x \eta_0 - S_y \xi_0 = \oint p q_b \, ds + 2A q_{s,0}$$

<div align="right">(7.5)</div>

$$M_q = 2A q_{12}$$

<div align="right">(7.6)</div>

7.1 Bending Stresses

The skin/stringer arrangement is idealized into one comprising booms and skin. The direct stress in each boom is then calculated using either Eqs. (7.1) or (7.2) in which the reference axes and the section properties refer to the direct stress carrying areas of the cross-section.

Example 7.1: The fuselage of a light passenger carrying aircraft has the circular cross-section shown in Fig. 7.1(a). The cross-sectional area of each stringer is 100 mm² and the vertical distances given in Fig. 7.1(b) are to the mid-line of the section wall at the corresponding stringer position. If the fuselage is subjected to a bending moment of 200 kNm applied in the vertical plane of symmetry, at this section, calculate the direct stress distribution.

The section is first idealized using the method described in Section 20.3. As an approximation we shall assume that the skin between adjacent stringers is flat so that:
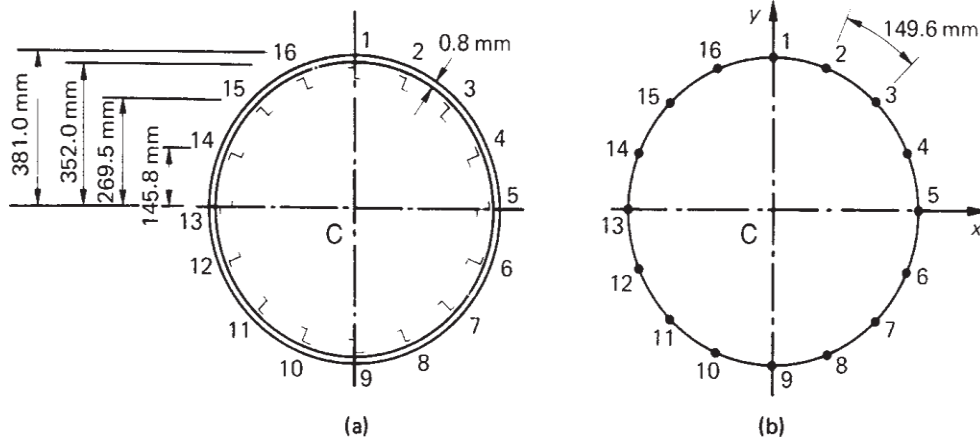
Fig. 7.1

we may use either Eq. (7.3) to determine the boom areas. From symmetry $B1 = B9$, $B2 = B8 = B10 = B16$, $B3 = B7 = B11 = B15$, $B4 = B6 = B12 = B14$ and $B5 = B13$. From Eq. (7.3)

$$B_1 = 100 + \frac{0.8 \times 149.6}{6}\left(2 + \frac{\sigma_2}{\sigma_1}\right) + \frac{0.8 \times 149.6}{6}\left(2 + \frac{\sigma_{16}}{\sigma_1}\right)$$

i.e.

$$B_1 = 100 + \frac{0.8 \times 149.6}{6}\left(2 + \frac{352.0}{381.0}\right) \times 2 = 216.6 \, \text{mm}^2$$

Similarly, $B2 = 216.6 \text{ mm}^2$, $B3 = 216.6 \text{ mm}^2$, $B4 = 216.7 \text{ mm}^2$. We note that stringers 5 and 13 lie on the neutral axis of the section and are therefore unstressed; the calculation of boom areas $B5$ and $B13$ does not then arise. For this particular section $Ixy = 0$ since Cx (and Cy) is an axis of symmetry. Further, $My = 0$ so that Eq. (7.1) reduces to

$$\sigma_z = \frac{M_x y}{I_{xx}}$$

in which

$$I_{xx} = 2 \times 216.6 \times 381.0^2 + 4 \times 216.6 \times 352.0^2 + 4 \times 216.6 \times 2695^2$$
$$+ 4 \times 216.7 \times 145.8^2 = 2.52 \times 10^8 \, \text{mm}^4$$

The solution is completed in Table 7.1.

Stringer/boom	y (mm)	σ_z (N/mm^2)
1	381.0	302.4
2, 16	352.0	279.4
3, 15	269.5	213.9
4, 14	145.8	115.7
5, 13	0	0
6, 12	−145.8	−115.7
7, 11	−269.5	−213.9
8, 10	−352.0	−279.4
9	−381.0	−302.4

7.2 Shear Flow Distribution

For a fuselage having a cross-section of the type shown in Fig. 7.1(a), the determination of the shear flow distribution in the skin produced by shear is basically the analysis of an idealized single cell closed section beam. The shear flow distribution is therefore given by Eq. (7.4) in which the direct stress carrying capacity of the skin is assumed to be zero, i.e. $t_D = 0$, thus

$$q_s = -\left(\frac{S_x I_{xx} - S_y I_{xy}}{I_{xx}I_{yy} - I_{xy}^2}\right)\sum_{r=1}^{n} B_r y_r - \left(\frac{S_y I_{yy} - S_x I_{xy}}{I_{xx}I_{yy} - I_{xy}^2}\right)\sum_{r=1}^{n} B_r x_r + q_{s,0}$$

Equation (7.5) is applicable to loading cases in which the shear loads are not applied through the section shear centre so that the effects of shear and torsion are included simultaneously. Alternatively, if the position of the shear centre is known, the loading system may be replaced by shear loads acting through the shear centre together with a pure torque, and the corresponding shear flow distributions may be calculated separately and then superimposed to obtain the final distribution.

Example 7.2: The fuselage of Example 7.1 is subjected to a vertical shear load of 100 kN applied at a distance of 150 mm from the vertical axis of

symmetry as shown, for the idealized section, in Fig. 7.2. Calculate the distribution of shear flow in the section.

As in Example 7.1, $Ixy = 0$ and, since $Sx = 0$, Eq. (7.4) reduces to

$$q_s = -\frac{S_y}{I_{xx}} \sum_{r=1}^{n} B_r y_r + q_{s,0} \tag{i}$$

in which $I_{xx} = 2.52 \times 10^8$ mm^4 as before. Then

$$q_s = \frac{-100 \times 10^3}{2.52 \times 10^8} \sum_{r=1}^{n} B_r y_r + q_{s,0}$$

or

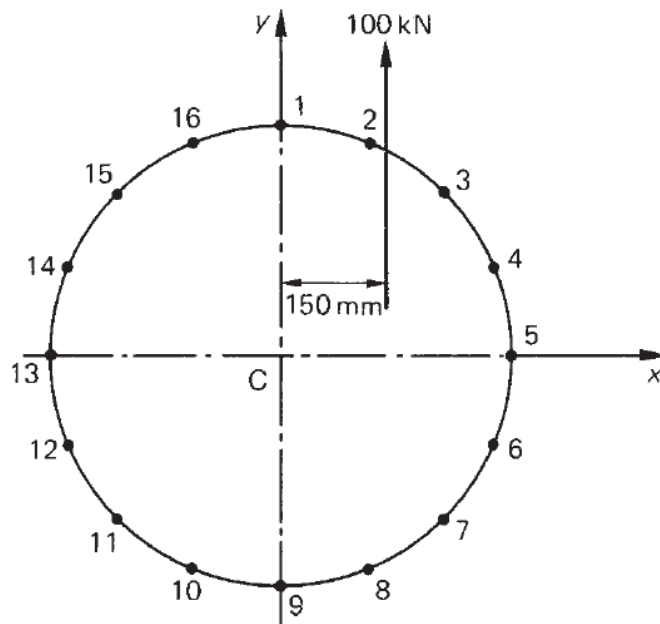$$q_s = -3.97 \times 10^{-4} \sum_{r=1}^{n} B_r y_r + q_{s,0} \tag{ii}$$

Fig. 7.2

Table 7.2

Skin panel	Boom	B_r (mm^2)	y_r (mm)	q_b (N/mm)
1 2		–	–	0
2 3	2	216.6	352.0	−30.3
3 4	3	216.6	269.5	−53.5
4 5	4	216.7	145.8	−66.0
5 6	5	–	0	−66.0
6 7	6	216.7	−145.8	−53.5
7 8	7	216.6	−269.5	−30.3
8 9	8	216.6	−352.0	0
1 16	1	216.6	381.0	−32.8
16 15	16	216.6	352.0	−63.1
15 14	15	216.6	269.5	−86.3
14 13	14	216.6	145.8	−98.8
13 12	13	–	0	−98.8
12 11	12	216.7	−145.8	−86.3
11 10	11	216.6	−269.5	−63.1
10 9	10	216.6	−352.0	−32.8

The first term on the right-hand side of Eq. (ii) is the 'open section' shear flow q_b. We therefore 'cut' one of the skin panels, say 12, and calculate q_b. The results are presented in Table 7.2. Note that in Table 7.2, the column headed Boom indicates the boom that is crossed when the analysis moves from one panel to the next. Note also that, as would be expected, the q_b shear flow distribution is symmetrical about the Cx axis. The shear flow $q_{s,0}$ in the panel 12 is now found by taking moments about a convenient moment centre, say C. Therefore, from Eq. (7.6):

$$100 \times 10^3 \times 150 = \oint q_b \, p \, ds + 2Aq_{s,0} \qquad \text{(iii)}$$

in which $A = \pi \times 381.02 = 4.56 \times 105 \text{ mm}^2$. Since the q_b shear flows are constant between the booms, Eq. (iii) may be rewritten in the form (see Eq. (7.7))

$$100 \times 10^3 \times 150 = -2A_{12}q_{b,12} - 2A_{23}q_{b,23} - \cdots - 2A_{161}q_{b,161} + 2Aq_{s,0} \qquad \text{(iv)}$$

in which $A12$, $A23$, ..., $A161$ are the areas subtended by the skin panels 12, 23,…, 16 1 at the centre C of the circular cross-section and anticlockwise moments are taken as positive. Clearly $A12 = A23 = \cdots = A16\ 1 = 4.56 \times 105/16 = 28\ 500 \text{ mm}^2$. Equation (iv) then becomes

$$100 \times 10^3 \times 150 = 2 \times 28\,500(-q_{b12} - q_{b23} - \cdots - q_{b161}) + 2 \times 4.56 \times 10^5 q_{s,0} \qquad \text{(v)}$$

Substituting the values of q_b from Table 7.2 in Eq. (v), we obtain

$$100 \times 10^3 \times 150 = 2 \times 28\,500(-262.4) + 2 \times 4.56 \times 10^5 q_{s,0}$$

from which $q_{s,0} = 32.8$ N/mm (acting in an anticlockwise sense) The complete shear flow distribution follows by adding the value of $q_{s,0}$ to the q_b shear flow distribution, giving the final distribution shown in Fig. 7.3. The solution may be checked by calculating the resultant of the shear flow distribution parallel to the Cy axis. Thus

$$2[(98.8 + 66.0)145.8 + (86.3 + 53.5)123.7 + (63.1 + 30.3)82.5$$
$$+ (32.8 - 0)29.0] \times 10^{-3} = 99.96\,\text{kN}$$

Fig. 7.3

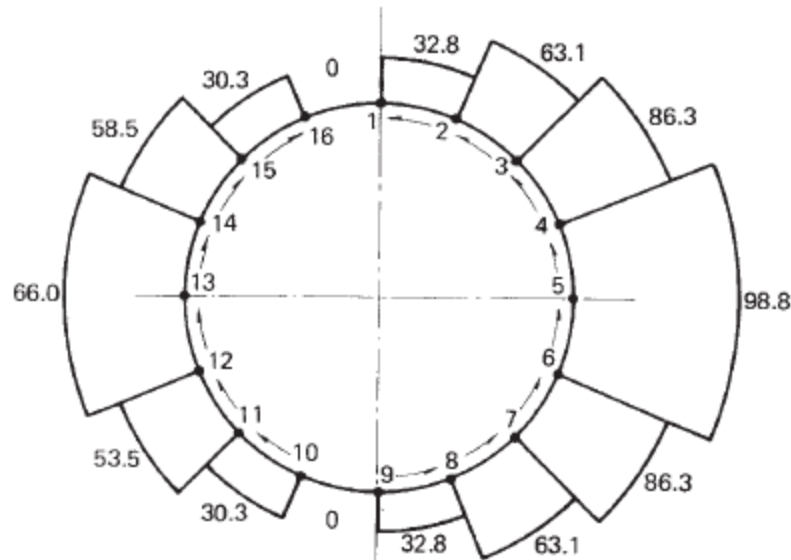## 7.2 Shear Flow Due to Torque

A fuselage section is basically a single cell closed section beam. The shear flow distribution produced by a pure torque is therefore given by:

$$q = \frac{T}{2A}$$

(7.8)

It is immaterial whether or not the section has been idealized since, in both cases, the booms are assumed not to carry shear stresses. Equation (7.8) provides an alternative approach to that illustrated in Example 7.2 for the solution of shear loaded sections in which the position of the shear centre is known. In Fig. 7.1 the shear centre coincides with the centre of symmetry so that the loading system may be replaced by the shear load of 100 kN acting through the shear centre together with a pure torque equal to 100×103 ×150=15×106 Nmm as shown in Fig. 7.4. The shear flow distribution due to the shear load may be found using the method of Example 7.2 but with the left-hand side of the moment equation (iii) equal to zero for moments about the centre of symmetry. Alternatively, use may be made of the symmetry of the section and the fact that the shear flow is constant between adjacent

108

booms. Suppose that the shear flow in the panel 21 is $q_{2\,1}$. Then from symmetry and using the results of Table 7.2

$$q_{98} = q_{9\,10} = q_{16\,1} = q_{21}$$

$$q_{32} = q_{87} = q_{10\,11} = q_{15\,16} = 30.3 + q_{21}$$
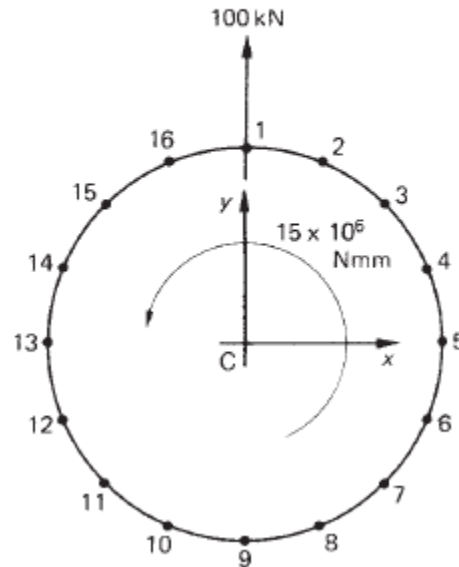
$$q_{43} = q_{76} = q_{11\,12} = q_{14\,15} = 53.5 + q_{21}$$

$$q_{54} = q_{65} = q_{12\,13} = q_{13\,14} = 66.0 + q_{21}$$

Fig. 7.4

The resultant of these shear flows is statically equivalent to the applied shear load so that

$$4(29.0q_{21} + 82.5q_{32} + 123.7q_{43} + 145.8q_{54}) = 100 \times 10^3$$

$$4(381q_{21} + 18\,740.5) = 100 \times 10^3$$

whence

$$q_{21} = 16.4\,\text{N/mm}$$

$$q_{32} = 46.7\,\text{N/mm}, \quad q_{43} = 69.9\,\text{N/mm}, \quad q_{54} = 83.4\,\text{N/mm etc.}$$

The shear flow distribution due to the applied torque is,

$$q = \frac{15 \times 10^6}{2 \times 4.56 \times 10^5} = 16.4\,\text{N/mm}$$

acting in an anticlockwise sense completely around the section. This value of shear flow is now superimposed on the shear flows produced by the shear load; this gives the solution shown in Fig. 7.3, i.e.

$$q_{21} = 16.4 + 16.4 = 32.8\,\text{N/mm}$$
$$q_{161} = 16.4 - 16.4 = 0 \text{ etc.}$$

7.4 Cutouts in Fuselage

So far we have considered fuselages to be closed sections stiffened by transverse frames and longitudinal stringers. In practice it is necessary to provide openings in these closed stiffened shells for, for example, doors, cockpits, bomb bays, windows in passenger cabins, etc. These openings or 'cut-outs' produce discontinuities in the otherwise continuous shell structure so that loads are redistributed in the vicinity of the cut-out thereby affecting loads in the skin, stringers and frames. Frequently these regions must be heavily reinforced resulting in unavoidable weight increases. In some cases, for example door openings in passenger aircraft, it is not possible to provide rigid fuselage frames on each side of the opening because the cabin space must not be restricted. In such situations a rigid frame is placed around the opening to resist shear loads and to transmit loads from one side of the opening to the other.

The effects of smaller cut-outs, such as those required for rows of windows in passenger aircraft, may be found approximately as follows. Figure 7.5 shows a fuselage panel provided with cut-outs for windows which are spaced a distance l apart. The panel is subjected to an average shear flow q_{av} which would be the value of the shear
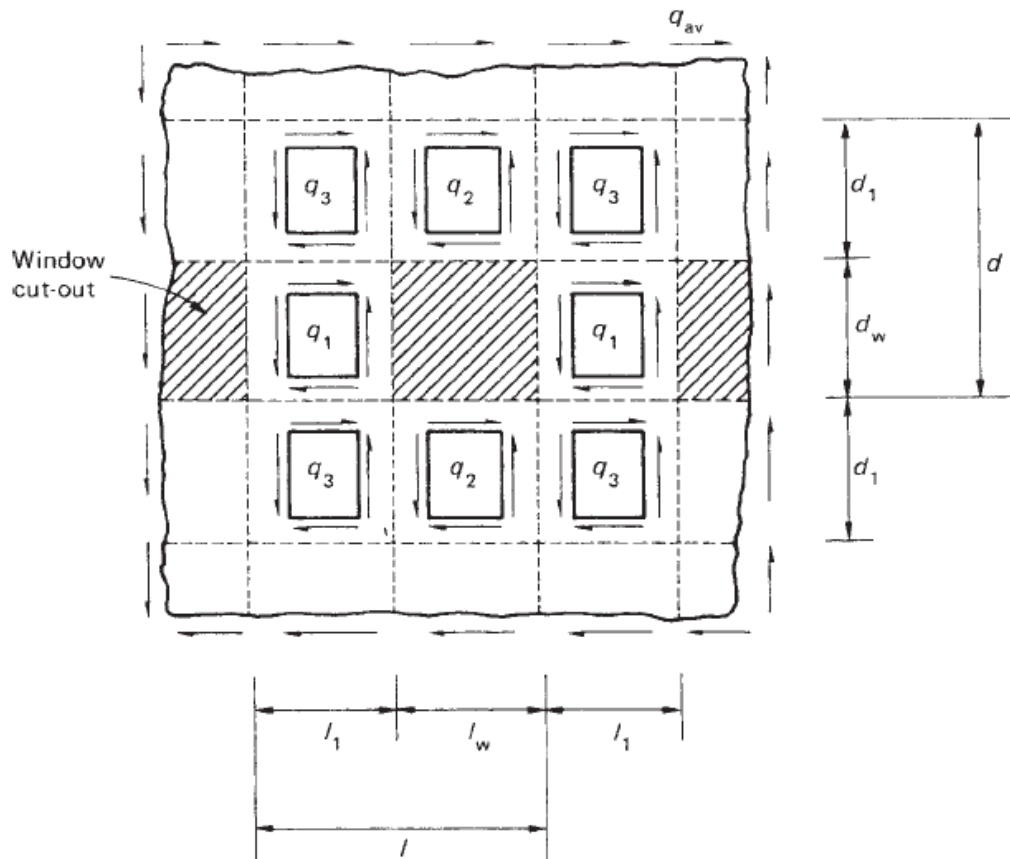
Fig. 7.5

flow in the panel without cut-outs. Considering a horizontal length of the panel through the cut-outs we see that

$$q_1 l_1 = q_{av} l$$

or

$$q_1 = \frac{l}{l_1} q_{av}$$

<div align="right">(7.9)</div>

Now considering a vertical length of the panel through the cut-outs

$$q_2 d_1 = q_{av} d$$

or

$$q_2 = \frac{d}{d_1} q_{av}$$

The shear flows q_3 may be obtained by considering either vertical or horizontal sections not containing the cut-out. Thus

$$q_3 l_1 + q_2 l_w = q_{av} l$$

Substituting for $q2$ from Eq. (7.10) and noting that $l = l1 + lw$ and $d = d1 + dw$, we obtain

$$q_3 = \left(1 - \frac{d_w}{d_1} \frac{l_w}{l_1} \right) q_{av}$$

Chapter Eight

Wing with Multi cell section

Wing sections consist of thin skins stiffened by combinations of stringers, spar webs, and caps and ribs. The resulting structure frequently comprises one, two or more cells, and is highly redundant.

8.1 Bending

Bending moments at any section of a wing are usually produced by shear loads at other sections of the wing. The direct stress system for such a wing section (Fig. 8.1) is given by:

$$\sigma = \left(\frac{M_y\, I_{xx} - M_x\, I_{xy}}{I_{xx}\, I_{yy} - I^2_{xy}}\right).x + \left(\frac{M_x\, I_{yy} - M_y\, I_{xy}}{I_{xx}\, I_{yy} - I^2_{xy}}\right).y$$

(8.1)

In which the coordinates (x, y) of any point in the cross-section and the sectional properties are referred to axes C_{xy} in which the origin C coincides with the centroid of the direct stress carrying area.
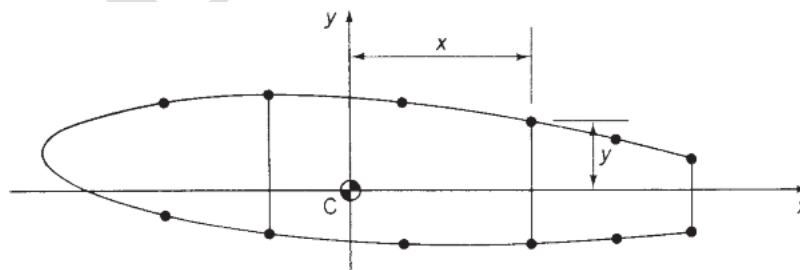
Fig. 8.1

Example 8.1

The wing section shown in Fig. 8.2 has been idealized such that the booms carry all the direct stresses. If the wing section is subjected to a bending moment of 300 kN. m applied in a vertical plane, calculate the direct stresses in the booms.

Boom areas: $B_1 = B_6 = 2580 \ mm^2$ $B_2 = B_5 = 3880 \ mm^2$ $B_3 = B_4 \ 3230 \ mm^2$

Solution:

The distribution of the boom areas is symmetrical about the horizontal x axis. $I_{xy} = 0$, $M_x = 300$ kN.m and $M_y = 0$, so that Eq. (8.1) becomes,

$$\sigma = \left(\frac{M_x}{I_{xx}}\right).y$$

In which,

$$I_{xx} = 2(2580 \times 165^2 + 3880 \times 230^2 + 3230 \times 200^2) = 809 \times 10^2 \ mm^2$$

Hence,

$$\sigma = \left(\frac{300 \times 10^6}{809 \times 10^2}\right).y \ \ = \ 0.371 \ y$$

Fig. 8.2

Boom	y (mm)	σ_z (N/mm^2)
1	165	61.2
2	230	85.3
3	200	74.2
4	−200	−74.2
5	−230	−85.3
6	−165	−61.2

8.2 Torsion

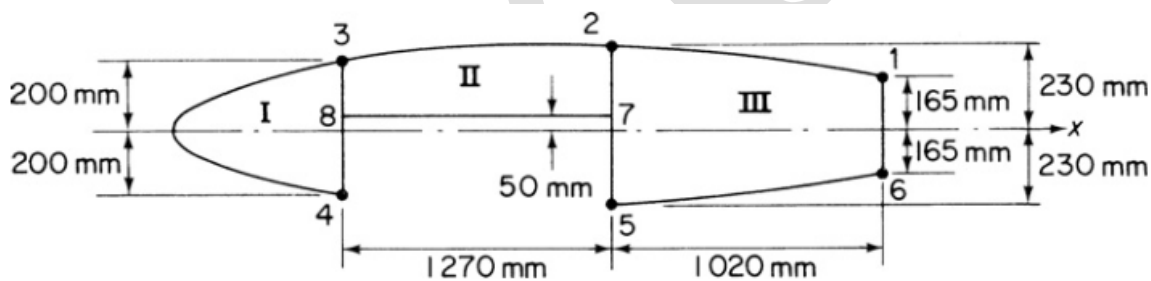The chord wise pressure distribution on an aerodynamic surface may be represented by shear loads (lift and drag loads) acting through the aerodynamic center together with a pitching moment M_O. This system of shear loads may be transferred to the shear center of the section in the form of shear loads S_x and S_y together with a torque T. It is the pure torsion case that is considered here. In the analysis it is assumed that no axial constraint effects are present and that the shape of the wing section remains unchanged by the load application. In the absence of axial constraint there is no development of direct stress in the wing section so that only shear stresses are present. It follows that the presence of booms does not affect the analysis in the pure torsion case.

The wing section shown in Fig. 8.3 comprises N cells and carries a torque T which generates individual but unknown torques in each of the N cells. Each cell therefore develops a constant shear flow $q_I, q_{II}, \ldots, q_R, \ldots q_N$ given by:
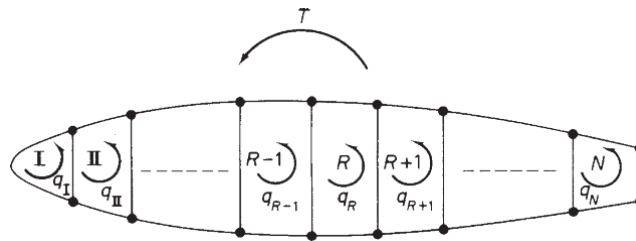

Fig. 8.3

$T = 2Aq$

The total therefore

$T = \sum_{R=1}^{N} 2A_R q_R$ (7.2)

This is sufficient for single cell.

For N cell section additional equations are required, this obtained by considering the rate of twist in each cell and the compatibility of displacement condition that all N cells possess the same rate of twist $d\theta/dz$

Consider the Rth cell of the wing section shown in Fig. 8.4. The rate of twist in the cell is:

$$\frac{d\theta}{dz} = \frac{1}{2A_R G} \oint_R q \frac{ds}{t} \qquad (8.3)$$

The shear flow in Eq. (8.3) is constant along each wall of the cell and has the value shown in Fig. 8.3 q_{R-1}, q_R, q_{R+1}.

Let $\frac{ds}{t} = \delta$ then Eq. (8.3) becomes:

In general terms, this equation may be rewritten in the form,

$$\frac{d\theta}{dz} = \frac{1}{2A_R G} \left[-q_{R-1} \delta_{R-1,R} + q_R \delta_R - q_{R+1} \delta_{R+1,R} \right] \qquad (8.4)$$

For Fig. 7.4, we can apply Eq. (8.4) as follows,

$$\frac{d\theta}{dz} = \frac{1}{2A_R G} \left[q_R \delta_{12} + (q_R - q_{R-1}) \delta_{23} + q_R \delta_{34} + (q_R - q_{R+1}) \delta_{41} \right]$$

Or, rearranging the terms in squares brackets

$$\frac{d\theta}{dz} = \frac{1}{2A_R G} \left[-q_{R-1} \delta_{23} + q_R (\delta_{12} + \delta_{23} + \delta_{34} + \delta_{41}) - q_{R+1} \delta_{41} \right]$$

In which $\delta_{R-1,R}$ is $\frac{ds}{t}$ for the wall common to the Rth and (R-1) the cells, δ_R is $\frac{ds}{t}$ for all the walls enclosing the Rth cell and $\delta_{R+1,R}$ is $\frac{ds}{t}$ for the wall common to the Rth and (R+1) the cells.

Eq. (8.4) is applicable to multi cell sections in which the cells are connected consecutively. Cell I connected to cell II, cell II to cells I and III and so on.

Note: if the skin panels and spar webs are fabricated from materials possessing different properties such that the shear modulus G is not constant. The analysis of such sections is simplified if the actual thickness t of a wall is converted to a modulus weighted thickness t* .

For the Rth cell of an N-cell wing section in which G varies from wall to wall, Eq. (8.4) takes the form:

$$\frac{d\theta}{dz} = \frac{1}{2A_R} \oint_R q \frac{ds}{Gt} \tag{8.5}$$

This equation may be rewritten as,

$$\frac{d\theta}{dz} = \frac{1}{2A_R} \oint_R q \frac{ds}{(G/G_{REF})t} \tag{8.6}$$

In which G_{REF} is a convenient reference value of the shear modulus. Eq. (8.6) is now rewritten as,

$$\frac{d\theta}{dz} = \frac{1}{2A_R G_{REF}} \oint_R q \frac{ds}{t^*} \tag{8.7}$$

Modulus – weighted thickness,

$$t^* = \left(\frac{G}{G_{REF}}\right) t \tag{8.7a}$$

Then $\delta = \int \frac{ds}{t^*}$ in Eq. (8.4).

Example 8.2

Calculate the shear stress distribution in the walls of the three- cell wing section shown in Fig. 8.4 when it is subjected to an anticlockwise torque of 11.3 kN.m.

Wall	Length (mm)	Thickness (mm)	G (N/mm²)	Cell area (mm²)
12º	1650	1.22	24 200	$A_I = 258\,000$
12ⁱ	508	2.03	27 600	$A_{II} = 355\,000$
13, 24	775	1.22	24 200	$A_{III} = 161\,000$
34	380	1.63	27 600	
35, 46	508	0.92	20 700	
56	254	0.92	20 700	

Note: The superscript symbols o and i are used to distinguish between outer and inner walls connecting the same two booms.
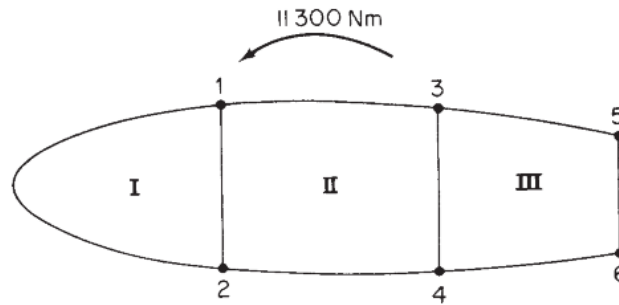
Fig. 8.4

Since the wing section is loaded by a pure torque the presence of the booms has no effect on the analysis.

Choosing $G_{REF} = 27600$ N/mm²

$$t_{12^\circ}^* = \frac{24\,200}{27\,600} \times 1.22 = 1.07 \text{ mm}$$

Similarly:

$$t_{13}^* = t_{24}^* = 1.07 \text{ mm} \quad t_{35}^* = t_{46}^* = t_{56}^* = 0.69 \text{ mm}$$

$$\delta_{12^\circ} = \int_{12^\circ} \frac{ds}{t^*} = \frac{1650}{1.07} = 1542$$

Similarly

$$\delta_{12i} = 250 \quad \delta_{13} = \delta_{24} = 725 \quad \delta_{34} = 233 \quad \delta_{35} = \delta_{46} = 736 \quad \delta_{56} = 368$$

- For cell I

$$\frac{d\theta}{dz} = \frac{1}{2 \times 258\,000 G_{REF}} [q_I(1542 + 250) - 250q_{II}] \qquad \text{(i)}$$

- For cell II

$$\frac{d\theta}{dz} = \frac{1}{2 \times 355\,000 G_{REF}} [-250q_I + q_{II}(250 + 725 + 233 + 725) - 233q_{III}] \qquad \text{(ii)}$$

- For cell III

$$\frac{d\theta}{dz} = \frac{1}{2 \times 161\,000 G_{REF}} [-233q_{II} + q_{III}(736 + 233 + 736 + 368)] \qquad \text{(iii)}$$

118

$$T = \sum_{R=1}^{N} 2A_R q_R$$

$$11.3 \times 10^6 = 2(258\,000 q_{\mathrm{I}} + 355\,000 q_{\mathrm{II}} + 161\,000 q_{\mathrm{III}}) \tag{iv}$$

Solving Eqs. (i) – (iv) simultaneously gives

$$q_{\mathrm{I}} = 7.1\,\mathrm{N/mm} \quad q_{\mathrm{II}} = 8.9\,\mathrm{N/mm} \quad q_{\mathrm{III}} = 4.2\,\mathrm{N/mm}$$

The shear stress in any wall is obtained by dividing the shear flow by the actual wall thickness. Hence the shear distribution is as shown in Fig. 8.6.
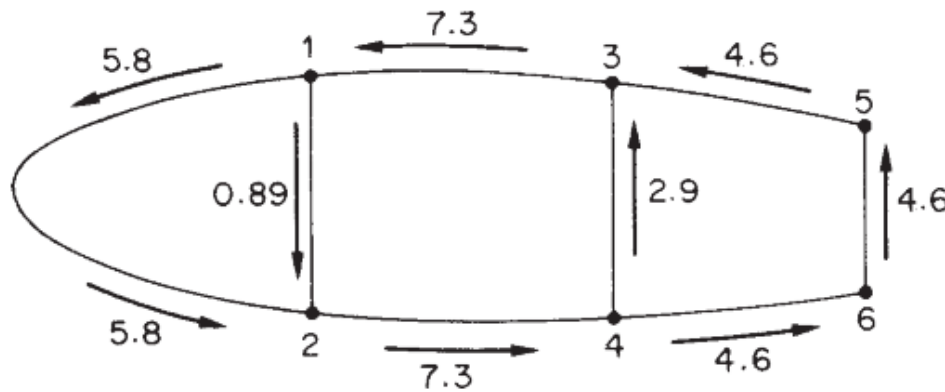

Fig. 8.6

8.3 Shear

Consider the general case of an N-cell wing section comprising booms and skin panels, the latter being capable of resisting both direct and shear stresses. The wing section is subjected to shear loads S_x and S_y whose line of action do not necessarily pass through the shear center S. the resulting shear flow distribution is therefore due to the combined effects of shear and torsion. The method for determining the shear flow distribution and the rate of twist is based on a simple extension of the analysis of a single cell beam subjected to shear loads. The complete distribution of shear flow around the cell is given by the summation of the open section shear flow q_b and the value of shear flow at the cut,

The open section shear flow q_b in the section is given by $q_{s,o,R}$, it could be suppose $q_{s,o,R}$ as a constant shear flow acting around the cell.

$$q_s = -\left(\frac{S_x I_{xx} - S_y I_{xy}}{I_{xx}I_{yy} - I_{xy}^2}\right)\left(\int_0^s t_D x\, ds + \sum_{r=1}^n B_r x_r\right) - \left(\frac{S_y I_{yy} - S_x I_{xy}}{I_{xx}I_{yy} - I_{xy}^2}\right)\left(\int_0^s t_D y\, ds + \sum_{r=1}^n B_r y_r\right)$$

(8.8)

The unknowns shear flows at each of the cuts $q_{s,o,I}$, $q_{s,o,II}$, ..., $q_{s,o,N}$ plus the unknown rate of twist $d\theta/dz$ which, from the assumption of an undistorted cross-section, is the same for each cell.

The rate of twist is:

$$\frac{d\theta}{dz} = \frac{1}{2A_R G}\oint_R q\frac{ds}{t} = \frac{1}{2A_R G}\oint_R (q_b + q_{s,0,R})\frac{ds}{t}$$

(8.9)

Fig. 8.7
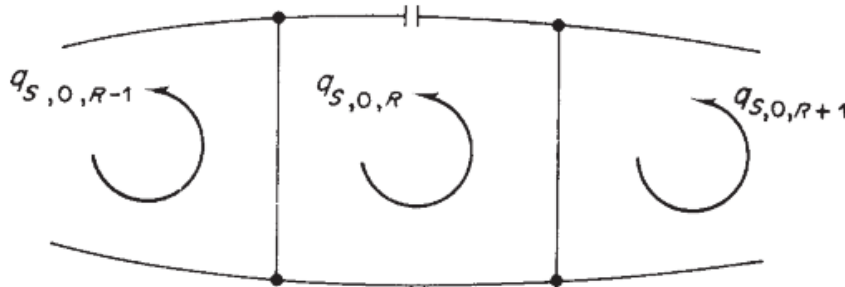
By comparison with pure torsion case:

$$\frac{d\theta}{dz} = \frac{1}{2A_R G}\left(-q_{s,0,R-1}\delta_{R-1,R} + q_{s,0,R}\delta_R - q_{s,0,R+1}\delta_{R+1,R} + \oint_R q_b\frac{ds}{t}\right)$$

(8.10)

q_b has previously been determined. There are N Eqs. , so that a further equation is required to solve for the N+1 unknowns. This obtained by considering the moment equilibrium of Rth cell.

The moment $M_{q,R}$ produced by the total shear flow about any convenient moment center O is given by :

$$M_{q,R} = \oint q_R p_0 \, ds$$

(8.11)

Substituting for q_R in terms of the open section shear flow q_b and the redundant shear flow $q_{s,o,R}$:

$$M_{q,R} = \oint_R q_b p_0 \, ds + q_{s,0,R} \oint_R p_0 \, ds$$

$$M_{q,R} = \oint_R q_b p_0 \, ds + 2A_R q_{s,0,R}$$

(8.12)

The sum of the moments from the individual cells is equivalent to the moment of the externally applied loads about the same point:

$$S_x \eta_0 - S_y \xi_0 = \sum_{R=1}^{N} M_{q,R} = \sum_{R=1}^{N} \oint_R q_b p_0 \, ds + \sum_{R=1}^{N} 2A_R q_{s,0,R}$$

(8.13)

If the moment center is chosen to coincide with the point of intersection of the lines of action of external forces:

$$0 = \sum_{R=1}^{N} \oint_R q_b p_0 \, ds + \sum_{R=1}^{N} 2A_R q_{s,0,R}$$

(8.14)

Example 8.3
The wing section of previous example carries a vertically upward shear load of 86.8 kN in the plane of the web 572. The section has been idealized such that the booms resist all the direct stresses while the walls are effective only in shear. If the shear modulus of all walls is 27 600 N/mm² except for the wall 78 for which it is three times this value, calculate the shear flow distribution in the section and the rate of twist.
Boom areas: $B_1 = B_6 = 2580$ mm² $B_2 = B_5 = 3880$ mm² $B_3 = B_4$ 3230 mm²

121

Wall	Length (mm)	Thickness (mm)	Cell area (mm^2)
12, 56	1023	1.22	$A_I = 265\,000$
23	1274	1.63	$A_{II} = 213\,000$
34	2200	2.03	$A_{III} = 413\,000$
483	400	2.64	
572	460	2.64	
61	330	1.63	
78	1270	1.22	
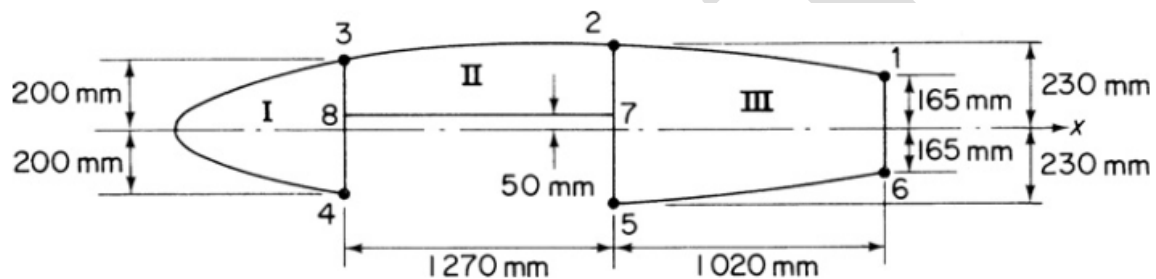
Fig. 8.8

Choosing G_{REF} as 27600 N/mm^2 then

$$t^*_{78} = \frac{3 \times 27\,600}{27\,600} \times 1.22 = 3.66 \text{ mm}$$

$$\delta_{78} = \frac{1270}{3.66} = 347$$

Also

$$\delta_{12} = \delta_{56} = 840 \quad \delta_{23} = 783 \quad \delta_{34} = 1083 \quad \delta_{38} = 57 \quad \delta_{84} = 95 \quad \delta_{87} = 347$$

$$\delta_{27} = 68 \quad \delta_{75} = 106 \quad \delta_{16} = 202$$

Cut the top skin panels in each cell and calculate the open section shear flows

The section is singly symmetric about the x-axis.

$$q_b = \frac{-S_y}{I_{xx}} \sum_{r=1}^{n} B_r y_r \qquad\qquad\qquad (i)$$

where, from Example 23.1, $I_{xx} = 809 \times 10^6 \text{ mm}^4$. Thus, from Eq. (i)

$$q_b = -\frac{86.8 \times 10^3}{809 \times 10^6} \sum_{r=1}^{n} B_r y_r = -1.07 \times 10^{-4} \sum_{r=1}^{n} B_r y_r \qquad\qquad (ii)$$

Since $q_b = 0$ at each 'cut', then $q_b = 0$ for the skin panels 12, 23 and 34. The remaining q_b shear flows are now calculated using Eq. (ii). Note that the order of the numerals in the subscript of q_b indicates the direction of movement from boom to boom.

$$q_{b,27} = -1.07 \times 10^{-4} \times 3880 \times 230 = -95.5 \text{ N/mm}$$

$$q_{b,16} = -1.07 \times 10^{-4} \times 2580 \times 165 = -45.5 \text{ N/mm}$$

$$q_{b,65} = -45.5 - 1.07 \times 10^{-4} \times 2580 \times (-165) = 0$$

$$q_{b,57} = -1.07 \times 10^{-4} \times 3880 \times (-230) = 95.5 \text{ N/mm}$$

$$q_{b,38} = -1.07 \times 10^{-4} \times 3230 \times 200 = -69.0 \text{ N/mm}$$

$$q_{b,48} = -1.07 \times 10^{-4} \times 3230 \times (-200) = 69.0 \text{ N/mm}$$

Therefore, as $q_{b,83} = q_{b,48}$ (or $q_{b,72} = q_{b,57}$), $q_{b,78} = 0$.

The values of δ and q_b are now for each cell in turn

- For cell I

$$\frac{d\theta}{dz} = \frac{1}{2 \times 265\,000 G_{REF}} [q_{s,0,I}(1083 + 95 + 57) - 57 q_{s,0,II} + 69 \times 95 + 69 \times 57] \quad (iii)$$

- For cell II

$$\frac{d\theta}{dz} = \frac{1}{2 \times 213\,000 G_{REF}} [-57 q_{s,0,I} + q_{s,0,II}(783 + 57 + 347 + 68) - 68 q_{s,0,III}$$

$$+ 95.5 \times 68 - 69 \times 57] \qquad\qquad (iv)$$

- For cell III

$$\frac{d\theta}{dz} = \frac{1}{2 \times 413\,000 G_{REF}}[-68q_{s,0,II} + q_{s,0,III}(840 + 68 + 106 + 840 + 202)$$

$$+ 45.5 \times 202 - 95.5 \times 68 - 95.5 \times 106] \qquad (v)$$
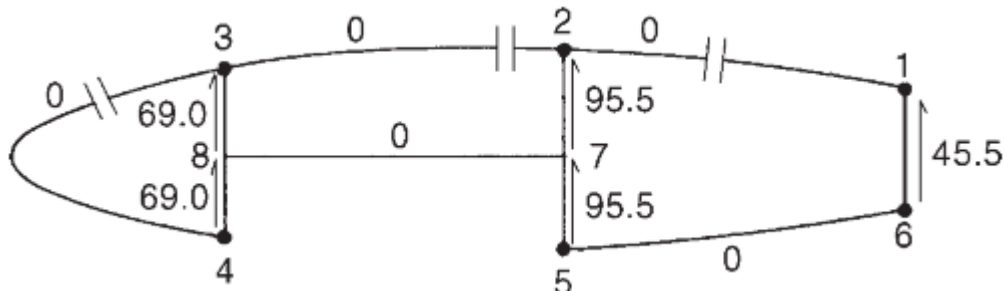

Fig. 8.9

The solely numerical terms in Eqs (iii)–(v) represent $\oint_R q_b(ds/t)$ for each cell. Care must be taken to ensure that the contribution of each q_b value to this term is interpreted correctly. The path of the integration follows the positive direction of $q_{s,0}$ in each cell, i.e. anticlockwise. Thus, the positive contribution of $q_{b,83}$ to $\oint_I q_b(ds/t)$ becomes a negative contribution to $\oint_{II} q_b(ds/t)$ and so on.

The fourth equation required for a solution is obtained by taking moments about the intersection of the x axis and the web 572. Thus

$$0 = -69.0 \times 250 \times 1270 - 69.0 \times 150 \times 1270 + 45.5 \times 330 \times 1020$$

$$+2 \times 265\,000q_{s,0,I} + 2 \times 213\,000q_{s,0,II} + 2 \times 413\,000q_{s,0,III} \qquad (vi)$$

Simultaneous solution of Eqs (iii)–(vi) gives

$$q_{s,0,I} = 5.5\,\text{N/mm} \quad q_{s,0,II} = 10.2\,\text{N/mm} \quad q_{s,0,III} = 16.5\,\text{N/mm}$$

Superimposing these shear flows on the q_b distribution

$$q_{34} = 5.5\,\text{N/mm} \quad q_{23} = q_{87} = 10.2\,\text{N/mm} \quad q_{12} = q_{56} = 16.5\,\text{N/mm}$$

$$q_{61} = 62.0\,\text{N/mm} \quad q_{57} = 79.0\,\text{N/mm} \quad q_{72} = 89.2\,\text{N/mm}$$

$$q_{48} = 74.5\,\text{N/mm} \quad q_{83} = 64.3\,\text{N/mm}$$

Finally, from any of Eqs (iii)–(v)

$$\frac{d\theta}{dz} = 1.16 \times 10^{-6} \, \text{rad/mm}$$

8.4 Tapered wings

$$S_x \eta_0 - S_y \xi_0 = \sum_{R=1}^{N} \oint_R q_b p_0 \, ds + \sum_{R=1}^{N} 2A_R q_{s,0,R} - \sum_{r=1}^{m} P_{x,r} \eta_r + \sum_{r=1}^{m} P_{y,r} \xi_r \tag{8.15}$$

Example 8.4

A two-cell beam has singly symmetrical cross-sections 1.2 m apart and tapers symmetrically in the y direction about a longitudinal axis. The beam supports load which produce a shear force S_y=10 kN and a bending moment M_x= 1.65 kN m at the larger cross-section; the shear load is applied in the plane of the internal spar web. If booms 1 and 6 lie in a plane which is parallel to the yz plane calculate the forces in the booms and the shear flow distribution in the walls at the larger cross-section. The booms are assumed to resist all the direct stresses while the walls are effective only in shear. The shear modulus is constant throughout, the vertical webs are all 1mm thick while the remaining walls are all 0.8 mm thick.

Boom areas: B_1=B_3=B_4=B_6= 600mm² B_2=B_5= 900mm²

Sol/

At the larger cross-section

$$I_{xx} = 4 \times 600 \times 90^2 + 2 \times 900 \times 90^2 = 34.02 \times 10^6 \, \text{mm}^4$$

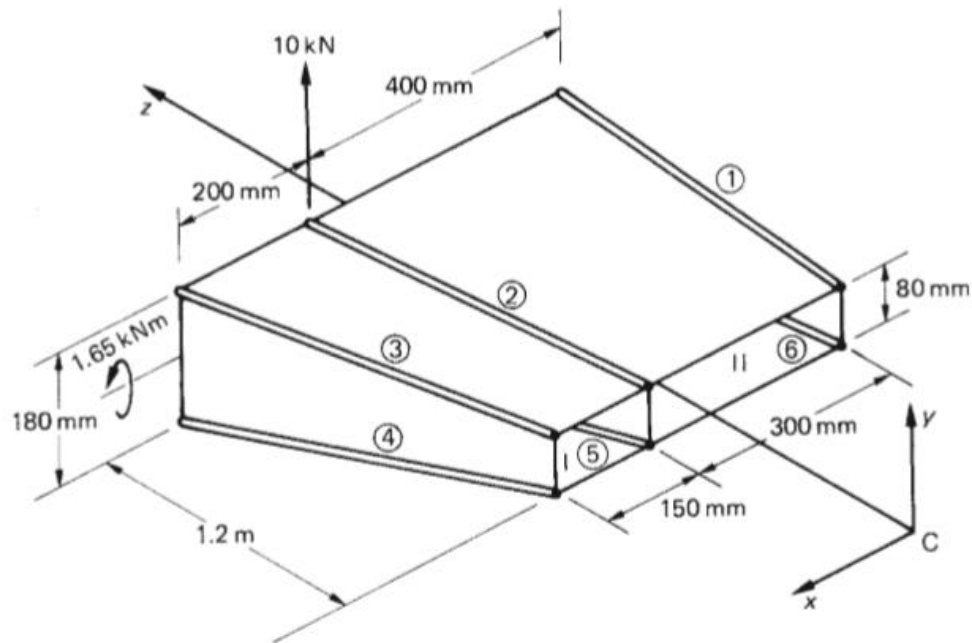I_{xy} =0 and M_y=0 , the direct stress

Fig. 8.10

$$\sigma_{z,r} = \frac{M_x y_r}{I_{xx}}$$

$$P_{z,r} = \frac{M_x y_r}{I_{xx}} B_r$$

$$P_{z,r} = \frac{1.65 \times 10^6 y_r B_r}{34.02 \times 10^6} = 0.08 y_r B_r \qquad \text{(i)}$$

The value of $P_{z,r}$ is calculated from equation (i) in column (2) of table below $P_{x,r}$ and P_{yr} were calculated as single cell respectively (column 5 and 6) . the axial load P_r is given by ($P_{x,r}^2 + P_{yr}^2 + P_{z,r}^2$) in column (7) and has the same sign as $P_{z,r}$. the moments of $P_{x,r}$ and P_{yr} columns (10) and (11), are calculated for a moment center at the mid-point of the internal web taking anticlockwise moments as positive.

126

①	②	③	④	⑤	⑥	⑦	⑧	⑨	⑩	⑪
	$P_{z,r}$	$\dfrac{\delta_{x_r}}{\delta_z}$	$\dfrac{\delta_{y_r}}{\delta_z}$	$P_{x,r}$	$P_{y,r}$	P_r	ξ_r	η_r	$P_{x,r}\eta_r$	$P_{y,r}\xi_r$
Boom	(N)			(N)	(N)	(N)	(mm)	(mm)	(N mm)	(N mm)
1	2619.0	0	0.0417	0	109.2	2621.3	400	90	0	43 680
2	3928.6	0.0833	0.0417	327.3	163.8	3945.6	0	90	−29 457	0
3	2619.0	0.1250	0.0417	327.4	109.2	2641.6	200	90	−29 466	21 840
4	−2619.0	0.1250	−0.0417	−327.4	109.2	−2641.6	200	90	−29 466	21 840
5	−3928.6	0.0833	−0.0417	−327.3	163.8	−3945.6	0	90	−29 457	0
6	−2619.0	0	−0.0417	0	109.2	−2621.3	400	90	0	−43 680

From column (5)

$$\sum_{r=1}^{6} P_{x,r} = 0$$

From column (6)

$$\sum_{r=1}^{6} P_{y,r} = 764.4\,\text{N}$$

From column (10)

$$\sum_{r=1}^{6} P_{x,r}\eta_r = -117\,846\,\text{N mm}$$

From column (11)

$$\sum_{r=1}^{6} P_{y,r}\xi_r = -43\,680\,\text{N mm}$$

$S_{x,w} = 0 \quad S_{y,w} = 10 \times 10^3 - 764.4 = 9235.6\,\text{N}$

C_x is axis of symmetry, $I_{xy} = 0$

$$q_b = -\frac{S_{y,w}}{I_{xx}} \sum_{r=1}^{n} B_r y_r$$

$$q_b = -\frac{9235.6}{34.02 \times 10^6} \sum_{r=1}^{n} B_r y_r = -2.715 \times 10^{-4} \sum_{r=1}^{n} B_r y_r \qquad \text{(ii)}$$

Cutting the top walls of each cell and using equation (ii) to evaluate q_b distribution as shown in Fig. 8.11.
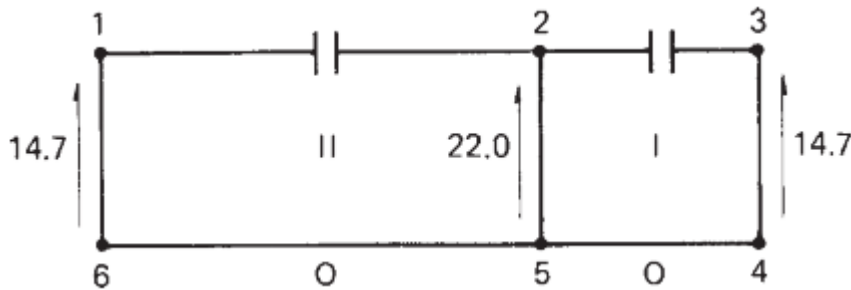

Fig. 8.11

Evaluating δ for each wall,

for cell I

$$\frac{d\theta}{dz} = \frac{1}{2 \times 36\,000G}(760q_{s,0,\mathrm{I}} - 180q_{s,0,\mathrm{II}} - 1314) \qquad \text{(iii)}$$

for cell II

$$\frac{d\theta}{dz} = \frac{1}{2 \times 72\,000G}(-180q_{s,0,\mathrm{I}} + 1160q_{s,0,\mathrm{II}} + 1314) \qquad \text{(iv)}$$

Taking moments about the mid-point of web 25 gives,

$$0 = -14.7 \times 180 \times 400 + 14.7 \times 180 \times 200 + 2 \times 36\,000q_{s,0,\mathrm{I}} + 2 \times 72\,000q_{s,0,\mathrm{II}}$$
$$-117\,846 - 43\,680$$

$0= -690726 + 72000\, q_{s,o,I} + 144000\, q_{s,o,II}$ <div style="text-align:right">(v)</div>

Solving Eqs (iii) –(v) gives

$$q_{s,0,I} = 4.6\,\text{N/mm} \quad q_{s,0,II} = 2.5\,\text{N/mm}$$

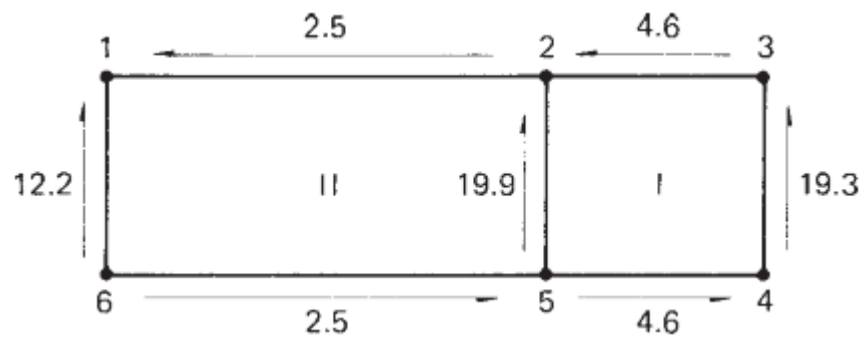The resulting shear flow distribution shown in   Fig. 8.12

Fig. 8.12

Principles: Wings, as well as fuselages, have openings in their surfaces to accommodate under carriages, engine nacelles and weapons installations, etc. In addition, inspection panel are required at specific positions so that, as for fuselages, the loads in adjacent portions of the wing structure are modified. Fig. 9.1 shows an opening in the bay 2 wing structure.
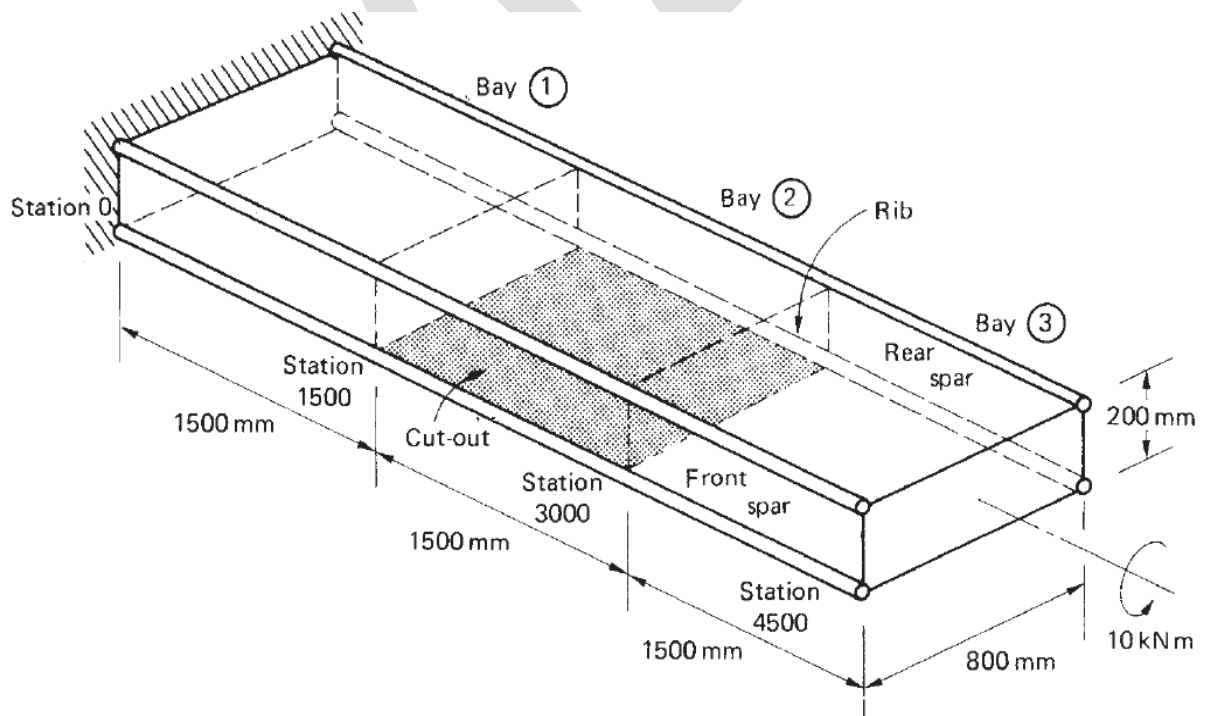

Fig. 9.1 Three-bay wing structure with cut-out.

Initially, <mark>consider the case of a wing subjected to a pure torque in which one bay of the wing has the skin on its undersurface removed.</mark> This will be illustrated by the following the numerical example.

Example 9.1

The structural portion of a wing consists of a three-bay rectangular section box which may be assumed to be firmly attached at all points around its periphery to the aircraft fuselage at its inboard end. The skin on the undersurface of the central bay has been removed and the wing is subjected to a torque of 10 kN.m at its tip (Fig. 9.1).

Calculate:
1. The shear flows in the skin panels ant the shear flows in the spar webs.
2. The loads in the corner flanges the forces in the ribs on each side of the cut-out

Assuming that the spar flanges carry all the direct loads while the skin panels and spar webs are effective only in shear.

Solution:
1. If the wing structure were continuous and the effects of restrained warping at the built-in end ignored, the shear flows in the skin panels would be given by the <mark>Bredit Batho Theorem</mark>, i.e.

$$q = \frac{T}{2A} = \frac{10 \times 10^6}{2 \times 200 \times 800} = 31.3 \, \text{N/mm}$$

and the flanges would be unloaded. However, the removal of the lower skin panel in bay ② results in a <mark>torsionally weak channel section</mark> for the length of bay ② which must in any case still transmit the applied torque to bay ① and subsequently to the wing support points.

<mark>Although open section beams are inherently weak in torsion, the channel section in this case is attached at its inboard and outboard ends to torsionally stiff closed boxes so that</mark>, in effect, it is built-in at both ends The effect of axial constraint will be examined on open section beams subjected to torsion. An alternative approach is to assume that the torque is transmitted
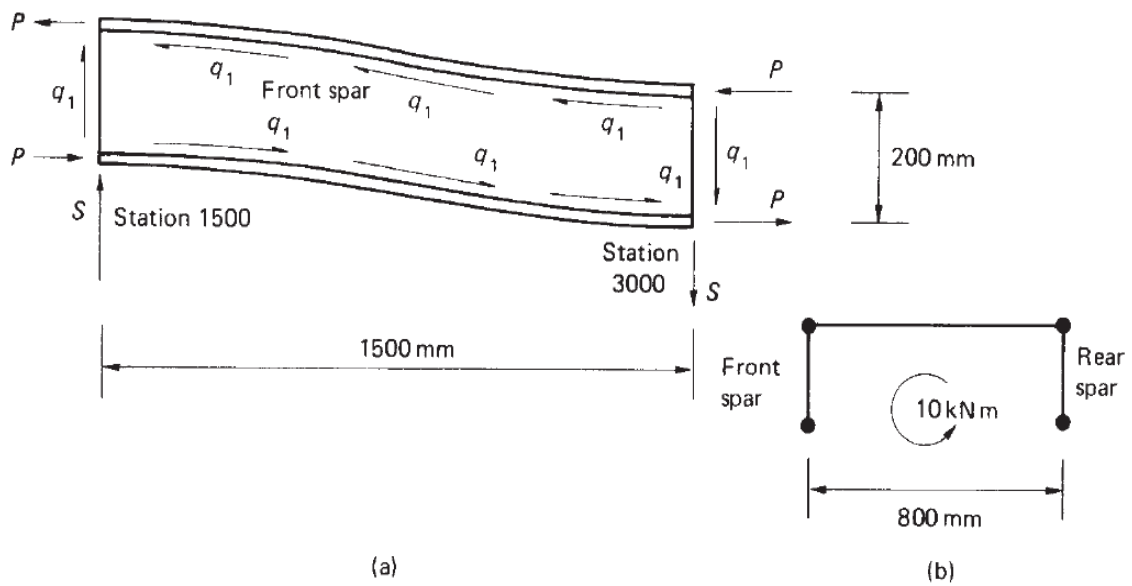
Fig. 9.2: Differential bending of front spar.

. The bending moment in each spar is resisted by the flange loads P as shown, for the front spar, in Fig. 9.2(a). The shear loads in the front and rear spars form a couple at any station in bay ② which is equivalent to the applied torque. Thus, from Fig. 9.2(b)

$$800S = 10 \times 10^6 \, \text{N mm}$$

i.e.

$$S = 12\,500 \, \text{N}$$

The shear flow $q1$ in Fig. 9.2(a) is given by

$$q_1 = \frac{12\,500}{200} = 62.5 \, \text{N/mm}$$

Midway between stations 1500 and 3000 a point of contraflexure occurs in the front and rear spars so that at this point the bending moment is zero. Hence

132

$$200P = 12\,500 \times 750 \, \text{N mm}$$

so that

$$P = 46\,875 \, \text{N}$$

Alternatively, P may be found by considering the equilibrium of either of the spar flanges. Thus

$$2P = 1500q_1 = 1500 \times 62.5 \, \text{N}$$

whence

$$P = 46\,875 \, \text{N}$$

The flange loads P are reacted by loads in the flanges of bays ① and ③. These flange loads are transmitted to the adjacent spar webs and skin panels as shown
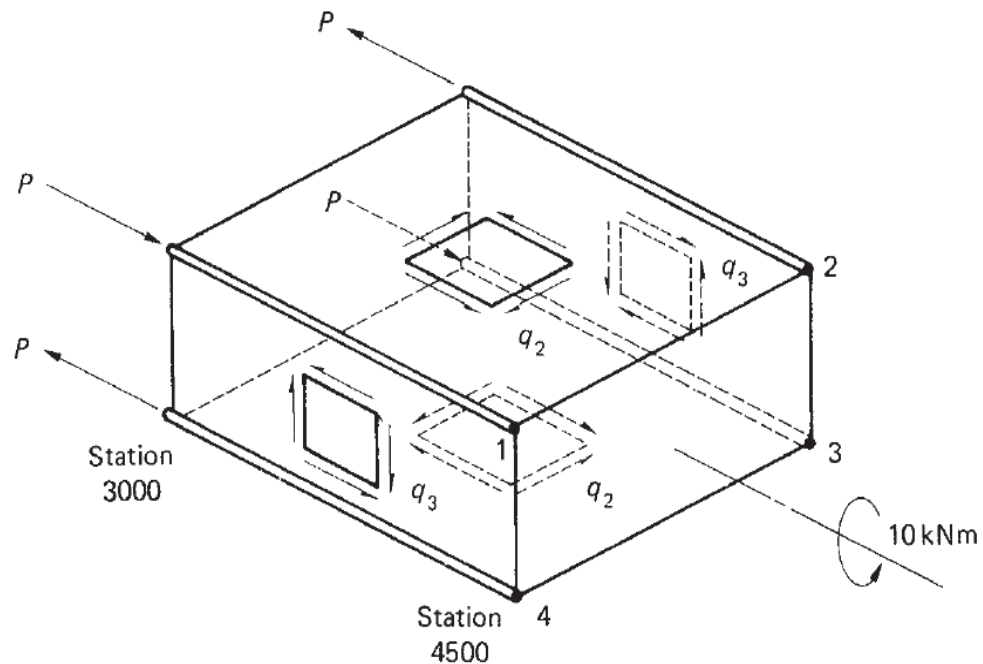

Fig. 9.3 Loads on bay ③ of the wing.

in Fig. 9.3 for bay ③ and modify the shear flow distribution given by Bredit Batho Theorem. For equilibrium of flange 1

$$1500q_2 - 1500q_3 = P = 46\,875\,\text{N}$$

or

$$q_2 - q_3 = 31.3 \qquad\qquad (i)$$

The resultant of the shear flows $q2$ and $q3$ must be equivalent to the applied torque. Hence, for moments about the centre of symmetry at any section in bay ③ as follows

$$200 \times 800q_2 + 200 \times 800q_3 = 10 \times 10^6\,\text{N mm}$$

or

$$q_2 + q_3 = 62.5 \qquad\qquad (ii)$$

Solving Eqs (i) and (ii) we obtain

$$q_2 = 46.9\,\text{N/mm} \qquad q_3 = 15.6\,\text{N/mm}$$

Comparison with the results of Bredit Batho Theorem show that the shear flows are increased by a factor of 1.5 in the upper and lower skin panels and decreased by a factor of 0.5 in the spar webs.

2. The flange loads are in equilibrium with the resultants of the shear flows in the adjacent skin panels and spar webs. Thus, for example, in the top flange of the front spar

$$P(\text{st.}4500) = 0$$

$$P(\text{st.}3000) = 1500q_2 - 1500q_3 = 46\,875\,\text{N (compression)}$$

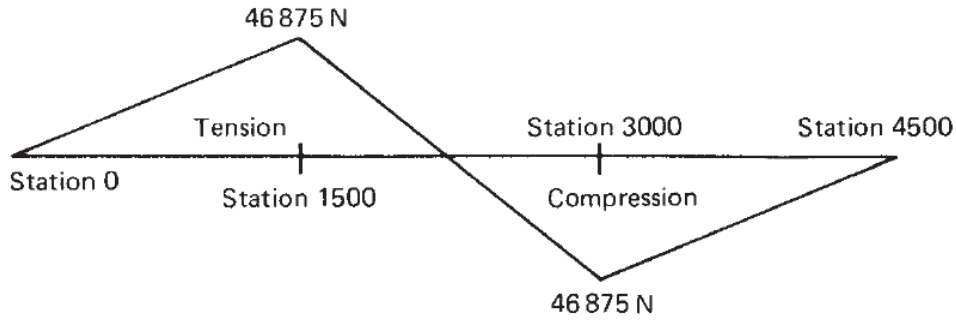$$P(\text{st.}2250) = 1500q_2 - 1500q_3 - 750q_1 = 0$$

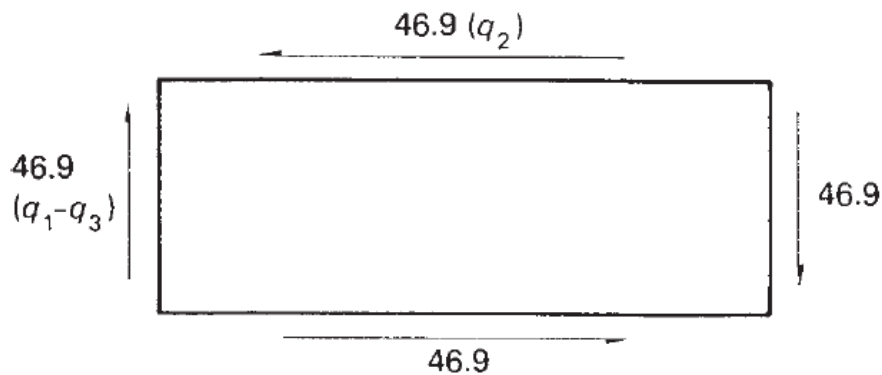**Fig. 9.4 Distribution of load in the top flange of the front spar of the wing.**

Fig. 9.5 Shear flows (N/mm) on wing rib at station 3000 in the wing.

Comments: The loads along the remainder of the flange follow from antisymmetry giving the distribution shown in Fig. 9.4. The load distribution in the bottom flange of the rear spar will be identical to that shown in Fig. 9.4 while the distributions in the bottom flange of the front spar and the top flange of the rear spar will be reversed. We note that the flange loads are zero at the built-in end of the wing (station 0). Generally, however, additional stresses are induced by the warping restraint at the built-in end. The loads on the wing ribs on either the inboard or outboard end of the cut-out are found by considering the shear flows in the skin panels and spar webs immediately inboard and outboard of the rib. Thus, for the rib at station 3000 we obtain the shear flow distribution shown in Fig. 9.5.

In this Example, we implicitly assumed in the analysis that the local effects of the cut-out were completely dissipated within the length of the adjoining bays which were equal in length to the cut-out bay. The validity of this assumption relies on St. Venant's principle. It may generally be assumed therefore that the effects of a cutout are restricted to spanwise lengths of the wing equal to the length of the cut-out on both inboard and outboard ends of

the cut-out bay. We shall now consider the more complex case of a wing having a cut-out and subjected to shear loads which produce both bending and torsion. Again the method is illustrated by a numerical example.

Example 9.2
A wing box has the skin panel on its undersurface removed between stations 2000 and 3000 and carries lift and drag loads which are constant between stations 1000 and 4000 as shown in Fig. 9.6(a). Determine:
1. The shear flows in the skin panels and spar webs.
2. The loads in the wing ribs at the inboard and outboard ends of the cut-out bay.
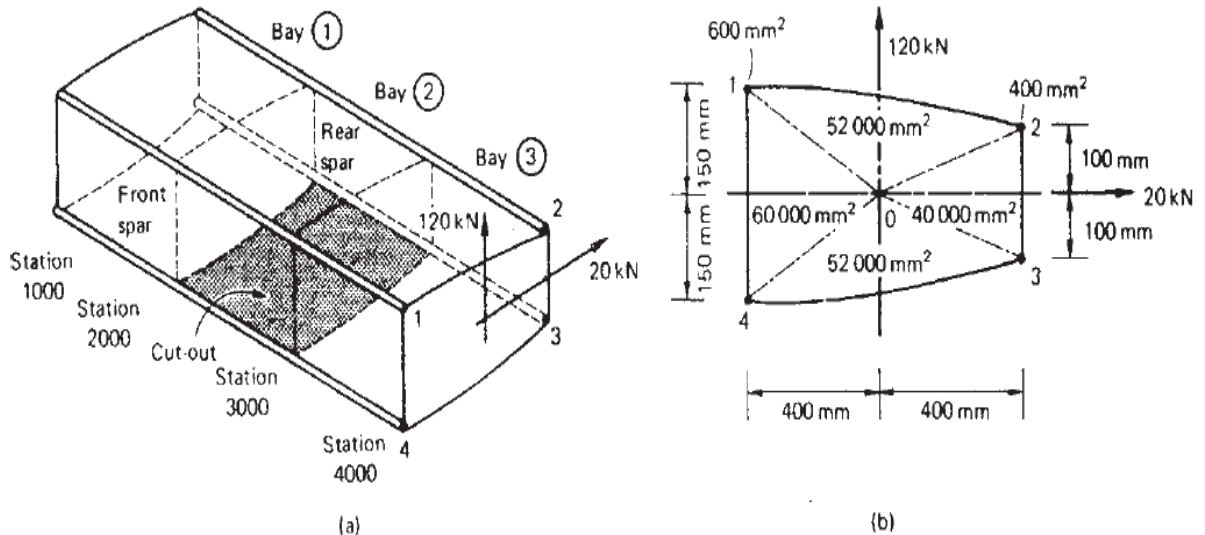

(a)   (b)

Fig. 9.6: Wing box of Example 9.1.

Assume that all bending moments are resisted by the spar flanges while the skin panels and spar webs are effective only in shear.
The simplest approach is first to determine the shear flows in the skin panels and spar webs as though the wing box were continuous and then to apply an equal and opposite shear flow to that calculated around the edges of the cut-out. The shear flows in the wing box without the cut-out will be the same in each bay and are calculated using the standard procedure of calculating the shear low. This gives the shear flow distribution shown in Fig. 9.7.
1. Now consider bay ② and apply a shear flow of 75.9 N/mm in the wall 34 in the opposite sense to that shown in Fig. 9.7. This reduces the shear flow in the wall 34 to zero and, in effect, restores the cut-out to bay ②.

The shear flows in the remaining walls of the cut-out bay will no longer be equivalent to the externally applied shear loads so that corrections are required.

Consider the cut-out bay (Fig. 9.8) with the shear flow of 75.9 N/mm applied in the opposite sense to that shown in Fig. 9.7.

The correction shear flows

$$q'_{12}, q'_{32} \text{ and } q'_{14}$$

may be found using statics. Thus, resolving forces horizontally we have

$$800q'_{12} = 800 \times 75.9 \,\text{N}$$

whence
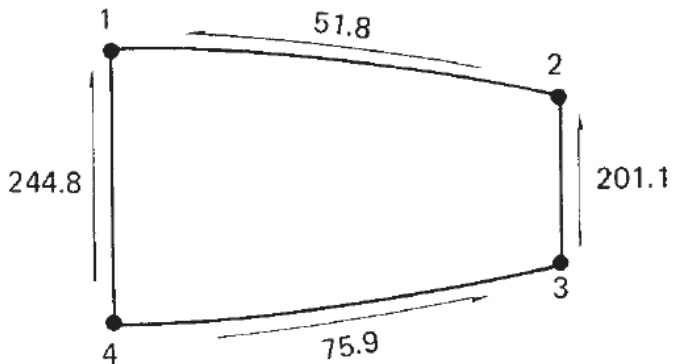
$$q'_{12} = 75.9 \,\text{N/mm}$$

Fig. 9.7: Shear flow (N/mm) distribution at any station in the wing without cut-out.
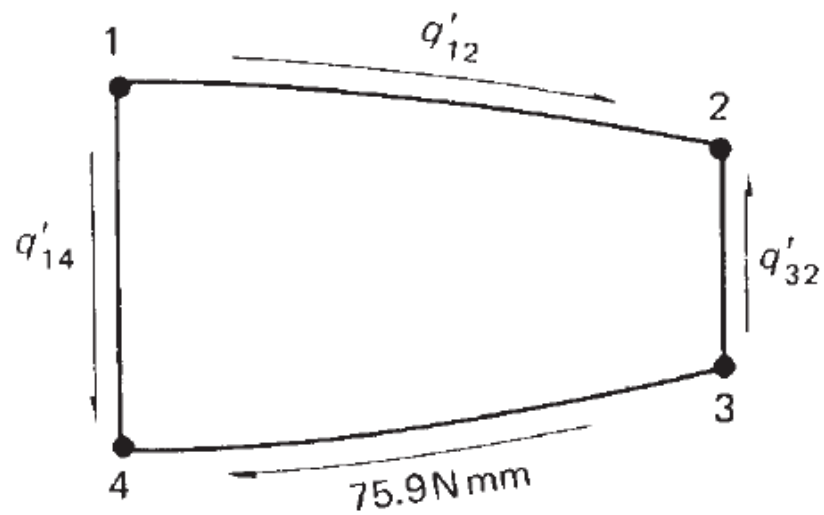
Fig. 9.8 Correction shear flows in the cut-out bay of the wing box of Example 23.7.

Resolving forces vertically

$$200q'_{32} = 50q'_{12} - 50 \times 75.9 - 300q'_{14} = 0 \qquad \text{(i)}$$

and taking moments about O in Fig. 9.6(b) we obtain

$$2 \times 52\,000q'_{12} - 2 \times 40\,000q'_{32} + 2 \times 52\,000 \times 75.9 - 2 \times 60\,000q'_{14} = 0 \quad \text{(ii)}$$

Solving Eqs (i) and (ii) gives

$$q'_{32} = 117.6\,\text{N/mm} \quad q'_{14} = 53.1\,\text{N/mm}$$

The final shear flows in bay ② are found by superimposing q'_{12}, q'_{32} and q'_{14} on the shear flows in Fig. 9.7, giving the distribution shown in Fig. 9.9. **Alternatively,** these shear flows could have been found directly by considering the equilibrium of the cut-out bay under the action of the applied shear loads.

The correction shear flows in bay ② (Fig. 9.8) will also modify the shear flow distributions in bays ① and ③. The correction shear flows to be applied to those shown in Fig. 9.7 for bay ③ (those in bay ① will be identical) may be found by determining the flange loads corresponding to the correction shear flows in bay ②. It can be seen from the magnitudes and directions of these correction shear flows (Fig. 9.8) that at any section in bay ② the loads in the upper and lower flanges of the front spar are equal in magnitude but opposite in direction. Similarly, for the rear spar.

Thus, the correction shear flows in bay ② produce an identical system of flange loads to that shown in Fig. 9.2 for the cut-out bays in the wing structure of example 9.1 are as follows,

$$1000q''_{41} + 1000q''_{21} = 64\,500\,\text{N} \tag{iii}$$

and for equilibrium of flange 2

$$1000q''_{21} + 1000q''_{23} = 96\,750\,\text{N} \tag{iv}$$

For equilibrium in the chordwise direction at any section in bay ③

$$800q''_{21} = 800q''_{43}$$

or

$$q''_{21} = q''_{43} \tag{v}$$

Finally, for vertical equilibrium at any section in bay ③

$$300q''_{41} + 50q''_{43} + 50q''_{21} - 200q''_{23} = 0 \tag{vi}$$
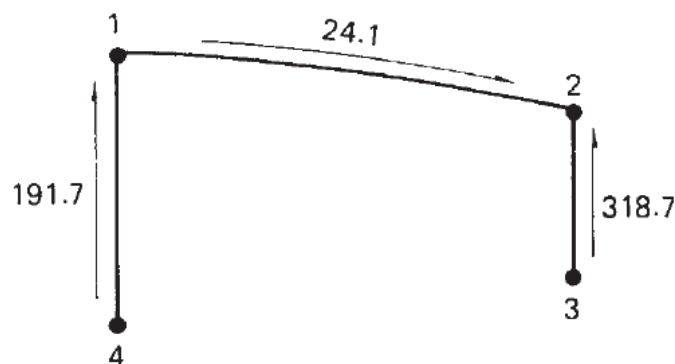
Fig. 9.9 Final shear flows (N/mm) in the cut-out bay of the wing box
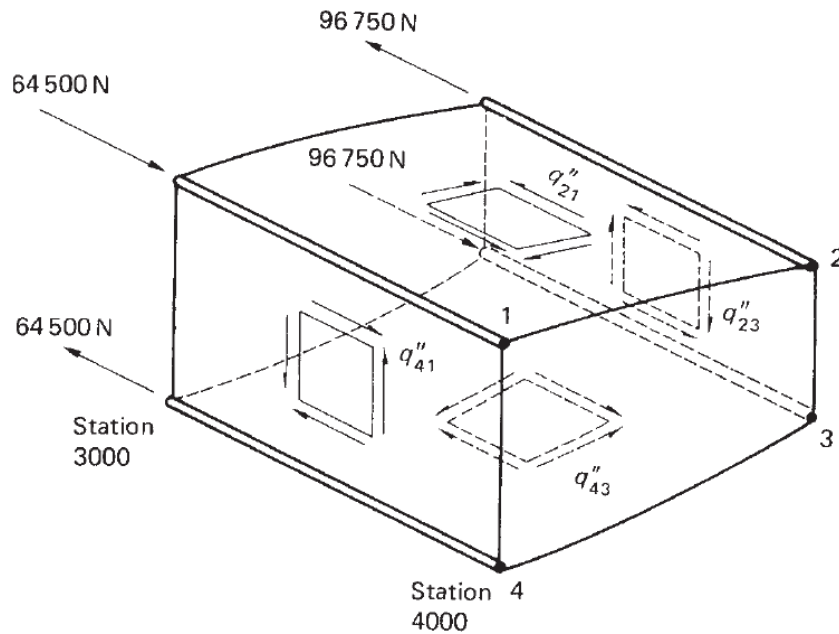
Fig. 9.10 Correction shear flows in bay ③ of the wing box.

Therefore, at station 3000 the flange loads are

$$P_1 = (75.9 + 53.1) \times 500 = 64\,500\,\text{N (compression)}$$

$$P_4 = 64\,500\,\text{N (tension)}$$

$$P_2 = (75.9 + 117.6) \times 500 = 96\,750\,\text{N (tension)}$$

$$P_3 = 96\,750\,\text{N (tension)}$$

These flange loads produce correction shear flows

$$q''_{21}, \; q''_{43}, \; q''_{23} \text{ and } q''_{41}$$

in the skin panels and spar webs of bay ③ as shown in Fig. 9.10. Thus for equilibrium of flange 1

140
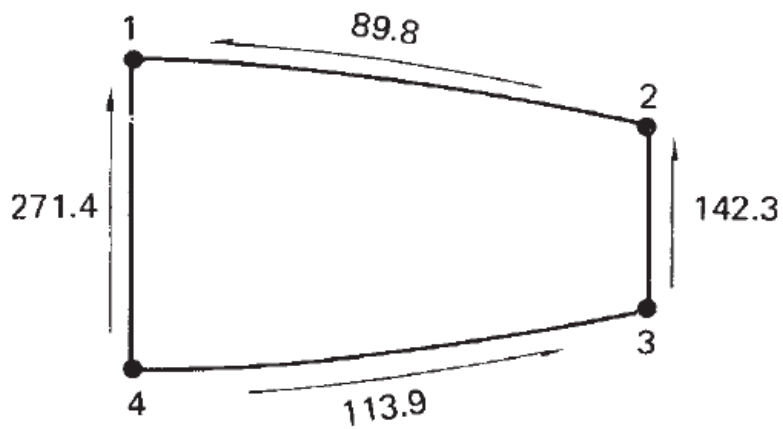
Fig. 9.11 Final shear flows in bay ③ (and bay ①) of the wing box
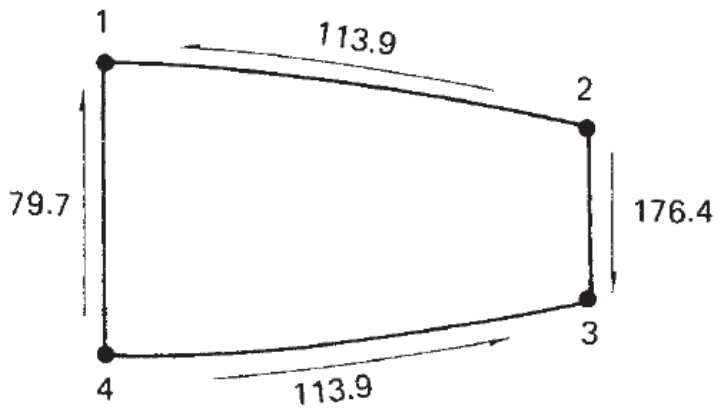
Fig. 9.12 Shear flows (N/mm) applied to the wing rib at station 3000 in the wing box.

$$1000q''_{41} + 1000q''_{21} = 64\,500\,\text{N} \qquad \text{(iii)}$$

and for equilibrium of flange 2

$$1000q''_{21} + 1000q''_{23} = 96\,750\,\text{N} \qquad \text{(iv)}$$

For equilibrium in the chordwise direction at any section in bay ③

$$800q''_{21} = 800q''_{43}$$

or

$$q''_{21} = q''_{43} \qquad \text{(v)}$$

Finally, for vertical equilibrium at any section in bay ③

$$300q''_{41} + 50q''_{43} + 50q''_{21} - 200q''_{23} = 0 \qquad \text{(vi)}$$

Simultaneous solution of Eqs (iii)–(vi) gives

$$q''_{21} = q''_{43} = 38.0\,\text{N/mm} \quad q''_{23} = 58.8\,\text{N/mm} \quad q''_{41} = 26.6\,\text{N/mm}$$

Superimposing these correction shear flows on those shown in Fig. 9.7 gives the final shear flow distribution in bay ③ as shown in Fig. 9.1. The rib loads at stations 2000 and 3000 are found as before by adding algebraically the shear flows in the skin panels and spar webs on each side of the rib. Thus, at station 3000 we obtain the shear flows acting around the periphery of the rib as shown in Fig. 9.12. The shear flows applied to the rib at the inboard end of the cut-out bay will be equal in magnitude but opposite in direction.

Note that in this example only the shear loads on the wing box between stations 1000 and 4000 are given. We cannot therefore determine the final values of the loads in the spar flanges since we do not know the values of the bending moments at these positions caused by loads acting on other parts of the wing.

Chapter Ten: Fuselage Frames and Wing Ribs

1. **Principles of stiffener/web construction**

Aircrafts are constructed primarily from thin metal skins which are capable of resisting in-plane tension and shear loads but they are weak in resisting buckling loads such as in the in-plane compressive loading. The skins are therefore stiffened by longitudinal stringers which resist the in-plane compressive loads and, at the same time, resist small distributed loads normal to the plane of the skin.
The fuselages structure is stiffened by transverse frames or bulkheads. The case of wings, they are stiffened by ribs. In addition, the frames and ribs resist concentrated loads in transverse
Thus, cantilever wings may be bolted to fuselage frames at the spar caps while undercarriage loads are transmitted to the wing through spar and rib attachment points.

Frames and ribs are themselves fabricated from thin sheets of metal and therefore require stiffening members to distribute the concentrated loads to the thin webs.
If the load is applied in the plane of a web, the stiffeners must be aligned with the direction of the load. Alternatively, if this is not possible, the load should be applied at the intersection of two stiffeners so that each stiffener resists the component of load in its direction. The basic principles of stiffener/web construction are illustrated in Example 10.1

Example 10.1
A cantilever beam (Fig. 10.1) carries concentrated loads as shown. Calculate the distribution of stiffener loads and the shear flow distribution in the web panels assuming that the latter are effective only in shear. We note that stiffeners HKD and JK are required at the point of application of the 4000N load to resist its vertical and horizontal

components. A further transverse stiffener GJC is positioned at the unloaded end J of the stiffener JK since stress concentrations are produced if a stiffener ends in the centre of a web panel. We note also that the web panels are only effective in shear so that the shear flow is constant throughout a particular web panel; the assumed directions of the shear flows are shown in Fig. 10.1.
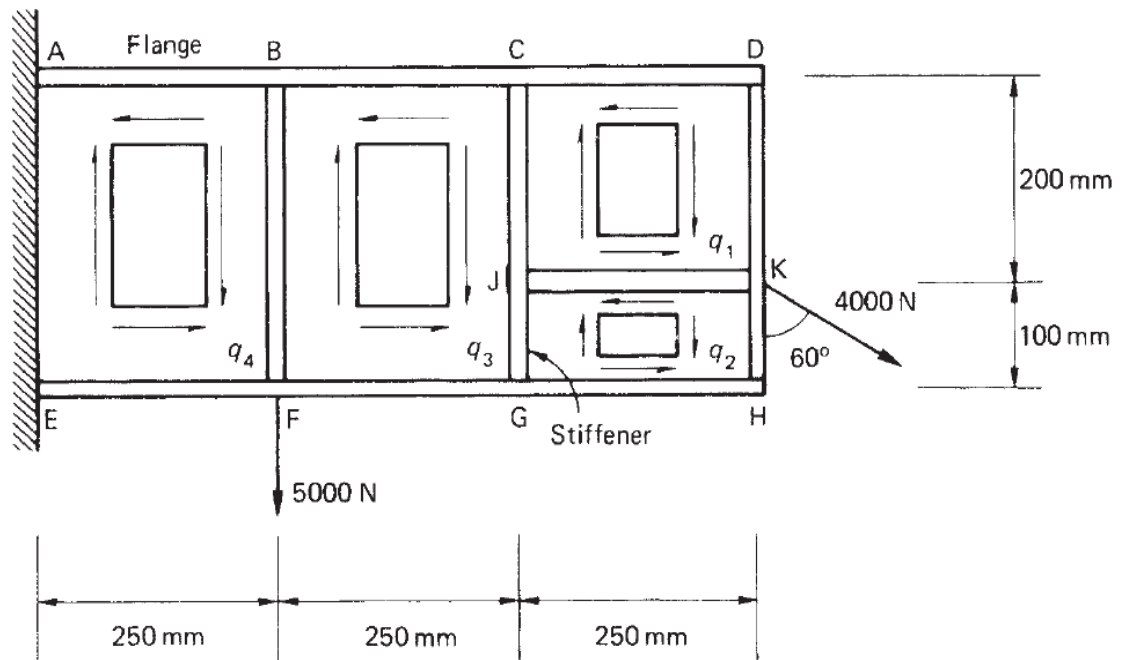
Fig. 10.1 Cantilever beam of Example 10.1.

To examine the physical role of the different structural components in supporting the applied loads. Generally, stiffeners are assumed to withstand axial forces only so that the horizontal component of the load at K is equilibrated locally by the axial load in the stiffener JK and not by the bending of stiffener HKD. By the same argument the vertical component of the load at K is resisted by the axial load in the stiffener HKD. These axial stiffener loads are equilibrated in turn by the resultants of the shear flows q_1 and q_2 in the web panels CDKJ and JKHG. Thus we see that the web panels resist the shear component of the externally applied load and at the same time transmit the bending and axial load of the externally applied load to the beam flanges; subsequently, the flange loads are reacted at the support points A and E. Consider the free body diagrams of the stiffeners JK and HKD shown in Figs. 10.2(a)

168

and (b).
From the equilibrium of stiffener JK we have

$$(q_1 - q_2) \times 250 = 4000 \sin 60° = 3464.1\,\text{N} \tag{i}$$
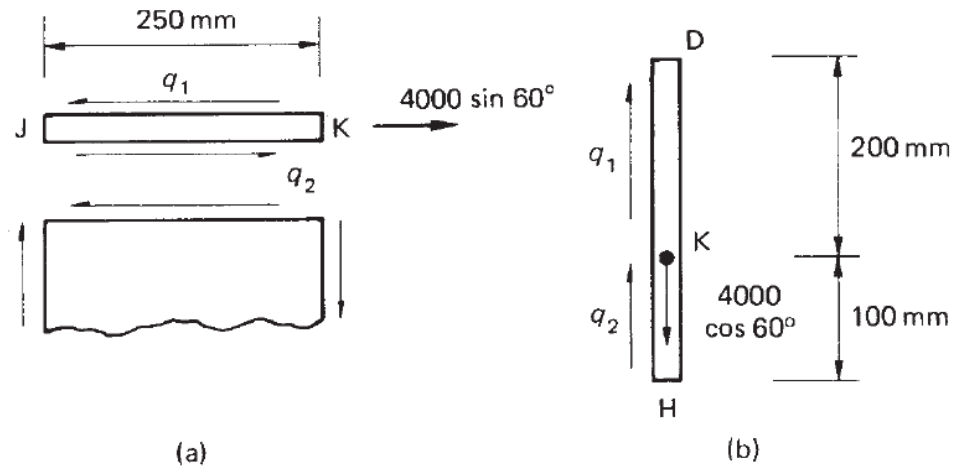
Fig. 10.2 Free body diagrams of stiffeners JK and HKD in the beam of Example 10.1.
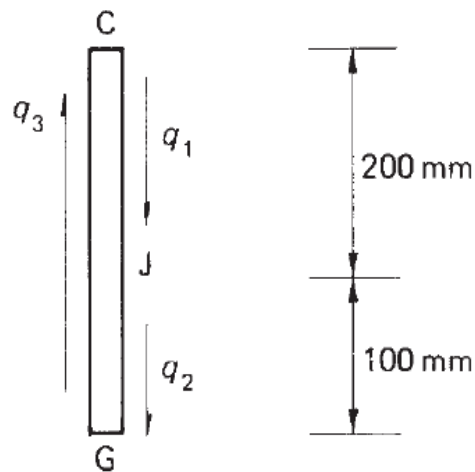
Fig. 10.3 Equilibrium of stiffener CJG in the beam of Example 10.1.

and from the equilibrium of stiffener HKD

$$200q_1 + 100q_2 = 4000 \cos 60° = 2000\,\text{N} \tag{ii}$$

Solving Eqs (i) and (ii) we obtain

$$q_1 = 11.3 \, \text{N/mm} \quad q_2 = -2.6 \, \text{N/mm}$$

The vertical shear force in the panel BCGF is equilibrated by the vertical resultant of the shear flow $q3$. Thus

$$300q_3 = 200q_1 + 100q_2$$

or

$$300q_3 = 200 \times 11.3 - 100 \times 2.6$$

from which

$$q_3 = 6.7 \, \text{N/mm}$$

The shear flow q_4 in the panel ABFE may be found using either of the above methods. Thus, considering the vertical shear force in the panel

$$300q_4 = 4000 \cos 60° + 5000 = 7000 \, \text{N}$$

whence

$$q_4 = 23.3 \, \text{N/mm}$$

Alternatively, from the equilibrium of stiffener BF

$$300q_4 - 300q_3 = 5000 \, \text{N}$$
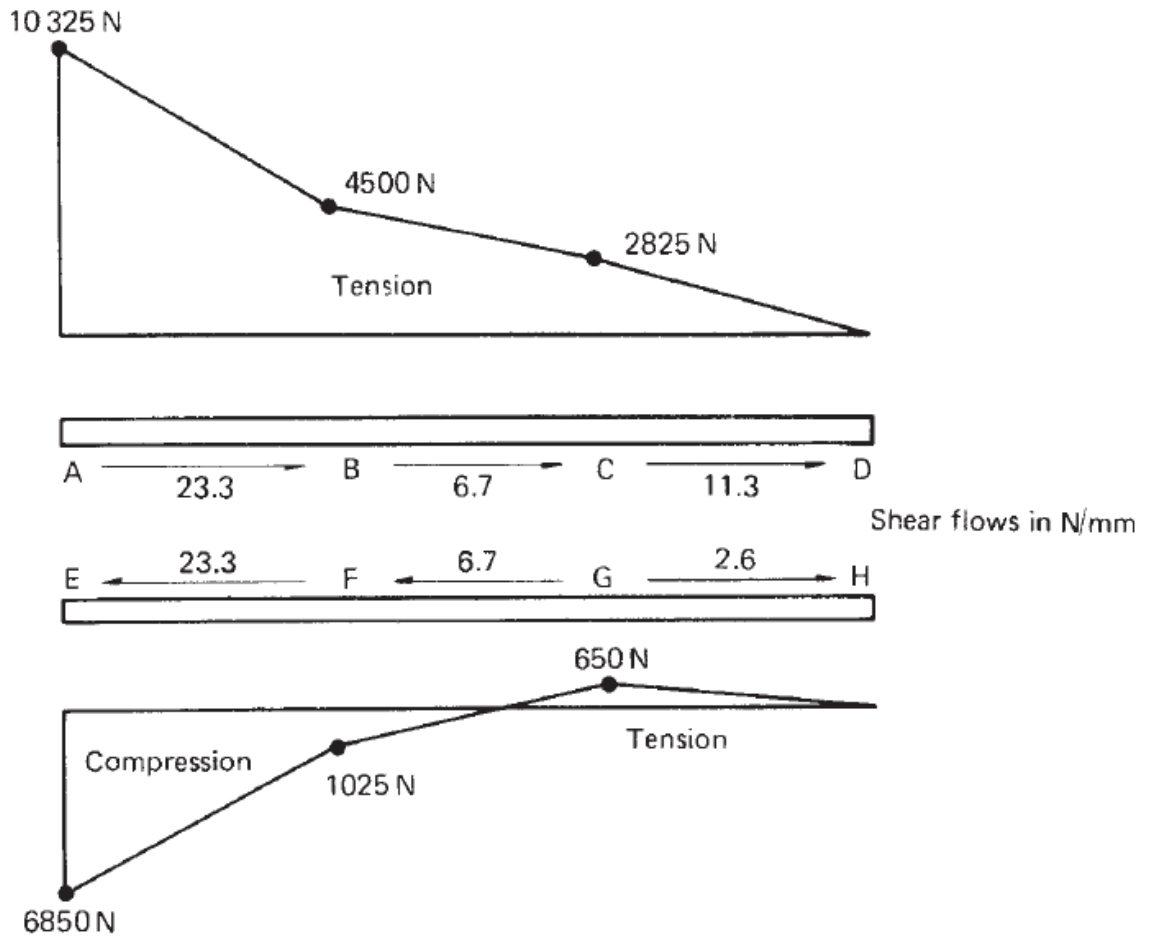
Fig. 10.4 Load distributions in flanges of the beam of Example 10.1.

whence

$$q_4 = 23.3 \, \text{N/mm}$$

The flange and stiffener load distributions are calculated in the same way and are obtained from the algebraic summation of the shear flows along their lengths. For example, the axial load P_A at A in the flange ABCD is given by

$$P_A = 250q_1 + 250q_3 + 250q_4$$

or

$$P_A = 250 \times 11.3 + 250 \times 6.7 + 250 \times 23.3 = 10\,325\,\text{N (tension)}$$

Similarly

$$P_E = -250q_2 - 250q_3 - 250q_4$$

i.e.

$$P_E = 250 \times 2.6 - 250 \times 6.7 - 250 \times 23.3 = -6850\,\text{N (compression)}$$

The complete load distribution in each flange is shown in Fig. 10.4. The stiffener load distributions are calculated in the same way and are shown in Fig. 10.5. The distribution of flange load in the bays ABFE and BCGF could have been obtained by considering the bending and axial loads on the beam at any section.
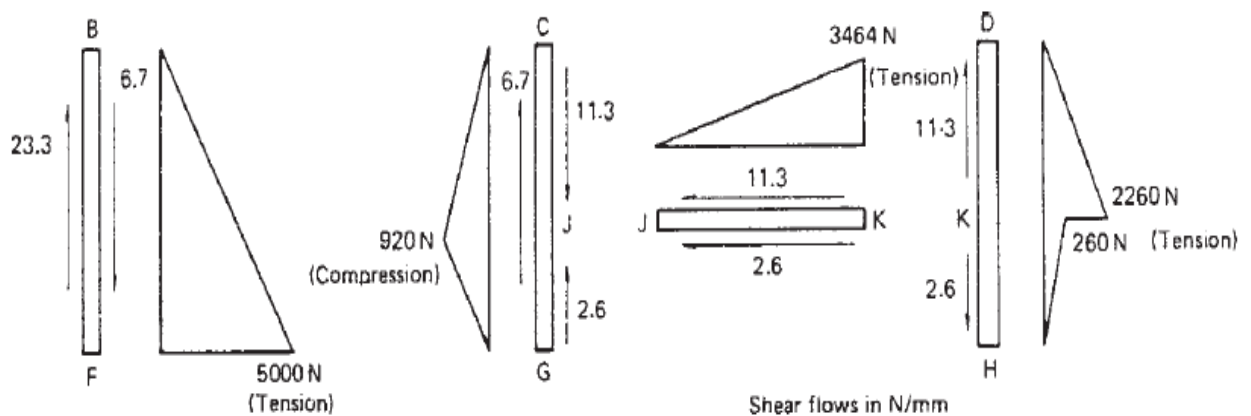
Fig. 10.5 Load distributions in stiffeners of the beam of Example 10.1.

For example, at the section AE we can replace the actual loading system by a bending

$$M_{AE} = 5000 \times 250 + 2000 \times 750 - 3464.1 \times 50 = 2\,576\,800\,\text{N mm}$$

and an axial load acting <mark>midway between the flanges</mark> (irrespective of whether or not the flange areas are symmetrical about this point) of

$$P = 3464.1\text{N}$$

Thus

$$P_A = \frac{2\,576\,800}{300} + \frac{3464.1}{2} = 10\,321\,\text{N (tension)}$$

and

$$P_E = \frac{-2\,576\,800}{300} + \frac{3464.1}{2} = -6857\,\text{N (compression)}$$

This approach cannot be used in the bay CDHG except at the section CJG since the axial load in the stiffener JK introduces an additional unknown. The above analysis assumes that the web panels in beams of the type shown in Fig. 10.1 resist pure shear along their boundaries. The thin webs <mark>may buckle</mark> under the action of such shear loads producing tension field stresses which,
in turn, induce additional loads in the stiffeners and flanges of beams. The tension field stresses may be calculated separately by the methods described previously superimposed on the stresses determined as described above. So far we have been concerned with web/stiffener arrangements in which the loads have been applied in the plane of the web so that two stiffeners are sufficient to resist the components of a concentrated load. Frequently, loads have an out-of-plane component in which case the structure should be arranged so that two webs meet at the point of load application with stiffeners aligned with the three component directions (Fig. 10.6). In some situations, it is not practicable to have two webs meeting at the point of load application so that a component normal to a web exists. If this component is small it may be resisted in bending by an in-plane stiffener, otherwise an additional member must be provided spanning between adjacent frames or ribs, as shown in Fig. 10.7. In general, no normal loads should be applied to an unsupported web no matter how small their magnitude.
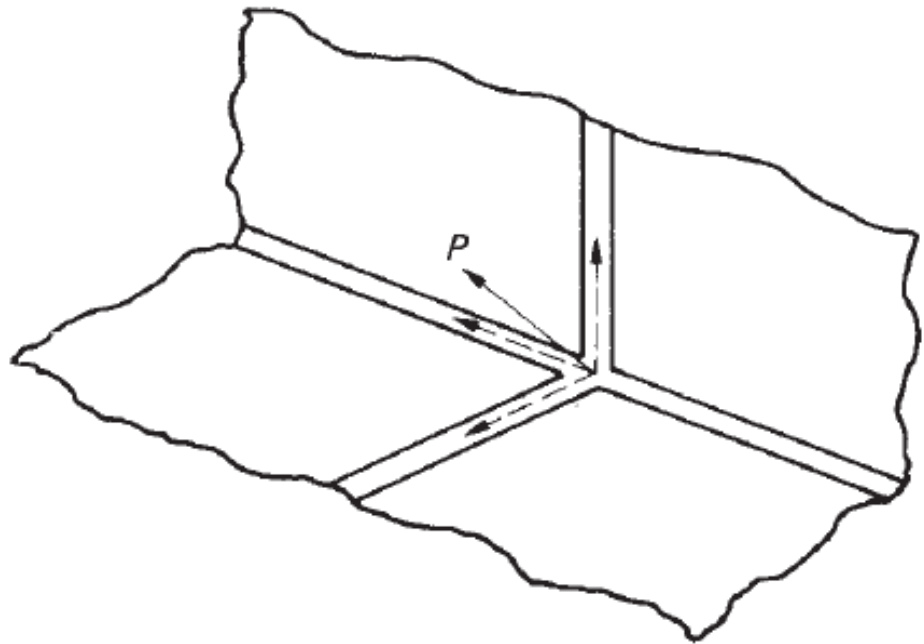
Fig. 10.6 Structural arrangement for an out of plane load.
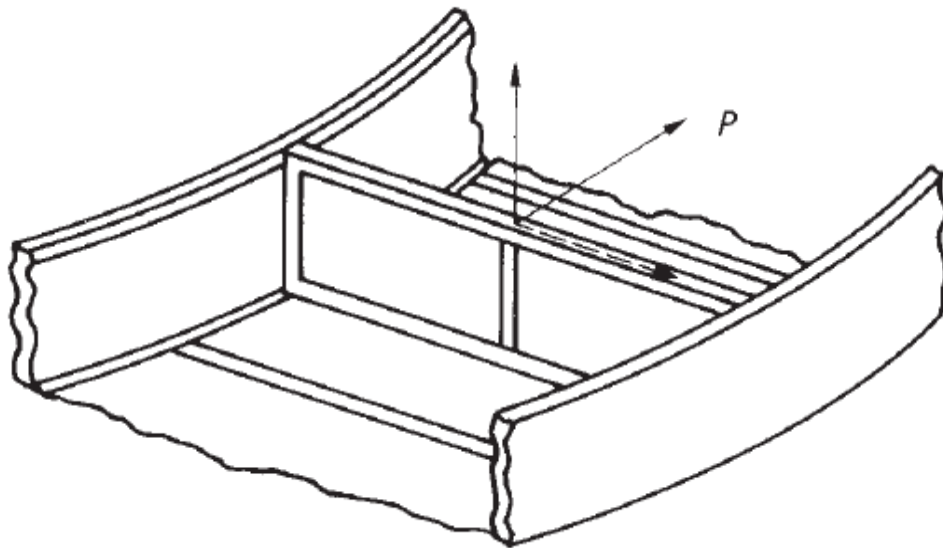
Fig. 10.7 Support of load having a component normal to a web.

2. Fuselage frames

The fuselage frames transfer loads to the fuselage shell and provide column support for the longitudinal stringers. The frames generally take the form of open rings so that the interior of the fuselage is not obstructed. They are

connected continuously around their peripheries to the fuselage shell and are not necessarily circular in form but will usually be symmetrical about a vertical axis. A fuselage frame is in equilibrium under the action of any external loads and the reaction shear flows from the fuselage shell. Suppose that a fuselage frame has a vertical axis of symmetry and carries a vertical external load W, as shown in Fig. 10.8(a) and (b). The fuselage shell/stringer section has been idealized such that the fuselage skin is effective only in shear. Suppose also that the shear force in the fuselage immediately to the left of the frame is $S_y,1$ and that the shear force in the fuselage immediately to the right of the frame is $S_{y,2}$; clearly, $S_{y,2} = S_{y,1} - W$. $S_{y,1}$ and $S_{y,2}$ generate shear flow distributions q_1 and q_2, respectively in the fuselage skin, each given by the following Eq. (A):

$$q_s = -\left(\frac{S_x I_{xx} - S_y I_{xy}}{I_{xx} I_{yy} - I_{xy}^2}\right)\sum_{r=1}^{n} B_r y_r - \left(\frac{S_y I_{yy} - S_x I_{xy}}{I_{xx} I_{yy} - I_{xy}^2}\right)\sum_{r=1}^{n} B_r x_r + q_{s,0}$$

(A)

in which $S_{x,1} = S_{x,2} = 0$ and $I_{xy} = 0$ (Cy is an axis of symmetry). The shear flow q_f transmitted to the periphery of the frame is equal to the algebraic sum of q_1 and q_2, i.e.

$$q_f = q_1 - q_2$$
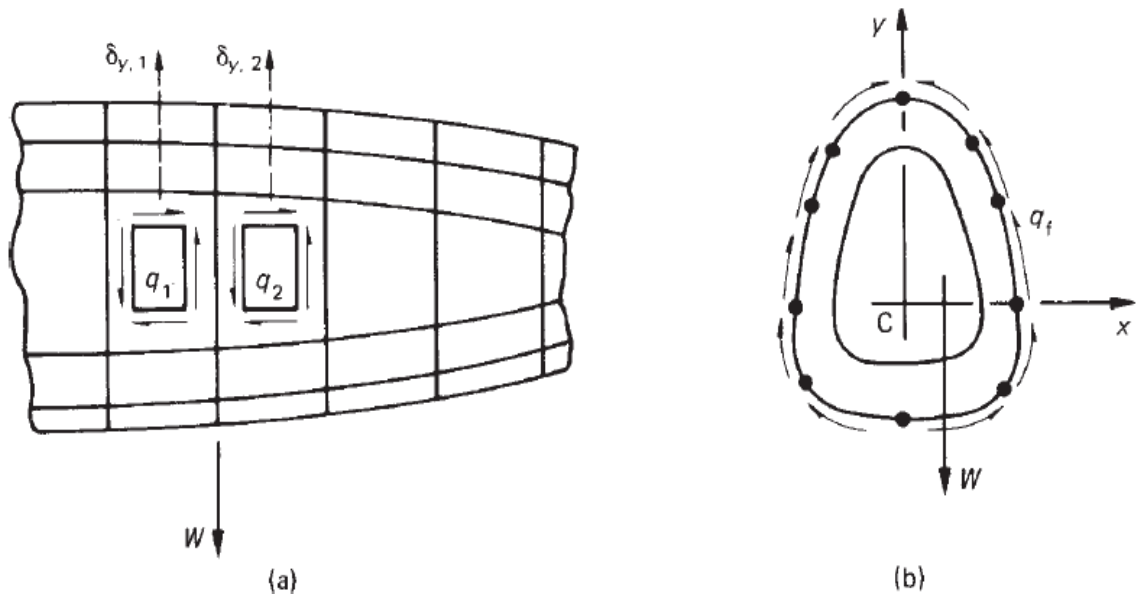
Fig. 10.8 Loads on a fuselage frame.

Thus, substituting for q_1 and q_2 obtained from Eq. (A) and noting that $S_{y,2} = S_{y,1} - W$, we have

$$q_\mathrm{f} = \frac{-W}{I_{xx}} \sum_{r=1}^{n} B_r y_r + q_{s,0}$$

in which $q_{s,o}$ is calculated using Eq. (17.17) where the shear load is W and

$$q_\mathrm{b} = \frac{-W}{I_{xx}} \sum_{r=1}^{n} B_r y_r$$

Having determined the shear flow distribution around the periphery of the frame, the frame itself may be analysed for distributions of bending moment, shear force and normal force, as described in previous chapters.

3. Wing ribs

Wing ribs perform similar functions to those performed by fuselage frames. They maintain the shape of the wing section, assist in transmitting external loads to the wing skin and reduce the column length of the stringers. Their geometry, however, is usually different in that they are frequently of unsymmetrical shape and possess webs which are continuous except for lightness holes and openings for control runs. Wing ribs are subjected to loading systems which are similar to those applied to fuselage frames. External loads applied in the plane of the rib produce a change in shear force in the wing across the rib; this induces reaction shear flows around its periphery.
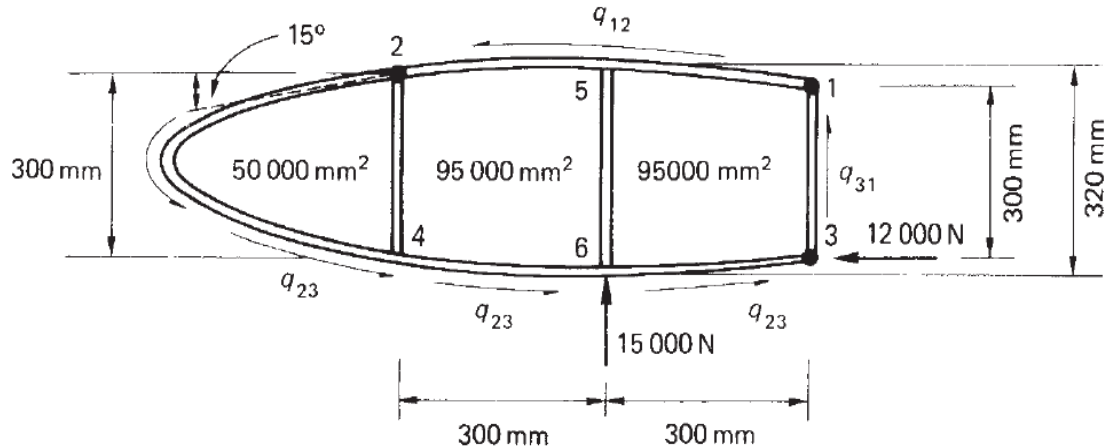
Fig. 10.9 Wing rib of Example 10.2.

To illustrate the method of rib analysis we shall use the example of a three-flange wing section in which the shear flow distribution is statically determinate.

Example 10.2

Calculate the shear flows in the web panels and the axial loads in the flanges of the wing rib shown in Fig. 10.9. Assume that the web of the rib is effective only in shear while the resistance of the wing to bending moments is provided entirely by the three flanges 1, 2 and 3. Since the wing bending moments are resisted entirely by the flanges 1, 2 and 3, the shear flows developed in the wing skin are constant between the flanges. Using the

For a three-flange wing section we have, resolving forces horizontally

$$600q_{12} - 600q_{23} = 12\,000\,\text{N} \tag{i}$$

Resolving vertically

$$300q_{31} - 300q_{23} = 15\,000\,\text{N} \tag{ii}$$

Taking moments about flange 3

$$2(50\,000 + 95\,000)q_{23} + 2 \times 95\,000q_{12} = -15\,000 \times 300\,\text{N mm} \tag{iii}$$

Solution of Eqs (i)–(iii) gives

$$q_{12} = 13.0\,\text{N/mm} \quad q_{23} = -7.0\,\text{N/mm} \quad q_{31} = 43.0\,\text{N/mm}$$

Consider now the nose portion of the rib shown in Fig. 10.10 and suppose that the shear flow in the web immediately to the left of the stiffener 24 is q_1. The total vertical shear force $S_{y,1}$ at this section is given by

177

$$S_{y,1} = 7.0 \times 300 = 2100N$$

The horizontal components of the rib flange loads resist the bending moment at this section. Thus

$$P_{x,4} = P_{x,2} = \frac{2 \times 50\,000 \times 7.0}{300} = 2333.3\,\text{N}$$
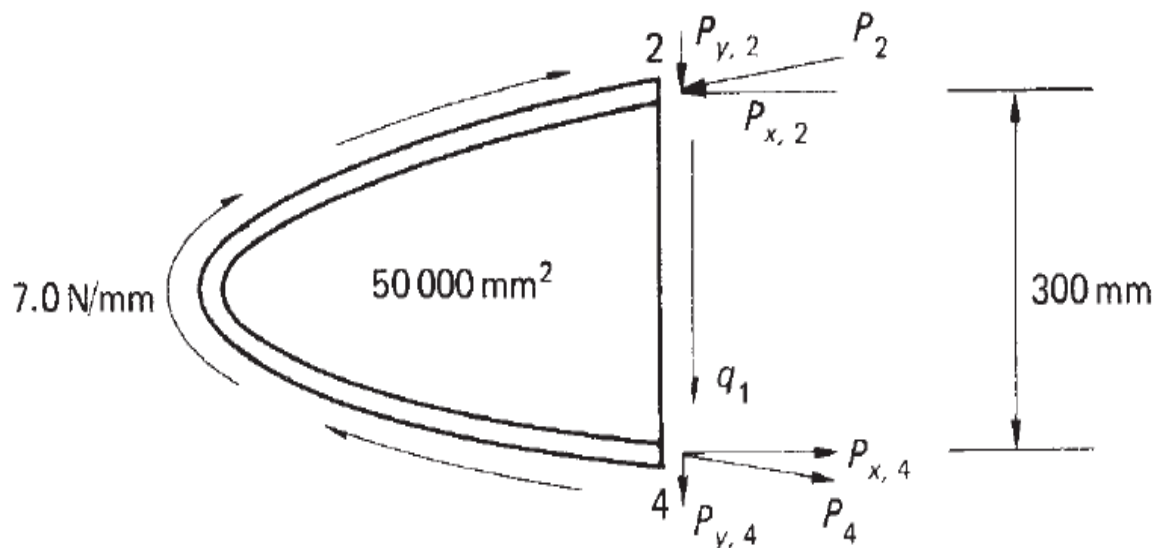
Fig. 10.10 Equilibrium of nose portion of the rib.

The corresponding vertical components are then

$$P_{y,2} = P_{y,4} = 2333.3 \tan 15° = 625.2N$$

Thus the shear force carried by the web is $2100 - 2 \times 625.2 = 849.6$ N. Hence

$$q_1 = \frac{849.6}{300} = 2.8\,\text{N/mm}$$

The axial loads in the rib flanges at this section are given by

$$P_2 = P_4 = (2333.3^2 + 625.2^2)^{1/2} = 2415.6\,\text{N}$$

The rib flange loads and web panel shear flows, at a vertical section immediately to the left of the intermediate web stiffener 56, are found by considering the free body diagram shown in Fig. 10.11. At this section, the rib flanges have zero slope so that the flange loads P_5 and $P6$ are obtained directly from the value of bending moment at this section. Thus

$$P_5 = P_6 = 2[(50\,000 + 46\,000) \times 7.0 - 49\,000 \times 13.0]/320 = 218.8\,\text{N}$$

тhe shear force at this section is resisted solely by the web. Hence

$$320q_2 = 7.0 \times 300 + 7.0 \times 10 - 13.0 \times 10 = 2040\,\text{N}$$
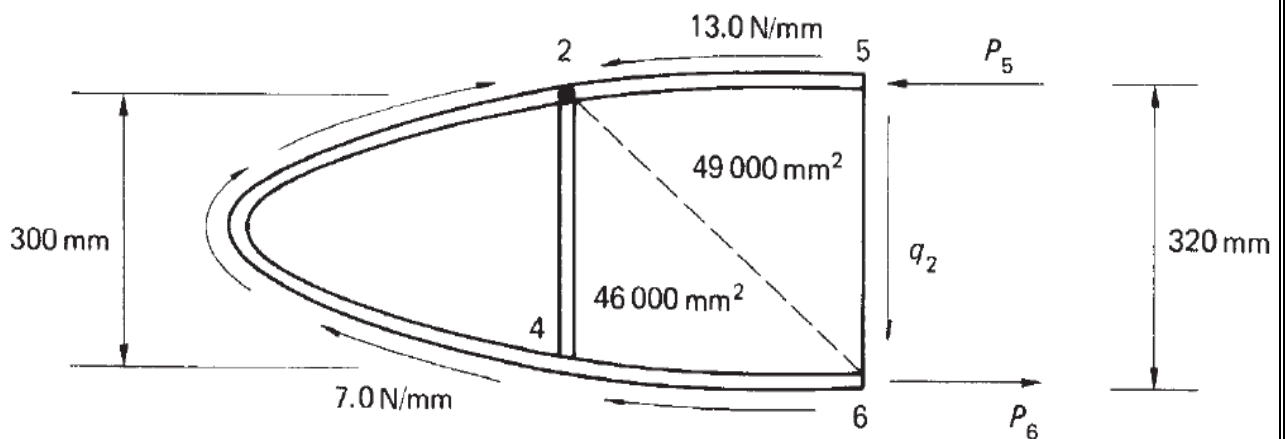
Fig. 10.11 Equilibrium of rib forward of intermediate stiffener 56.
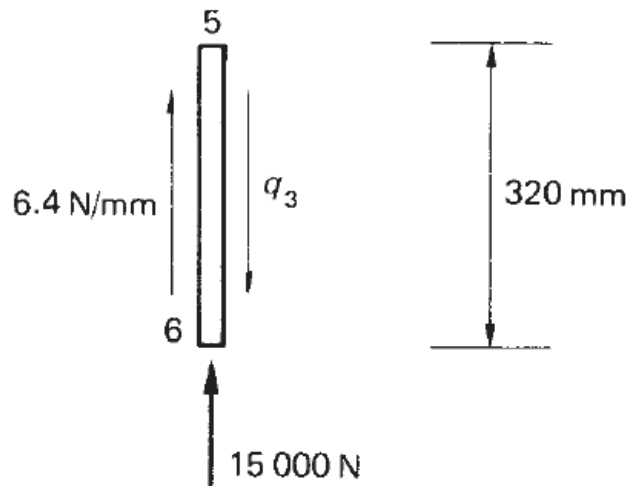
Fig. 10.12 Equilibrium of stiffener 56.
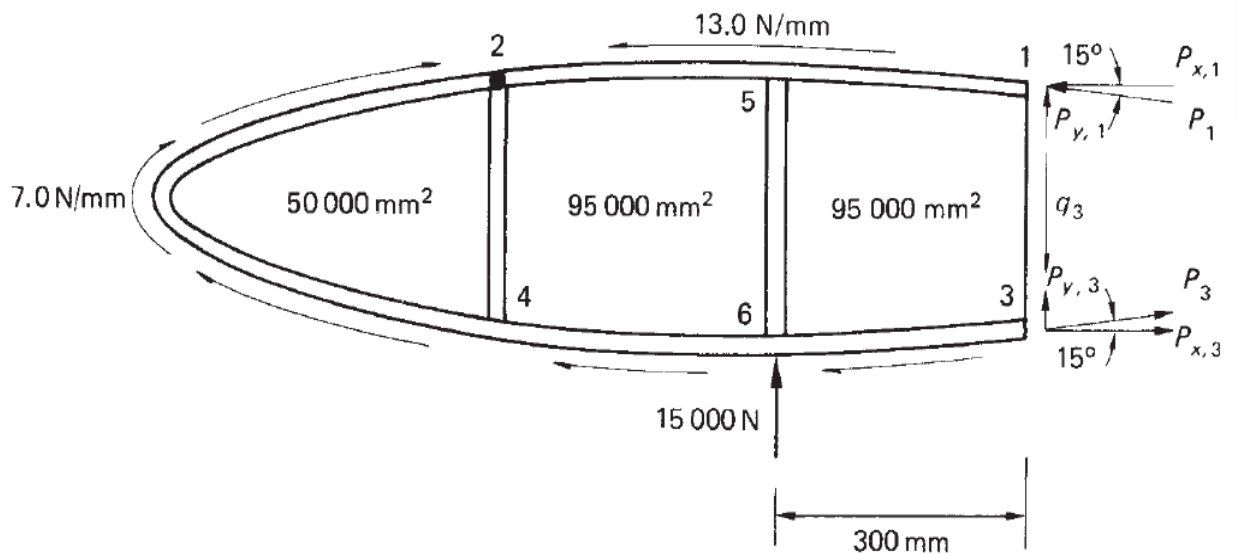
Fig. 10.13 Equilibrium of the rib forward of stiffener 31.

so that

$q_2 = 6.4$ N/mm

The shear flow in the rib immediately to the right of stiffener 56 is found most simply by considering the vertical equilibrium of stiffener 56 as shown in Fig. 10.12. Thus

$$320\,q_3 = 6.4 \times 320 + 15\,000$$

which gives

$$q_3 = 53.3\text{N/mm}$$

Finally, we shall consider the rib flange loads and the web shear flow at a section immediately forward of stiffener 31. From Fig. 10.13, in which we take moments about the point 3

$$M_3 = 2[(50\,000 + 95\,000) \times 7.0 - 95\,000 \times 13.0] + 15\,000 \times 300 = 4.06 \times 10^6\,\text{N mm}$$

The horizontal components of the flange loads at this section are then

$$P_{x,1} = P_{x,3} = \frac{4.06 \times 10^6}{300} = 13\,533.3\,\text{N}$$

and the vertical components are

$$P_{y,1} = P_{y,3} = 3626.2\,\text{N}$$

Hence

$$P_1 = P_3 = \sqrt{13\,533.3^2 + 3626.2^2} = 14\,010.7\,\text{N}$$

The total shear force at this section is $15\,000 + 300 \times 7.0 = 17\,100$ N. Therefore, the shear force resisted by the web is $17\,100 - 2 \times 3626.2 = 9847.6$N so that the shear flow q_3 in the web at this section is

$$q_3 = \frac{9847.6}{300} = 32.8\,\text{N/mm}$$

Chapter Eleven
Aircraft in Fatigue Structural Elements

12. General

In this respect, we consider the factors affecting the life of an aircraft including safe life and fail safe structures, designing against fatigue, the fatigue strength of components, the prediction of aircraft fatigue life and crack propagation.

Fatigue is defined as the progressive deterioration of the strength of a material or structural component during service such that failure can occur at much lower stress levels than the ultimate stress level. Fatigue is a dynamic phenomenon which initiates small (micro) cracks in the material or component and causes them to grow into large (macro) cracks; these, if not detected, can result in catastrophic failure. Fatigue damage can be produced in a variety of ways.

1. *Cyclic fatigue* is caused by repeated fluctuating loads.
2. *Corrosion fatigue* is accelerated by surface corrosion of the material penetrating inwards so that the material strength deteriorates.
3. Small scale rubbing movements and abrasion of adjacent parts cause *fretting fatigue*,
4. while *thermal fatigue* is produced by stress fluctuations induced by thermal expansions and contractions; the latter does not include the effect on material strength of heat.
5. Finally, high frequency stress fluctuations, due to vibrations excited by jet or propeller noise, cause *sonic* or *acoustic fatigue*.

Clearly an aircraft's structure must be designed so that fatigue does not become a problem. For aircraft in general, the requirements that the strength of an aircraft throughout its operational life shall be such as to ensure that the possibility of a disastrous fatigue failure shall be extremely remote (i.e. the probability of failure is less than 10^{-7}) under the action of the repeated loads of variable magnitude expected in service

12.2 Designing against fatigue

Various precautions may be taken to ensure that an aircraft has an adequate fatigue life. The following observations should be taken into considerations:

1. The early aluminium–zinc alloys possessed high ultimate and proof stresses but were susceptible to early failure under fatigue loading; choice of materials is therefore important. The naturally aged aluminium–copper alloys possess good fatigue resistance but with lower static strengths.

2. Modern research is concentrating on alloys which combine high strength with high fatigue resistance.

3. Stress concentrations can arise at sharp corners and abrupt changes in section. Fillets should therefore be provided at re-entrant corners, and cut-outs, such as windows and access panels, should be reinforced.

4. In machined panels the material thickness should be increased around bolt holes, while holes in primary bolted joints should be reamered to improve surface finish; surface scratches and machine marks are sources of fatigue crack initiation.

5. The *fatigue load spectrum* begins when the aircraft taxis to its take-off position. During taxiing the aircraft may be manoeuvring over uneven ground with a full payload so that wing stresses, for example, are greater than in the static case. Also, during take-off and climb and descent and landing the aircraft is subjected to the greatest load fluctuations.

6. The undercarriage is retracted and lowered; flaps are raised and lowered; there is the impact on landing; the aircraft has to carry out manoeuvres.

7. Finally, the aircraft, experiences a greater number of gusts than during the cruise. The loads corresponding to these various phases must be calculated before the associated stresses can be obtained. For example, during take-off, wing bending stresses and shear stresses due to shear and torsion are based on the total weight of the aircraft including full fuel tanks, and maximum payload all factored by 1.2 to allow for a bump during each take-off on a hard runway or by 1.5 for a take-off from grass.

8. The use of radar enables aircraft to avoid cumulus where guests are prevalent, but has little effect at low altitude in the climb and descent where clouds cannot be avoided. The ESDU (Engineering Sciences Data Unit) has produced gust data based on information collected by gust recorders carried by aircraft. Graphical forms are available in a form l_{10} versus h curves, h is altitude).

9. The average distance flown at various altitudes for a gust having a velocity greater than ±3.05 m/s to be encountered. In addition, *gust*

> *frequency curves* give the number of gusts of a given velocity per 1000
> gusts of velocity ±3.05 m/s.

Example:

The Airbus is required to have a life free from fatigue cracks of 24 000
flights or 30 000 hours, while its economic repair life is 48 000 flights or
60 000 hours; its landing gear, however, is designed for a safe life of 32
000 flights, after which it must be replaced.

12.3 Fatigue strength of components

As the stress level is decreased the number of cycles to failure increases,
resulting in a fatigue endurance curve (the *S–N* curve) of the type shown in
Fig. 12.1. Such a curve corresponds to the average value of N at each stress
amplitude since there will be a wide range of values of N for the given stress;
even under carefully controlled conditions the ratio of maximum N to
minimum N may be as high as 10: 1. Two other curves may therefore be
drawn, as shown in Fig. 12.1, enveloping all or nearly all the experimental
results; these curves are known as the *confidence limits*. If 99.9 per cent of all
the results lie between the curves, i.e. only 1 in 1000 falls outside, they
represent the 99.9 per cent confidence limits. If 99.99999 per cent of results
lie between the curves only 1 in 107 results will fall outside them and they
represent the 99.99999 per cent confidence limits. The results from tests on a
number of specimens may be represented as a histogram in which the number
of specimens failing within certain ranges R of N is plotted against N. Then if
N_{aV} is the average value of N at a given stress amplitude the probability of
failure occurring at N cycles is given by

$$p(N) = \frac{1}{\sigma\sqrt{2\pi}} \exp\left[-\frac{1}{2}\left(\frac{N - N_{\text{av}}}{\sigma}\right)^2\right]$$

(12.1)

in which σ is the standard deviation of the whole population of N values. The
derivation of Eq. (12.1) depends on the histogram approaching the profile of
a continuous function close to the *normal distribution*, which it does as the
interval N_{aV}/R becomes smaller and the number of tests increases. The
cumulative probability.
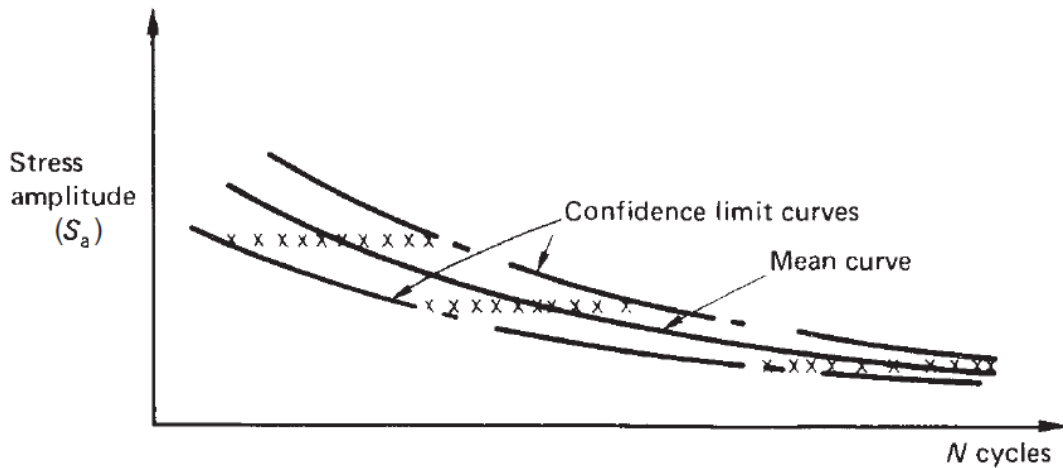
Fig. 12.1: S-N diagram

The probability that a particular specimen will fail at or below N cycles, is defined as

$$P(N) = \int_{-\infty}^{N} p(N)\, dN$$

(12.2)

The following points are to be noted:
1. The probability that a specimen will endure more than N cycles is then $1 - P(N)$. The normal distribution allows negative values of N, which is clearly impossible in a fatigue testing situation.
2. Other distributions, *extreme value distributions*, are more realistic and allow the existence of minimum fatigue endurances and fatigue limits.
3. The damaging portion of a fluctuating load cycle occurs when the stress is tensile; this causes cracks to open and grow.
4. Conversely, if the steady stress is compressive the maximum tensile stress will decrease and the number of cycles to failure will increase.
5. An approximate method of assessing the effect of a steady mean value of stress is provided by a Goodman diagram, as shown in Fig. 12.2. This shows the cyclic stress amplitudes which can be superimposed upon different mean stress levels to give a constant fatigue life.

In Fig. 12.2, Sa is the allowable stress amplitude, $Sa,0$ is the stress amplitude required to produce fatigue failure at N cycles with zero mean stress,

S_m is the mean stress and S_u the ultimate tensile stress.
If $S_m = S_u$ any cyclic stress will cause failure, while if $S_m = 0$ the allowable stress amplitude is $S_{a,0}$.
The equation of the straight line portion of the diagram is

$$\frac{S_a}{S_{a,0}} = \left(1 - \frac{S_m}{S_u} \right)$$

(12.3)

Experimental evidence suggests a non-linear relationship for particular materials. Equation (12.3) then becomes

$$\frac{S_a}{S_{a,0}} = \left[1 - \left(\frac{S_m}{S_u} \right)^m \right]$$

(12.4)

in which m lies between 0.6 and 2.
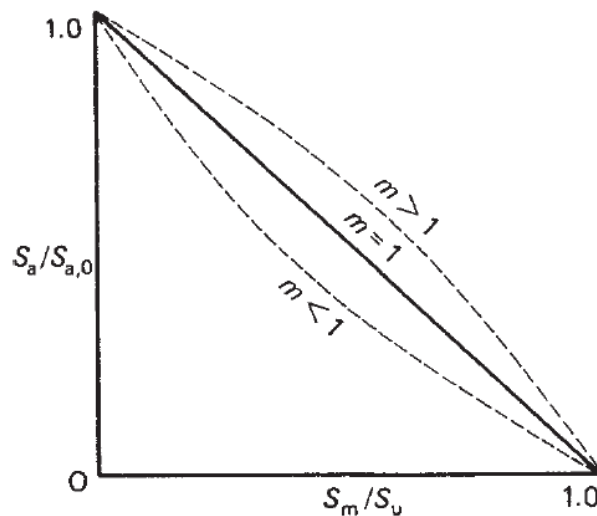
Fig. 12.2: Goodman diagram

In practical situations, fatigue is not caused by a large number of identical stress cycles but by many different stress amplitude cycles. The prediction of the number of cycles to failure therefore becomes complex. **Miner and**

Palmgren have proposed a *linear cumulative damage law* as follows. If N cycles of stress amplitude S_a cause fatigue failure, then 1 cycle produces $1/N$ of the total damage to cause failure. Therefore, if r different cycles are applied in which a stress amplitude S_j ($j = 1, 2, \ldots, r$) would cause failure in N_j cycles the number of cycles n_j required to cause total fatigue failure is given by

$$\sum_{j=1}^{r} \frac{n_j}{N_j} = 1$$

(12.5)

Although *S–N* curves may be readily obtained for different materials by testing a large number of small specimens (*coupon tests*), it is not practicable to adopt the same approach for aircraft components since these are expensive to manufacture and the test program too expensive to run for long periods of time. Stresses were measured at points where fatigue was expected (and actually occurred) and *S–N* curves plotted for the complete structure. The curves had the usual appearance and at low stress levels had such large endurances that fatigue did not occur; thus a fatigue limit existed. It was found that the average *S–N* curve could be approximated to by the equation

$$S_a = 10.3(1 + 1000/\sqrt{N})$$

(12.6)

in which the mean stress was 90 N/mm². In general terms, Eq. (12.6) may be written as

$$S_a = S_\infty(1 + C/\sqrt{N})$$

(12.7)

in which S_∞ is the fatigue limit and C is a constant. Thus $S_a \rightarrow S_\infty$ as $N \rightarrow \infty$. Equation (12.7) may be rearranged to give the endurance directly, i.e.

$$N = C^2 \left(\frac{S_\infty}{S_a - S_\infty} \right)^2$$

(12.8)

which shows clearly that as $S_a \rightarrow S_\infty$, $N \rightarrow \infty$.

It has been found ==experimentally== that N is inversely proportional to the mean stress as the latter varies in the region of 90 N/mm^2 while C is virtually constant. This suggests a method of determining a 'standard' endurance curve (corresponding to a mean stress level of 90 N/mm^2) from tests carried out on a few specimens at other mean stress levels. Suppose S_m is the mean stress level, not 90 N/mm^2, in tests carried out on a few specimens at an alternating stress level $S_{a,m}$ where failure occurs at a mean number of cycles N_m. Then assuming that the S–N curve has the same form as Eq. (12.7)

$$S_{a,m} = S_{\infty,m}(1 + C/\sqrt{N_m})$$

(12.9)

in which $C = 1000$ and S_∞,m is the fatigue limit stress corresponding to the mean stress S_m. Rearranging Eq. (12.9) we have

$$S'_{\infty,m} = S_{a,m}/(1 + C/\sqrt{N'})$$

(12.10)

The number of cycles to failure at a mean stress of 90 N/mm^2 would have been, from the above

$$N' = \frac{S_m}{90} N_m$$

(12.11)

The corresponding fatigue limit stress would then have been, from a comparison with Eq. (12.10)

$$S'_{\infty,m} = S_{a,m}/(1 + C/\sqrt{N'})$$

$$(12.12)$$

The standard endurance curve for the component at a mean stress of 90 N/mm^2 is from Eq. (12.7)

$$S_a = S'_{\infty,m}/(1 + C/\sqrt{N})$$

$$(12.13)$$

Substituting in Eq. (12.13) for $S_{\infty,m}$ from Eq. (12.12) we have

$$S_a = \frac{S_{a,m}}{(1 + C/\sqrt{N'})}(1 + C/\sqrt{N})$$

$$(12.14)$$

in which N'' is given by Eq. (12.11).

Equation (12.14) will be based on a few test results so that a 'safe' fatigue strength is usually taken to be three standard deviations below the mean fatigue strength. Hence we introduce *a scatter factor Kn (>1)* to allow for this; Eq. (12.14) then becomes

$$S_a \frac{S_{a,m}}{K_n(1 + C/\sqrt{N'})}(1 + C/\sqrt{N})$$

$$(12.15)$$

K_n varies with the number of test results available and for a coefficient of variation of 0.1, $K_n = 1.45$ for 6 specimens, $K_n = 1.445$ for 10 specimens, $K = 1.44$ for 20 specimens and for 100 specimens or more $K_n = 1.43$. For typical S–N curves a scatter factor of 1.43 is equivalent to a life factor of 3 to 4.

12.4 Prediction of aircraft fatigue life

We have seen that an aircraft suffers fatigue damage during all phases of the ground–air– ground cycle. The various contributions to this damage may be calculated separately and hence the safe life of the aircraft in terms of the

number of flights calculated. In the ground–air–ground cycle the maximum vertical acceleration during take-off is 1.2 g for a take-off from a runway or 1.5 g for a take-off from grass.

It is assumed that these accelerations occur at zero lift and therefore produce compressive (negative) stresses, $-S_{TO}$, in critical components such as the undersurface of wings. The maximum positive stress for the same component occurs in level flight (at 1 g) and is $+S_{1g}$. The ground–air–ground cycle produces, on the undersurface of the wing, a fluctuating stress $S_{GAG} = (S_{1g} +S_{TO})/2$ about a mean stress $SGAG(mean) = (S_{1g} -S_{TO})/2$. Suppose that tests show that for this stress cycle and mean stress, failure occurs after N_G cycles. For a life factor of 3 the safe life is $N_G/3$ so that the damage done during one cycle is $3/N_G$. This damage is multiplied by a factor of 1.5 to allow for the variability of loading between different aircraft of the same type so that the damage per flight D_{GAG} from the ground–air–ground cycle is given by:

$$D_{GAG} = 4.5/N_G$$

$$(12.16)$$

Fatigue damage is also caused by gusts encountered in flight, particularly during the climb and descent. Suppose that a gust of velocity u_e causes a stress S_u about a mean stress corresponding to level flight, and suppose also that the number of stress cycles of this magnitude required to cause failure is $N(S_u)$; the damage caused by one cycle is then $1/N(S_u)$.

From the Palmgren–Miner hypothesis, when sufficient gusts of this and all other magnitudes together with the effects of all other load cycles produce acumulative damage of 1.0, fatigue failure will occur.

The ESDU data sheets [Reference: ESDU Data Sheets, Fatigue, No. 80036] present the data in two forms.

1. First, $l10$ against altitude curves show the distance which must be flown at a given altitude in order that a gust (positive or negative) having a velocity ≥ 3.05 m/s be encountered. It follows that $1/l10$ is the number of gusts encountered in unit distance (1 km) at a particular height.

2. Secondly, gust frequency distribution curves, $r(u_e)$ against u_e, give the number of gusts of velocity u_e for every 1000 gusts of velocity 3.05 m/s. From these two curves the gust exceedance $E(u_e)$ is obtained; $E(u_e)$ is the number of times a gust of a given magnitude (u_e) will be equaled or exceeded in 1 km of flight.

Thus, from the above

number of gusts ≥ 3.05 m/s per km $= 1/l_{10}$

number of gusts equal to u_e per 1000 gusts equal to 3.05 m/s $= r(u_e)$

Hence

number of gusts equal to u_e per single gust equal to 3.05 m/s $= r(u_e)/1000$

It follows that the gust exceedance $E(u_e)$ is given by

$$E(u_e) = \frac{r(u_e)}{1000 l_{10}}$$

(12.17)

in which $l10$ is dependent on height. A good approximation for the curve of $r(u_e)$ against u_e in the region $u_e = 3.05$ m/s is:

$$r(u_e) = 3.23 \times 10^5 u_e^{-5.26}$$

(12.18)

Consider the typical gust exceedance curve shown in Fig. 12.3. In 1 km of flight there are likely to be $E(ue)$ gusts exceeding ue m/s and $E(ue) - \delta E(ue)$ gusts exceeding
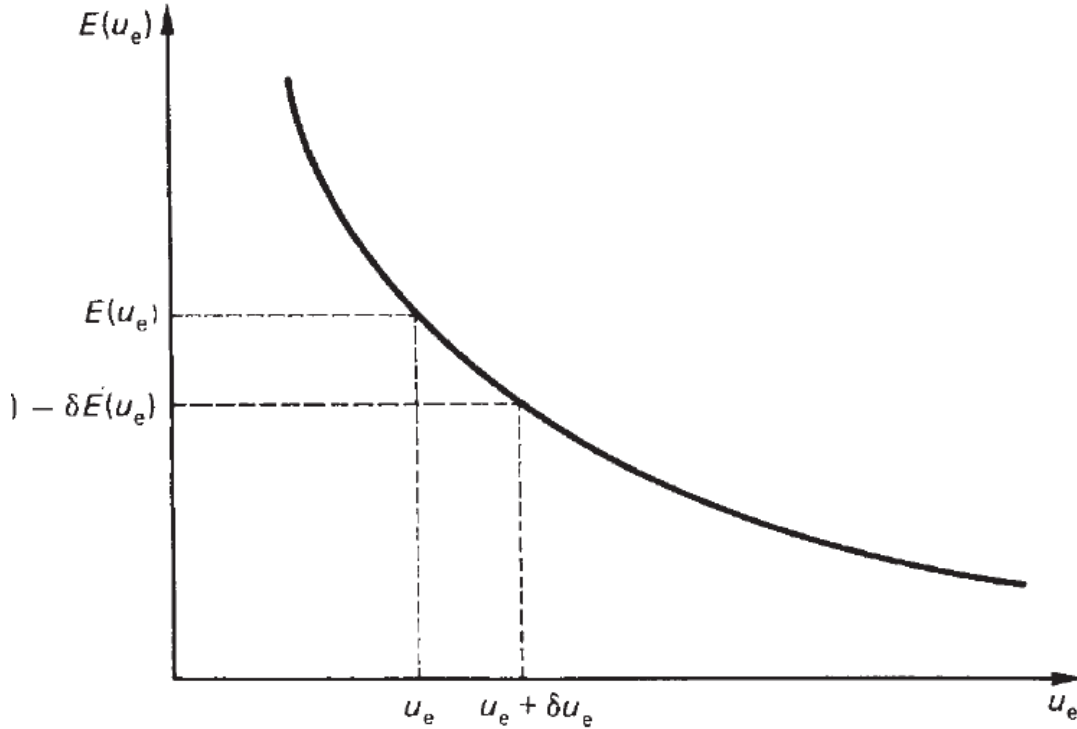
Fig. 12.3: Gust exceedance curve

$U_e + \delta_{ue}$ m/s. Thus, there will be $\delta E(u_e)$ *fewer* gusts exceeding $u_e + \delta u_e$ m/s than u_e m/s and the increment in gust speed δu_e corresponds to a number $-\delta E(u_e)$ of gusts at a gust speed close to u_e. Half of these gusts will be positive (upgusts) and half negative (downgusts) so that if it is assumed that each upgust is followed by a downgust of equal magnitude the number of complete gust cycles will be $-\delta E(u_e)/2$.

Suppose that each cycle produces a stress $S(u_e)$ and that the number of these cycles required to produce failure is $N(S_{u,e})$. The damage caused by one cycle is then $1/N(S_{u,e})$ and over the gust velocity interval δu_e the total damage δD is given by

$$\delta D = -\frac{\delta E(u_e)}{2N(S_{u,e})} = -\frac{dE(u_e)}{du_e}\frac{\delta u_e}{2N(S_{u,e})}$$

(12.19)

Integrating Eq. (12.19) over the whole range of gusts likely to be encountered, we obtain the total damage D_g per km of flight.

153

$$D_g = -\int_{u_f}^{\infty} \frac{1}{2N(S_{u,e})} \frac{dE(u_e)}{du_e} du_e$$

(12.20)

Further, if the average block length journey of an aircraft is R_{av}, the average gust damage per flight is D_gR_{av}. Also, some aircraft in a fleet will experience more gusts than others since the distribution of gusts is random. Therefore, if, for example, it is found that one particular aircraft encounters 50 per cent more gusts than the average its gust fatigue damage is $1.5D_g$/km.

The gust damage predicted by Eq. (12.20) is obtained by integrating over a complete gust velocity range from zero to infinity. Clearly there will be a gust velocity below which no fatigue damage will occur since the cyclic stress produced will be below the fatigue limit stress of the particular component. Equation (12.20) is therefore rewritten

$$D_g = -\int_{u_f}^{\infty} \frac{1}{2N(S_{u,e})} \frac{dE(u_e)}{du_e} du_e$$

(12.21)

in which u_f is the gust velocity required to produce the fatigue limit stress. We have noted previously that more gusts are encountered during climb and descent than during cruise. Altitude therefore affects the amount of fatigue damage caused by gusts and its effects may be determined as follows. Substituting for the gust exceedance $E(u_e)$ in Eq. (12.21) from Eq. (12.17) we obtain

$$D_g = -\frac{1}{1000l_{10}} \int_{u_f}^{\infty} \frac{1}{2N(S_{u,e})} \frac{dr(u_e)}{du_e} du_e$$

or

$$D_g = \frac{1}{l_{10}} d_g \text{ per km}$$

(12.22)

154

Suppose that the aircraft is climbing at a speed V with a rate of climb (ROC). The time taken for the aircraft to climb from a height h to a height $h+\delta h$ is $\delta h/\text{ROC}$ during which time it travels a distance $V\delta h/\text{ROC}$. Hence, from Eq. (12

.22) the fatigue damage experienced by the aircraft in climbing through a height δh is

$$\frac{1}{l_{10}} d_g \frac{V}{\text{ROC}} \delta h$$

The total damage produced during a climb from sea level to an altitude H at a constant speed V and ROC is

$$D_{\text{g,climb}} = d_g \frac{V}{\text{ROC}} \int_0^H \frac{dh}{l_{10}}$$

$$(12.23)$$

Plotting $1/l_{10}$ against h from ESDU data sheets for aircraft having cloud warning radar and integrating gives

$$\int_0^{3000} \frac{dh}{l_{10}} = 303 \qquad \int_{3000}^{6000} \frac{dh}{l_{10}} = 14 \qquad \int_{6000}^{9000} \frac{dh}{l_{10}} = 3.4$$

From the above 90000 dh/l10 =320.4, from which it can be seen that approximately 95 per cent of the total damage in the climb occurs in the first 3000 m.

An additional factor influencing the amount of gust damage is forward speed. For example, the change in wing stress produced by a gust may be represented by

$$S_{\text{u,e}} = k_1 u_e V_e$$

$$(12.24)$$

in which the forward speed of the aircraft is in equivalent airspeed (EAS). From Eq. (12.24) we see that the gust velocity u_f required to produce the fatigue limit stress $S\infty$ is

$$u_f = S_\infty / k_1 V_e$$

The gust damage per km at different forward speeds V_e is then found using Eq. (12.21) with the appropriate value of u_f as the lower limit of integration. The integral may be evaluated by using the known approximate forms of $N(S_{u,e})$ and $E(u_e)$ from Eqs (12.15) and (12.17). From Eq. (12.15)

$$S_a = S_{u,e} = \frac{S'_{\infty,m}}{K_n}(1 + C/\sqrt{N(S_{u,e})})$$

$$N(S_{u,e}) = \left(\frac{C}{K_n}\right)^2 \left(\frac{S'_{\infty,m}}{S_{u,e} - S'_{\infty,m}}\right)^2$$

where $S_{u,e} = k_1 V_e u_e$ and $S'_{\infty,m} = k_1 V_e u_f.$

From which from Equ. (12.17), we have,

$$E(u_e) = \frac{r(u_e)}{1000 l_{10}}$$

or, substituting for $r(u_e)$ from Eq. (12.18)

$$E(u_e) = \frac{3.23 \times 10^5 u_e^{-5.26}}{1000 l_{10}}$$

Equation (12.21) then becomes:

$$D_g = -\int_{u_f}^{\infty} \frac{1}{2} \left(\frac{K_n}{C}\right)^2 \left(\frac{S_{u,e} - S'_{\infty,m}}{S'_{\infty,m}}\right)^2 \left(\frac{-3.23 \times 5.26 \times 10^5 u_e^{-5.26}}{1000 l_{10}}\right) du_e$$

Substituting for $S_{u,e}$ and $S'_{\infty,m}$ we have

$$D_g = \frac{16.99 \times 10^2}{2 l_{10}} \left(\frac{K_n}{C}\right)^2 \int_{u_f}^{\infty} \left(\frac{u_e - u_f}{u_f}\right)^2 u_e^{-6.26} du_e$$

or

$$D_g = \frac{16.99 \times 10^2}{2 l_{10}} \left(\frac{K_n}{C}\right)^2 \int_{u_f}^{\infty} \left(\frac{u_e^{-4.26}}{u_f^2} - \frac{2u_e^{-5.26}}{u_f} + u_e^{-6.26}\right) du_e$$

from which

$$D_g = \frac{46.55}{2 l_{10}} \left(\frac{K_n}{C}\right)^2 u_f^{-5.26}$$

or, in terms of the aircraft speed V_e

$$D_g = \frac{46.55}{2 l_{10}} \left(\frac{K_n}{C}\right)^2 \left(\frac{k_1 V_e}{S'_{\infty,m}}\right)^{5.26} \text{ per km}$$

(12.26)

It can be seen from Eq. (12.26) that gust damage increases in proportion to $V_e^{5.26}$ so that increasing forward speed has a dramatic effect on gust damage.

The total fatigue damage suffered by an aircraft per flight is the sum of the damage caused by the ground–air–ground cycle, the damage produced by gusts and the damage due to other causes such as pilot induced manoeuvres, ground turning and braking, and landing and take-off load fluctuations.
The damage produced by these other causes can be determined from load exceedance data. Thus, if this extra damage per flight is Dextra the total fractional fatigue damage per flight is

$$D_{\text{total}} = D_{\text{GAG}} + D_{\text{g}}R_{\text{av}} + D_{\text{extra}}$$

or

$$D_{\text{total}} = 4.5/N_{\text{G}} + D_{\text{g}}R_{\text{av}} + D_{\text{extra}}$$

(12.27)

and the life of the aircraft in terms of flights is

$$N_{\text{flight}} = 1/D_{\text{total}}$$

(12.28)

12.5 Crack propagation

We have seen that the concept of fail-safe structures in aircraft construction relies on a damaged structure being able to retain sufficient of its load-carrying capacity to prevent catastrophic failure, at least until the damage is detected. It is therefore essential that the designer be able to predict how and at what rate a fatigue crack will grow. The ESDU data sheets provide a useful introduction to the study of crack propagation; some of the results are presented here. The analysis of stresses closes to a crack tip using elastic stress concentration factors breaks down since the assumption that the crack tip radius approaches zero results in the stress concentration factor tending to infinity. Instead, linear elastic fracture mechanics analyses the stress field around the crack tip and identifies features of the field common to all cracked elastic bodies.

12.5.1 Stress concentration factor

There are three basic modes of crack growth, as shown in Fig. 12.4. Generally, the stress field in the region of the crack tip is described by a two-dimensional model which may be used as an approximation for many practical three-dimensional loading cases. Thus, the stress system at a distance r $(r \leq a)$ from the tip of a crack of length $2a$, shown in Fig. 12.5, can be expressed in the form

$$S_r, S_\theta, S_{r,\theta} = \frac{K}{(2\pi r)^{\frac{1}{2}}} f(\theta)$$

(12.29)

in which $f(\theta)$ is a different function for each of the three stresses and K is the *stress intensity factor*; K is a function of the nature and magnitude of the applied stress levels and also of the crack size. The terms $(2\pi r)^{1/2}$ and $f(\theta)$ map the stress field in the
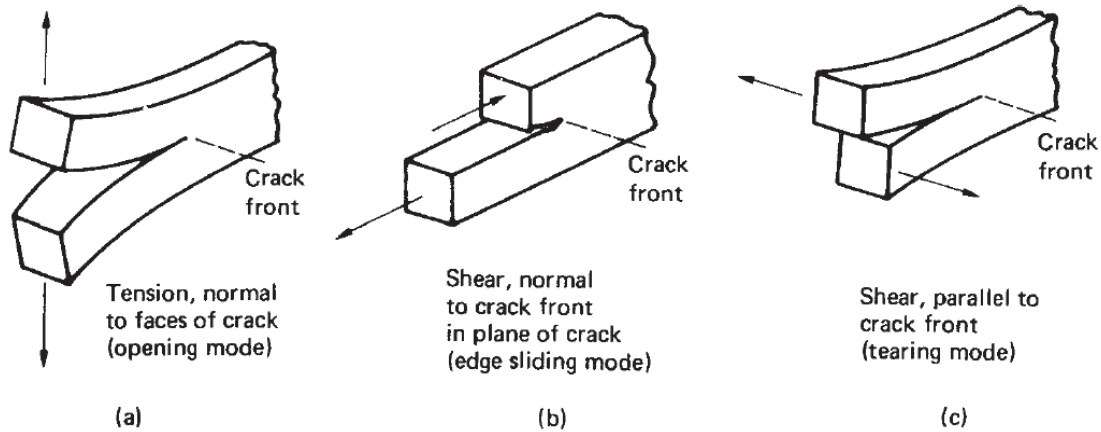

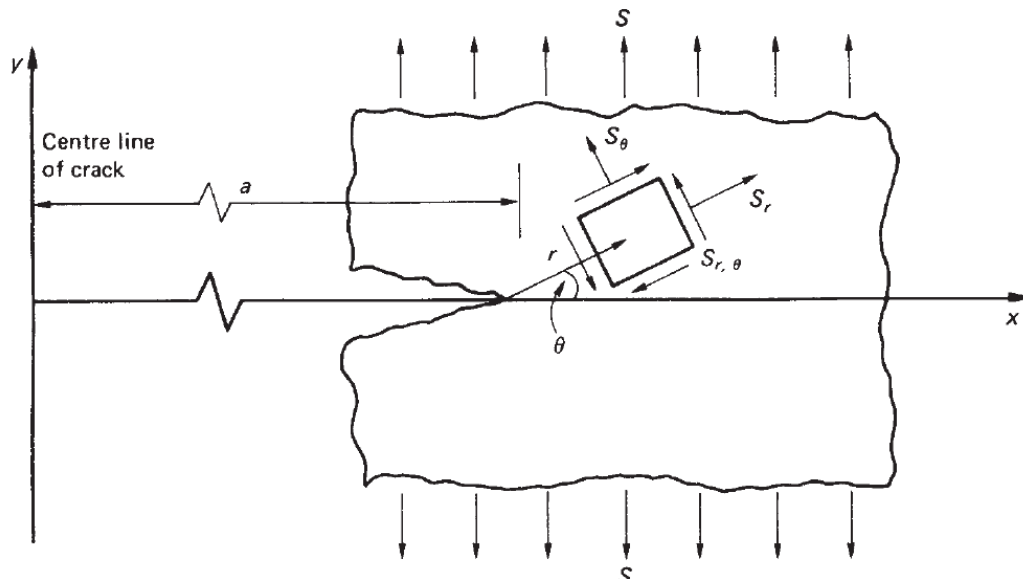**Fig. 12.4: Basic modes of crack growth**

Fig. 12.5: Stress Field in the vicinity of a crack

vicinity of the crack and are the same for all cracks under external loads that cause crack openings of the same type. Equation (12.29) applies to all modes of crack opening, with K having different values depending on the geometry

159

of the structure, the nature of the applied loads and the type of crack.Experimental data show that crack growth and residual strength data are better correlated using K than any other parameter. K may be expressed as a function of the nominal applied stress S and the crack length in the form:

$$K = S(\pi a)^{\frac{1}{2}} \alpha$$

$$(12.30)$$

in which α is a non-dimensional coefficient usually expressed as the ratio of crack length to any convenient local dimension in the plane of the component; for a crack in an infinite plate under an applied uniform stress level S remote from the crack, $\alpha=1.0$.

Alternatively, in cases where opposing loads P are applied at points close to the plane of the crack

$$K = \frac{P\alpha}{(\pi a)^{\frac{1}{2}}}$$

$$(12.31)$$

in which P is the load/unit thickness. Equations (12.30) and (12.31) may be rewritten as

$$K = K_0 \alpha$$

$$(12.32)$$

where K_0 is a reference value of the stress intensity factor which depends upon the loading. For the simple case of a remotely loaded plate in tension

$$K_0 = S(\pi a)^{\frac{1}{2}}$$

$$(12.33)$$

and Eqs (12.32) and (12.30) are identical so that for a given ratio of crack length to plate width α is the same in both formulations. In more complex cases, for example the in-plane bending of a plate of width $2b$ and having a central crack of length $2a$

$$K_0 = \frac{3Ma}{4b^3}(\pi a)^{\frac{1}{2}}$$

(12.34)

in which M is the bending moment per unit thickness. Comparing Eqs (12.34) and (12.30), we see that $S = 3Ma/4b3$ which is the value of direct stress given by basic bending theory at a point a distance $\pm a/2$ from the central axis. However, if S was specified as the bending stress in the outer fibres of the plate, i.e. at $\pm b$, then $S = 3M/2b2$.

clearly the different specifications of S require different values of α. On the other hand, the final value of K must be independent of the form of presentation used. Use of Eqs (12.30)–(12.32) depends on the form of the solution for K_0 and care must be taken to ensure that the formula used and the way in which the nominal stress is defined are compatible with those used in the derivation of α.

There are a number of methods available for determining the value of K and α. In one method the solution for a component subjected to more than one type of loading is obtained from available standard solutions using superposition or, if the geometry is not covered, two or more standard solutions may be compounded.

The coefficient α in Eq. (12.30) has different values depending on the plate and crack geometries. Listed below are values of α for some of the more common cases.

(i) A semi-infinite plate having an edge crack of length a; $\alpha=1.12$.

(ii) An infinite plate having an embedded circular crack or a semi-circular surface crack, each of radius a, lying in a plane normal to the applied stress; $\alpha=0.64$.

(iii) An infinite plate having an embedded elliptical crack of axes $2a$ and $2b$ or a semielliptical crack of width $2b$ in which the depth a is less than half the plate thickness each lying in a plane normal to the applied stress; $\alpha=1.12\ \phi$ in which ϕ varies with the ratio a/b as follows:

a/b	0	0.2	0.4	0.6	0.8
Φ	1.0	1.05	1.15	1.28	1.42

For $a/b = 1$ the situation is identical to case (ii).

(iv) A plate of finite width w having a central crack of length $2a$ where $a\leq0.3w$; $\alpha=[\ \sec\ (a\pi/w)]1/2$.

(v) For a plate of finite width w having two symmetrical edge cracks each of depth $2a$, Eq. (12.30) becomes

$$K = S[w \tan (\pi a/w) + (0.1w) \sin (2\pi a/w)]^{1/2}$$

From Eq. (12.29) it can be seen that the stress intensity at a point ahead of a crack can be expressed in terms of the parameter K. Failure will then occur when K reaches a critical value K_c. This is known as the <mark>*fracture toughness*</mark> of the material and has units MN/m$^{3/2}$ or N/mm$^{3/2}$.

12.5.2 Crack tip plasticity

In certain circumstances it may be necessary to account for the effect of plastic flow in the vicinity of the crack tip. This may be allowed for by estimating the size of the plastic zone and adding this to the actual crack length to form an effective crack length $2a_1$. Thus, if r_p is the radius of the plastic zone, $a_1 = a + r_p$ and Eq. (12.30) becomes

$$K_p = S(\pi a_1)^{\frac{1}{2}} \alpha_1$$

(12.35)

in which K_p is the stress intensity factor corrected for plasticity and α_1 corresponds to a_1. Thus for $r_p/t > 0.5$, i.e. a condition of plane stress

$$r_p = \frac{1}{2\pi} \left(\frac{K}{f_y} \right)^2 \quad \text{or} \quad r_p = \frac{a}{2} \left(\frac{S}{f_y} \right)^2 \alpha^2$$

(12.36)

in which f_y is the yield proof stress of the material. For $r_p/t < 0.02$, a condition of plane strain

$$r_p = \frac{1}{6\pi} \left(\frac{K}{f_y} \right)^2$$

(12.37)

For intermediate conditions the correction should be such as to produce a conservative solution. Dugdale[D. S., *J. Mech. Phys. Solids*, **8**, 1960.] showed

that the fracture toughness parameter K_c is highly dependent on plate thickness. In general, since the toughness of a material decreases with decreasing plasticity, it follows that the true fracture toughness is that corresponding to a plane strain condition. This lower limiting value is particularly important to consider in high strength alloys since these are prone to brittle failure. In addition, the assumption that the plastic zone is circular is not representative in plane strain conditions. Rice
and Johnson [Rice, J. R. and Johnson, M. A., *Inelastic Behaviour of Solids*, McGraw Hill, NewYork, 1970] showed that, for a small amount of plane strain yielding, the plastic zone extends as two lobes (Fig. 12.6) each inclined at an angle θ to the axis of the crack where $\theta = 70°$ and the greatest extent L and forward penetration (r_y for $\theta = 0$) of plasticity are given by

$$L = 0.155 \, (K/f_y)^2$$

$$r_y = 0.04 \, (K/f_y)^2$$
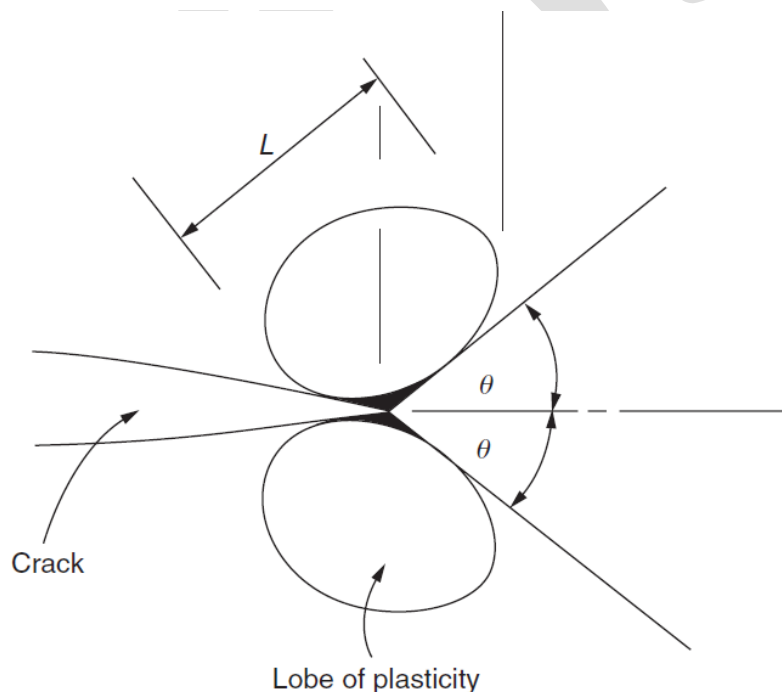
12.5.3 Crack propagation rates
Having obtained values of the stress intensity factor and the coefficient α, fatigue crack propagation rates may be estimated. From these, the life of a structure containing cracks or crack-like defects may be determined;

alternatively, the loading condition may be modified or inspection periods arranged so that the crack will be detected before failure. Under constant amplitude loading the rate of crack propagation may be represented graphically by curves described in general terms by the law[Paris, P. C. and Erdogan, F., A critical analysis of crack propagation laws, [*Trans. Am. Soc. Mech.Engrs.*, **85**, Series D, No. 4, December 1963.]

$$\frac{\mathrm{d}a}{\mathrm{d}N} = f(R, \Delta K)$$

(12.38)

in which ΔK is the stress intensity factor range and $R = S_{min}/S_{max}$. If Eq. (12.30) is used

$$\Delta K = (S_{max} - S_{min})(\pi a)^{\frac{1}{2}} \alpha$$

(12.39)

Equation (12.39) may be corrected for plasticity under cyclic loading and becomes

$$\Delta K_{\mathrm{p}} = (S_{max} - S_{min})(\pi a_1)^{\frac{1}{2}} \alpha_1$$

(12.40)

in which $a_1 = a + r_{\mathrm{p}}$, where, for plane stress

$$r_{\mathrm{p}} = \frac{1}{8\pi} \left(\frac{\Delta K}{f_{\mathrm{y}}} \right)^2$$

[Rice, J. R., Mechanics of crack tip deformation and extension by fatigue. In: *Fatigue Crack*]

The curves represented by Eq. (12.38) may be divided into three regions. The first corresponds to a very slow crack growth rate ($<10^{-8}$ m/cycle) where the curves approach a threshold value of stress intensity factor ΔK_{th} corresponding

to 4×10^{-11} m/cycle, i.e. no crack growth. In the second region (10^{-8}– 10^{-6} m/cycle) much of the crack life takes place and, for small ranges of ΔK, Eq. (12.38) may be represented by

$$\frac{\mathrm{d}a}{\mathrm{d}N} = C(\Delta K)^n$$

[Paris, P. C., The fracture mechanics approach to fatigue. In: *Fatigue – An Interdisciplinary*] **(12.41)**

in which C and n depend on the material properties; over small ranges of $\mathrm{d}a/\mathrm{d}N$ and ΔK, C and n remain approximately constant. The third region corresponds to crack growth rates $>10^{-6}$ m/cycle, where instability and final failure occur. An attempt has been made to describe the complete set of curves by the relationship

$$\frac{\mathrm{d}a}{\mathrm{d}N} = \frac{C(\Delta K)^n}{(1 - R)K_{\mathrm{c}} - \Delta K}$$

[Forman, R. G., Numerical analysis of crack propagation in cyclic-loaded structures, *Trans. Am.*] **(12.42)**

in which K_{c} is the fracture toughness of the material obtained from toughness tests. Integration of Eqs (12.41) or (12.42) analytically or graphically gives an estimate of the crack growth life of the structure, i.e. the number of cycles required for a crack to grow from an initial size to an unacceptable length, or the crack growth rate or failure, whichever is the design criterion. Thus, for example, integration of Eq. (12.41) gives, for an infinite width plate for which $\alpha=1.0$

$$[N]_{N_{\mathrm{i}}}^{N_{\mathrm{f}}} = \frac{1}{C[(S_{\max} - S_{\min})\pi^{\frac{1}{2}}]^n} \left[\frac{a^{(1-n/2)}}{1 - n/2}\right]_{a_{\mathrm{i}}}^{a_{\mathrm{f}}}$$

(12.43)

for $n>2$. An analytical integration may only be carried out if n is an integer and α is in the form of a polynomial, otherwise graphical or numerical techniques must be employed. Substituting the limits in Eq. (12.43) and taking $N_{\mathrm{i}} =0$, the number of cycles to failure is given by

$$N_f = \frac{2}{C(n-2)[(S_{max} - S_m)\pi^{1/2}]^n} \left[\frac{1}{a_i^{(n-2)/2}} - \frac{1}{a_f^{(n-2)/2}} \right]$$

(12.44)

An infinite plate contains a crack having an initial length of 0.2 mm and is subjected to a cyclic repeated stress range of 175 N/mm². If the fracture toughness of the plate is 1708 N/mm$^{3/2}$ and the rate of crack growth is $40 \times 10^{-15} (\Delta K)^4$ mm/cycle determine the number of cycles to failure.

The crack length at failure is given by Eq. (12.30) in which $\alpha=1$, $K=1708$ N/mm$^{3/2}$ and $S=175$ N/mm², i.e.

$$a_f = \frac{1708^2}{\pi \times 175^2} = 30.3 \text{ mm}$$

$$N_f = \frac{2}{C(n-2)[(S_{max} - S_m)\pi^{1/2}]^n} \left[\frac{1}{a_i^{(n-2)/2}} - \frac{1}{a_f^{(n-2)/2}} \right]$$

from which

$$N_f = 26919 \text{ cycles}$$